THESIS

CUT IT OUT: A NOVEL, QUANTIFIABLE APPROACH TO KERF MARK ANALYSIS USING 3D CONFOCAL MICROSCOPY AND MACHINE LEARNING

Submitted by

Wyatt H. Benson

Department of Anthropology and Geography

In partial fulfillment of the requirements

For the Degree of Master of Arts

Colorado State University

Fort Collins, Colorado

Spring, 2023

Master's Committee:

Advisor: Michael C. Pante

Andrew Du
Jessica Jackson

Copyright by Wyatt H. Benson 2023

All Rights Reserved

ABSTRACT

CUT IT OUT: A NOVEL, QUANTIFIABLE APPROACH TO KERF MARK ANALYSIS USING 3D CONFOCAL MICROSCOPY AND MACHINE LEARNING

Forensic methods must adhere to the *Daubert* standard to be deemed as admissible evidence in court. Current critiques regarding how well this standard is upheld have also challenged whether current forensic practices truly meet the *Daubert* standard. For example, kerf mark analyses can reveal trace evidence in sharp force trauma cases but a lack of quantitative studies and standardized analytical methods leave the field open to potential scrutiny.

While previous research frequently classifies marks as either the product of serrated or non-serrated blades, further identifications are rarely made confidently. The goal of this project is to determine whether variations in 3D micromorphological variables can be used to quantitatively discriminate between kerf marks made by different knife types and blade classes.

Here, kerf marks were produced using five different knives on bovid diaphyses, 3D scanned using profilometric microscopy, measured for both volumetric and profile variables, then analyzed using quadratic discriminant analysis. Results show individual knives were classified correctly in only 52% of attempts. However, blade class – serrated vs. non-serrated vs. partially serrated – was successfully identified in 97% of attempts. Significantly, our results differentiate between kerfs produced by serrated blades, non-serrated blades, and partially serrated blades, not only allowing for more specific blade identifications but also producing a quantifiable and replicable method meeting the *Daubert* criteria.

ACKNOWLEDGMENTS

I would first like to thank my advisor, Dr. Michael Pante, for his expertise, edits, and guidance throughout this research process and for taking me in as his graduate student when my research interests changed and developed. I also want to thank my other committee members – Dr. Andrew Du and Dr. Jessica Jackson – for their assistance with this thesis. Dr. Du, your guidance regarding my statistical analysis was invaluable to the success of this research. Dr. Jackson, your lessons on the importance of historical narratives were a necessity for making sense of the complexity behind forensic admittance. I would also like to acknowledge the Colorado State University Anthropology Department and College of Liberal Arts for funding my studies and for purchasing the Sensofar non-contact 3D surface metrology scanner.

Additionally, I am grateful for Elle Herner and Dr. Connie Fellmann for creating the kerf mark collection used in this analysis. The production of this collection back in 2017 allowed me to answer the questions I wanted to ask while saving substantial amounts of time and money. Furthermore, I am grateful for the entire customer service team at Sensofar for assisting me with all my technical questions regarding the scanner and Sensomap software.

This thesis would not have been possible if not for my family and friends. To my parents, Dale and Terry, you have always been there for me when I needed it most, thank you for your unconditional support throughout this process. To my friends and partner, thank you for helping me stay in a healthy mental state when times were difficult. Finally, I would like to thank my cohort and peers for providing me with academic advice and emotional support during the entirety of this graduate experience.

TABLE OF CONTENTS

LIST OF TABLES

LIST OF FIGURES

CHAPTER ONE: INTRODUCTION

1.1: Background and Research Problem

In court, all forensic practices must meet a certain standard to be deemed as admissible evidence in a case. Currently, those criteria are delineated by the *Daubert* standard (1993), stating expert witnesses and all forensic science must only be accepted by a judge if they meet specific scientific standards. Although the *Daubert* standard helped strengthen forensics as it led to more critical critiques of certain analyses – such as hair, fingerprints, bite mark, shoeprint, firearm, handwriting analysis, etc. – it is important to note these critiques are not directly translating over to practice (Giannelli, 2006; Garrett and Neufeld, 2009; NAS, 2009; Seaman, 2012; Cates et al., 2015; Lander and PCAST, 2016; Lander, 2018). Currently, the *Daubert* standard is not evenly upheld in courtrooms across America, with issues stemming from judges not effectively knowing whether forensic practices are scientifically valid to differences regarding forensic acceptance in civil vs criminal courts (Risinger, 2000; Moreno, 2003; Hans, 2007; Bernstein, 2009; Saks, 2009; Moriarty, 2010; Giannelli, 2013; Epstein, 2018; Hilbert, 2018; Garrett et al., 2021). Because current forensic standards are not being consistently upheld across courtrooms, forensic analysts must therefore become more critical of their respective fields and determine whether their practices and methods truly meet the standard outlined by *Daubert* (Grivas and Komar, 2008).

While more uncommon in the United States due to the accessibility of firearms, sharp force trauma (SFT) cases are highly relevant, with around 10% of all homicides in the United States (7,721) being the result of stabbings from 2015-2019 (Bohnert et al., 2006; DOJ, 2020). Similarly, stabbings are one of the most frequent forms of homicide in Europe, with 97,183 individuals being stabbed to death worldwide in 2017 (UNDOC, 2019). SFT can be best defined as "narrowly focused, dynamic, slow-loaded, compressive force with a sharp object that produces damage to hard tissue in the form of an incision (broad or narrow)" (Symes et al., 2002). When also taking Locard's Exchange Principle (1910) into account – or the assumption that trace evidence will always be transferred between the suspect, victim, and crime scene – it can be presumed there will always be evidence left behind at scenes involving SFT. Therefore, kerf marks (cut marks in forensic contexts) are one of the most important forms of evidence in SFT cases as they may be the only trace evidence left behind to help identify a murder weapon and seal a conviction.

Kerf mark analysis (KMA) is extremely important for identifying the agent used in SFT cases; however, studies of bone surface modifications (BSM) originated in paleoanthropology wherein researchers began studying marks left behind on bones and fossils to better interpret hominin behaviors and separate them from naturally occurring taphonomic processes (Bunn, 1981; Potts and Shipman, 1981; Shipman and Rose, 1983; Blumenschine and Selvaggio, 1988; Fisher, 1995; Blumenschine et al., 1996; Bartelink et al., 2001; Lupo and O'Connell, 2002; Bello and Soligo, 2008; Bello, 2011). Since the origination of BSM studies in paleoanthropology, numerous forensic analysts have reframed the ways researchers use BSM and taphonomy to better identify SFT in the courtroom, with results often distinguishing between kerf marks made by serrated and non-serrated blades (Bonte, 1975; Vao and Hart, 1983; Lewis, 2008; Thompson and Inglis, 2009; Love et al., 2012; Tegtmeyer, 2012; Tennick, 2012; Crowder et al., 2013; Cerutti et al., 2014; Smith, 2014; Norman et al., 2018; Sandras et al., 2018; Giraudo et al., 2019).

Even though individual kerf studies may succeed in making proper identifications of marks made by serrated vs. non-serrated knives, the field as a whole is riddled with issues including the relative absence of quantitative analyses, contradictory error rates, and a major lack of standardization across studies (Bartelink et al., 2001; Love et al., 2012; Crowder et al., 2013; Smith, 2014; Love, 2019). Because KMAs are not standardized and the results of individual studies often contradict one another, a universal error rate cannot be generated, methodologies and hypotheses cannot be retested, results are not replicable, and there is no maintenance of standards. The issues with KMAs emphasize there is no "widespread acceptance" of the methods used within this scientific community, meaning KMAs currently do not meet the criteria listed in *Daubert* and should not be used in court until new methods are developed which meet this standard of acceptance. However, as KMAs have been influenced by paleoanthropological BSM studies before, novel approaches for mark identification in paleoanthropology which use 3D optical profilometry and machine learning may be the key to solving the issues currently existing in KMA.

This thesis presents a novel approach to KMA using the protocol outlined by Pante et al. (2017) to develop a new, more replicable, quantifiable, and standardized method that researchers can easily use when analyzing kerf marks while still adhering to the *Daubert* standard. To do so, this study uses 3D optical profilometry to quantify the variation in micromorphological measurements of kerf marks made by four different knives: a chef's knife, boning knife, steak knife, and bread knife. Once marks were scanned and measured, quadratic discriminant analysis (QDA) was used to generate a model which determines whether knife type or blade class can be identified based on a marks' micromorphology.

1.2: Goal of this Study

As noted above, there are currently issues with the application of forensic standards and their translation over to forensic fields like KMA. Because of this disconnect, KMAs currently do not meet the *Daubert* standard and should therefore not be used in court until the necessary adjustments are made. Hence, the main goal of this study is to develop and test a new methodology for KMAs that meets all the criteria listed in *Daubert*. This thesis uses the method presented by Pante et al. (2017) as this protocol and subsequent research using this protocol have demonstrated the method produces results with minimal error rates which are consistently quantifiable, replicable, and retestable (Muttart et al., 2017; Gümrükçü et al., 2018; Gümrükçü and Pante, 2018; Keevil, 2018; Mwakyoma, 2021). Testing this new method is also crucial as it will not only alleviate the problems afflicting KMAs – in terms of *Daubert* – but may also lead to novel research using the same method, resulting in a standardized approach to KMA which can be maintained over time and used to produce a universal error rate. Moreover, identifying kerf marks using this new method can help kerf mark analysts asses the quality and reputability of prior research, further progressing KMAs forward.

1.3: Objectives of this Study

There are two primary objectives within this thesis. The first objective is to determine whether optical profilometry and the protocol outlined by Pante et al. (2017) can translate over from paleoanthropology to forensics. In other words, this thesis is testing whether variations in 3D micromorphological measurements can be used to identify the knife type or blade class responsible for producing certain kerf marks. Knife type refers to a specific kind of knife: chef's, boning, steak, bread, etc. Blade class refers to the type of blade: non-serrated, partially serrated, and fully serrated. To address this objective, marks were made by four different knives – chef, boning, steak, and bread – then scanned using the Sensofar non-contact 3D surface metrology scanner and its associated Sensoview® software. Once the 3D scans were captured, micromorphometric features of each mark were measured using Sensomap® software then analyzed using QDA to determine whether knife type or blade class could be surmised from the measurements taken on each mark. By doing so, this thesis not only tests the accuracy of each classification but also whether it is possible to identify the type of knife used or just blade class.

The second objective of this study is to identify which mircomorphometric variables are the most useful when making mark identifications. In total, 12 variables were measured; these include measurements from the 3D rendering such as surface area, volume, maximum depth, mean depth, maximum length, and maximum width as well as profile measurements like area, maximum width, maximum depth, roughness, opening angle, and floor radius. The value of each variable was assessed in two different ways. First, predictor screening was used to see which variables carried the most weight on the statistical model. Second, QDA models were run again omitting any variables deemed insignificant by predictor screening. The importance of each variable was then evaluated on whether the removal of certain variables strengthened or weakened the QDA model(s).

Current KMAs have demonstrated only blade class can be readily identified based predominately on qualitative analyses of mark morphology (Thompson and Inglis, 2009; Tegtmeyer, 2012; Crowder et al., 2013; Sandras et al., 2018). Additionally, while the consensus is knife identifications can typically only be made to the level of blade class, KMAs tend to use vastly different criteria and variables for analysis, making it difficult to compare the results of one study to those of another. Therefore, results from this study can help forensic analysts determine if more accurate identifications can be made beyond blade class as well as offer insight as to which quantified variables are the most useful when determining the knife responsible for producing kerf marks.

1.4: Hypothesis

Based on the proposed research questions, the null hypothesis (H_0) states there will be no significant differences between kerf marks made by different knife types of classes based on the micromorphometric variables measured in the 3D scans. In other words, we will fail to reject the null hypothesis if the QDA model cannot make correct mark classifications consistently. However, in order to reject the null hypothesis, we must fail to reject the alternative hypothesis (H_A) which states the QDA model can consistently classify marks accurately, meaning kerf marks are frequently attributed to the proper knife type or class.

1.5: Chapter Summaries

In order to answer the aforementioned research questions and efficiently achieve the goals and objectives of this research, this thesis is split into six chapters. Chapter One (the current chapter) outlines the research problems as well as the goals, objectives, questions, and hypotheses being tested through this research. Chapter Two summarizes all the literature necessary to understanding the problematic history of forensic admissibility, the origins and current state of KMA in relation to *Daubert*, and how current approaches using 3D profilometric microcopy in paleoanthropology may help alleviate the concerns afflicting KMA. Chapter Three defines the experimental procedures and protocol used in this study for data collection as well as the statistical analyses employed to interpret the data. Chapter Four provides an overview of the statistical analysis. Finally, Chapters Five and Six explain and summarize the results of this experiment and their overall implications for KMA.

CHAPTER TWO: BACKGROUND

The main goal of this study is to develop a new, standardized, and quantifiable approach for kerf mark analysis (KMA). While taphonomic and bone surface modification (BSM) studies originally rose to prominence in paleoanthropology, the analyses and methods used have also gained traction in forensics. Based on Locard’s Exchange Principle (1910), KMA is vital in sharp force trauma (SFT) cases as kerf marks left behind on bone may be the necessary evidence for identifying the tool used to produce the marks and ensuring a conviction. However, it is important to be skeptical of the validity of KMA studies as there are currently discrepancies about what is considered admissible scientific evidence in court. Put differently, because there are issues with how judges and juries interpret the *Daubert* standard to determine what forensic evidence can and cannot be used in court, there are also problems regarding the reliability of KMA studies and whether they truly meet the standard for forensic admissibility. Nevertheless, there is the potential that new approaches which use profilometric microscopy and 3D analysis to better identify cut marks in the fossil record could also become commonplace in KMA.

This chapter begins by providing a background of the theoretical framework upon which all forensic practices are built, Locard’s Exchange Principle. This chapter then outlines the history of forensic admissibility in court, detailing the *Frye* and *Daubert* standards as well as the problems with each standard through time to present day. Next, this chapter discusses the history of taphonomic and BSM studies, from their origin in paleoanthropology to more recent developments of KMA in forensics. Finally, this chapter explains the current issues regarding KMA and how novel approaches in paleoanthropology which use profilometric microscopy, 3D imaging, and machine learning are potentially the answer to resolving the problems defining KMA.

2.1: Locard's Exchange Principle: A Theoretical Framework

Although forensic science has existed for centuries, the current state of forensic evidence and analysis stems from Edmund Locard's Exchange Principle (1910), or the theory that "every contact leaves a trace." Trace evidence can be further defined as any evidence found at a crime scene, on a suspect, or on a victim (Mistek et al., 2018). In other words, Locard's Exchange Principle stresses when two objects – for example, a suspect and victim/crime scene – come into contact with one another, each will take something from the other object or leave something behind. More eloquently, Kirk and Kirk (1953, p. 4) explained this theory as follows:

> "Wherever he steps, whatever he touches, whatever he leaves, even unconsciously, will serve as a silent witness against him. Not only his fingerprints or his footprints, but his hair, the fibers from his clothes, the glass he breaks, the tool mark he leaves, the paint he scratches, the blood or semen he deposits or collects. All of these and more, bear mute witness against him. This is evidence that does not forget. It is not confused by the excitement of the moment. It is not absent because human witnesses are. It is factual evidence. Physical evidence cannot be wrong, it cannot perjure itself, it cannot be wholly absent. Only human failure to find it, study and understand it, can diminish its value."

According to this aforementioned quote, Locard's Exchange Principle is crucial to any forensic study as it emphasizes the assumption that some form of evidence will always be left behind, regardless of the crime committed. Moreover, this theory is important as it accentuates the forensic analysts' job to uncover any trace evidence; since this principle assumes evidence is always present, it becomes the analysts' job to uncover said evidence (Kirk and Kirk, 1953). Therefore, Locard's Exchange Principle is a vital theoretical framework for numerous fields in forensics – including KMA – as it demarcates the argument that trace evidence can always be found at a crime scene, further warranting the need for reliable, reputable forensic methods.

2.2: *Frye* v *Daubert*: A History of Forensic Admissibility

While Locard's Exchange Principle set the foundation for the discovery of forensic evidence, it is mandatory to also address the history of forensic admissibility in court. From the mid-late 1800s to present-day, forensic admissibility has undergone numerous transitions, further delineating the standards forensic methods must meet to be used by a prosecutor or defense (*Frye v United States*, 1923; *Daubert v Merrell Dow Pharmaceuticals Inc.,* 1993). Even though these standards have become stricter over the years, the current state of forensic admissibility is still plagued with concerns and conflicts regarding how the legislation is interpreted and practiced (Risinger, 2000; Giannelli, 2006; Hans, 2007; Bernstein, 2009; Garrett and Neufeld, 2009; Moriarty, 2010; Seaman, 2012; Giannelli, 2013; Cates et al., 2015; Epstein, 2018; Lander, 2018; Garrett et al., 2021). The following sections will provide context and outline the history of forensic admissibility from the time before the *Frye* standard, between the *Frye* standard and *Daubert* standard, and present day during the *Daubert* era. Additionally, the following sections will outline the critiques and conflicts which have influenced the development of these different forensic standards.

2.2.1: A Time Before Frye

In the mid-late 1800s, standards for forensic admissibility were relatively lacking in terms of scientific influence, as most of the criteria for acceptance were based on the judge's perception of the expert as an individual, but not the true value of the method (Dillon, 2017). For instance, expert witness in the late 1800s was frequently based on whether the findings of the expert went beyond the range of knowledge for an average juror (Faigman et al., 1993). Similarly, at this time forensic evidence was oftentimes allowed in court if the expert witness was "commercially successful" in their field, demonstrating a level of professional excellence that was profitable (Saks, 2009). Thus, the earliest forms of forensic admissibility are best summarized as placing more emphasis on the success of the expert witness rather than the validity of the science being practiced.

By the beginning of the 20th Century, the legal community was calling for stricter guidelines for the admission of scientific evidence and expert testimony because these early forensic standards were highly subjective and focused more on the expert rather than the scientific method employed. By this time, judges, state supreme courts, and even the public demonstrated a lack of confidence in forensic admissibility based on an experts' "success," as these experts oftentimes disguised pseudoscience as scientific fact by obscuring the truth and using jargon-laden rhetoric to confuse and influence juries (Hilbert, 2018). Therefore, because there were contradictions between the perception of expert "success" and the public's understanding of forensic evidence, the legal community began calling for a legalized standard for forensic admissibility which placed more emphasis on the validity of evidence presented.

2.2.2: The Frye Standard

Since legal constituents and policymakers were expressing concerns over the admissibility of forensic evidence at the beginning of the 20th Century, the legal community was searching for a way to implement a new, stricter standard. In *Frye v United States* (1923), Joseph Alphonzo Frye was on appeal for second degree murder, in which he attempted to present an expert witness who would testify on behalf of Frye recanting his guilt. However, the trial judge denied the expert's testimony because there was not enough data to support the use of a systolic blood pressure test – an early version of a lie detector test – within the physiological and psychological scientific communities, resulting in the dismissal of Frye's appeal. In turn, this court case led to the first standardized legal criteria for the admissibility of forensic evidence.

The *Frye* standard was then created, stating "scientific evidence presented to the court must be interpreted by the court as 'generally accepted' by a meaningful segment of the associated scientific community" (*Frye v United States*, 1923). In other words, if a forensic method was "generally accepted" amongst those in the respective scientific community, that method was deemed admissible in court.

2.2.3: The Caveats of Frye

While pivotal for its time, the *Frye* standard was also deemed problematic as judges frequently ignored or overlooked the standard until the 1970s-1980s (Gottesman, 1998; Saks, 2009). Even though the *Frye* standard did not take hold until the late 1900s, some courts were rejecting the "general acceptance" test as they saw the criteria as antiquated and outdated (Giannelli, 1993). Juries were also skeptical of the court or judges' abilities to make an informed decision on whether a forensic method was "generally accepted" within their scientific circles (Bernstein, 2000; Mnookin, 2008). As a result of these conflicts, it became apparent some courts offered contradictory rulings in different jurisdictions based on the variable interpretations of "general acceptance," resulting in a lack of standardized forensic admissibility (Bernstein, 2000). Hence, because different jurisdictions were interpreting the *Frye* standard in various ways, the new standard was unsuccessful in effectively creating a universal approach to assessing the validity of forensic methods in court.

The *Frye* standard underwent further scrutiny resulting from parties taking advantage of the standard's loopholes. In the 1980s, "toxic tort" cases – cases involving injuries to plaintiffs by toxic substances – appeared more and more frequently in civil courts, with prosecutors calling upon expert witnesses who presented "junk science" to help plaintiffs win lawsuits and make large profits (Eggen, 1993; Posin, 1995; Billauer, 2016). Since the scientific methods used in “toxic tort” cases were complex, judges and juries had a difficult time assessing whether these intricate, novel studies should be deemed admissible, resulting in forensic evidence being taken at face value (Hilbert, 2018). Due to discrepancies in the application of the *Frye* standard and the increasing complexity of scientific studies in the late 1900s, judges and juries had a difficult time determining what forensic studies should be deemed “generally accepted,” resulting in individuals profiting off the flaws defining forensic admissibility.

2.2.4:The Daubert Standard and its Application

With the *Frye* standard being taken advantage of in civil courts, the legal community once again called for a review of forensic admissibility in the late 1980s, early 1990s to combat the inclusion of questionable science in courtrooms. In *Daubert v Merrell Dow Pharmaceuticals Inc. (1993)*, Merrell Dow – a pharmaceutical company manufacturing a morning sickness drug called Benedictin – was sued by a mother who argued the use of Benedictin during her pregnancy resulted in her two sons being born with birth defects. The Ninth Court stated the plaintiff’s experts had not submitted their reanalysis to peer review, nor were the methods published or accepted by their peers, meaning the forensic evidence was insufficient and did not meet the scientific standard to be used in court (*Daubert v Merrell Dow Pharmaceuticals, 1993*).

The implications stemming from this case were pivotal as this court case demonstrated the need for further delineation and discrimination in the admissibility of forensic evidence. In this case, the plaintiff’s argument was deemed inadmissible because their expert failed to present a method which had been peer reviewed, published, or accepted by any of their colleagues, demonstrating beyond a reasonable doubt the methodology used was not scientific or “generally accepted”. Because of these more rigorous criteria used specifically in this case, the *Daubert* standard was created, ushering in a new era of scientific standards in court. Under this new standard, all forensic evidence was only deemed admissible if it met the following criteria:

> "(1) The theory/methodology used can be and had been tested, (2) it has to have been subjected to peer review and publication, (3) there must be a known potential error rate, (4) there should be an existence and maintenance of standards, and (5) the method/theory must demonstrate widespread acceptance within a relevant scientific community" (*Daubert v Merrell Dow Pharmaceuticals*, 1993).

Therefore, while the *Daubert* standard did echo the *Frye* standard in terms of "widespread" or "general" acceptance, this new standard provided clearer criteria for judges and juries to consider when assessing whether a method was truly accepted by its scientific community.

2.2.5: Current Issues with the Daubert Standard

Although the *Daubert* standard generated new, more rigorous standards for judges and juries to follow when assessing the admissibility of forensic evidence, there are still numerous problems with how the standard is employed. To begin, there are inconsistencies in how often the *Daubert* standard is applied in practice, with judges oftentimes varying in their interpretation of the legislation. It is argued this lack of consistency stems from a widespread lack of scientific competency, wherein judges either receive little to no instruction about general scientific methods or principles, the training they do receive is oftentimes outdated, and many judges have little to no training in mathematical or statistical analysis (Moreno, 2003; Hans, 2007; Epstein, 2018; Garrett et al., 2021). Moreover, considering how complex some cases can be and the time it would take to fully assess the method's admissibility, some judges may be incentivized to bypass the time-consuming analysis required in cases with hard science expert testimony (Hilbert, 2018). Since judges are often inadequately trained in forensic methods and cannot spend the necessary time to fully assess every forensic method presented to them, it can be argued judges are unequipped to truly assess whether a forensic method meets the *Daubert* standard's criteria.

2.2.6: The Fallout of a Faulty Daubert

Although it is important to address where the *Daubert* standard is failing, it is also crucial to see the consequences arising from not critiquing the standard sooner. For instance, in 2009 the National Academy of Science (NAS) stated besides DNA analysis, all other forensic methods have not been able to "rigorously and consistently demonstrate a connection between evidence and a specific individual or source" (NAS, 2009). The President's Council of Advisors on Science and Technology (PCAST) reported similar findings, stating bite mark comparison evidence, shoeprint, and firearm evidence were not valid forensic methods with too high of error rates (Lander and PCAST, 2016). Various other forensic methods have faced even further scrutiny since the passing of *Daubert* such as hair, fingerprint, and handwriting analysis, but the issue is these methods are still used in the court of law (Giannelli, 2006; Garett and Neufeld, 2009; Seaman, 2012; Cates et al., 2015). Therefore, even though the *Daubert* standard had led researchers to further critique their respective fields, the critiques are not directly translating over to judges and juries, with many faulty forensic methods still being used and upheld in court cases throughout the country.

Finally, since the *Daubert* standard had been implemented, hundreds of people have been exonerated for their crimes, with nearly half of these cases involving faulty forensic science that was never excluded by the courts (Lander, 2018). In other words, even though *Daubert* is supposed to help catch faulty forensic practice in the courtroom, cases keep slipping through the cracks with any sort of solutions or reconciliations occurring *post-hoc*. In summation, there are numerous disparities in how the *Daubert* standard is assessed and upheld in both civil and criminal courts, with these discrepancies stemming from systemic issues as well as naivety on the judges' behalf; even though the standard itself is useful, its implementation in the courts has been inconsistent. Thus, if the system cannot reliably enforce and uphold this forensic standard, it is up to each respective scientific field to be critical of themselves and assess whether the current state of their field truly meets the requirements outlined by *Daubert*.

2.3: From Paleoanthropology to Forensics: A History of KMA

Sharp force trauma (SFT) can be defined as "narrowly focused, dynamic, slow-loaded, compressive force with a sharp object that produces damage to hard tissue in the form of an incision (broad or narrow)" (Symes et al., 2002). While SFT is not as common in the United States – due to the accessibility of firearms – it is one of the most frequent methods of homicide throughout countries in Europe, with over 97,183 individuals being killed worldwide by SFT in 2017 while a total of 7,721 individuals were murdered by sharp instruments in the US from 2015-2019 (Bohnert et al., 2006; UNDOC, 2019; DOJ, 2020). When taking into account Locard's Exchange Principle and the relatively high frequency of SFT in homicide cases, it has become apparent SFT often impacts bone or cartilage, leaving behind trace evidence (Banasr et al., 2003). Therefore, because SFT is common in homicide cases, it becomes the responsibility of forensic anthropologists to identify the kerf marks, the tool used to produce the marks, and how that tool was used (Crowder et al., 2013; Rainwater, 2015).

Due to the increased prevalence of SFT, KMA has become more common in the courtroom, but the field has a more extensive history going beyond forensics into the field of paleoanthropology. Early taphonomic studies of BSM in paleoanthropological contexts focused on identifying marks left behind by ancestral hominins to better understand human evolution and behavior (Bunn, 1981; Potts and Shipman, 1981; Shipman and Rose, 1983; Blumenschine and

Selvaggio, 1988; Blumenschine et al., 1996; Bartelink et al., 2001; Lupo and O'Connell, 2002; Bello and Soligo, 2008; Bello, 2011). Since the value of BSM studies has been highlighted within paleoanthropology, numerous forensic studies have reframed the way researchers use taphonomy and BSM to better identify evidence of SFT in court (Bonte, 1975; Vao and Hart, 1983; Lewis, 2008; Thompson and Inglis, 2009; Love et al., 2012; Tegtmeyer, 2012; Tennick, 2012; Crowder et al., 2013; Cerutti et al., 2014; Smith, 2014; Norman et al., 2018; Sandras et al., 2018; Giraudo et al., 2019). The following sections explain the history of taphonomic and BSM studies in both paleoanthropology and forensics. Additionally, the following sections highlight the current issues afflicting the field of KMA and present potential solutions to these concerns.

2.3.1: Taphonomy and BSM Within Paleoanthropology

Taphonomy can first be defined as everything that happens to an organism from when it dies to when it is found, or all the transitions an organism undergoes from the biosphere to the lithosphere (Efremov, 1940; Lyman and Lyman, 1994). While taphonomic studies apply to a wide variety of fields, they first rose to prominence in paleoanthropology, or the sub-field of anthropology focused on human evolution. Within paleoanthropology, taphonomic studies concentrated on distinguishing human-produced marks on bone from those produced by naturally occurring processes to better identify and understand human hunting and scavenging behaviors. In the beginning, BSM studies used macroscopic, qualitative descriptions of length, width, and mark profile shape to differentiate between naturally occurring marks – these include tooth marks from carnivores, rodent gnawing, root etching, trampling, bioerosion, rockfall, etc. – from human-produced marks like cut marks and percussion pits at East African sites like Olduvai Gorge and Koobi Fora (Bunn, 1981; Blumenschine and Selvaggio, 1988; Blumenschine et al., 1996).

While these seminal works helped lay the foundation of BSM studies in paleoanthropology, they were critiqued because the morphological criteria used for proper mark identification were macroscopic and qualitative, resulting in a lack of standardized approaches to BSM studies (Lupo and O'Connell, 2002). Even though Blumenschine et al. (1996) determined experts could correctly differentiate cut marks from tooth marks 97% to 99% of the time while novices with several hours of training could make correct identifications 86% to 95% of the time, the lack of standardization across research teams severely limited comparisons across studies and made it impossible to retest each other's work.

Since there were concerns over the use of macroscopic BSM studies, paleoanthropologists began implementing scanning electron microscopy (SEM) and digital microscopy to aid in the identification of cut marks from the fossil record (Potts and Shipman, 1981; Shipman and Rose, 1983). However, like macroscopic analyses, SEM and digital microscopy studies were also criticized because the technology only generates 2D images, meaning quantitative, volumetric measurements cannot be taken (Bartelink et al., 2001; Bello and Soligo, 2008; Bello, 2011). Advancements have recently been made within paleoanthropology to implement 3D imaging and quantitative analyses to create more reputable and replicable approaches for interpreting and detecting human-produced BSM; these approaches will be discussed at length later in this chapter (Bello and Soligo, 2008; Bello, 2011; Maté-González et al., 2015; Pante et al., 2017; Keevil, 2018; Mwakyoma, 2021).

2.3.2: The Origin of KMA Within Forensic Taphonomy

While taphonomic studies rose to prominence within paleoanthropology and archaeology, they were also deemed crucial to forensic studies. Ubelaker (1997) recognized taphonomic studies assisted forensic anthropologists with estimating the postmortem interval, reconstructing the environment in which a crime was committed, and determining if trauma was caused by a perimortem event related to the crime or naturally occurring post-mortem events. Likewise, even though the value of BSM studies was uncovered by paleoanthropologists, forensic analysts were interested in similar information.

Although KMAs did not gain traction until the mid-late 1980s, following the success of BSM research in paleoanthropology, kerf mark studies originated as early as 1942 when researchers noted marks produced by different metal instruments would leave behind certain morphological characteristics useful for tool identification on mediums like wood and metal (Burd and Kirk, 1942). Comparably, Bonte (1975) argued SFT patterns on human bone paralleled those found on inanimate mediums like wood and metal, emphasizing qualitative patterns could be documented to assist in weapon identification. Finally, Rao and Hart (1983) stated when comparing crime marks in human costal cartilage to marks made by the same knife in experimental settings on cellulose acetate butyrate, the crime marks and test marks matched. Though these seminal works were beneficial for helping lay the foundation for KMA, the macroscopic, morphological variables used for making the identifications were rarely listed or explained, meaning the results could be replicated or retested. Like seminal BSM work in paleoanthropology, early kerf mark studies were also considered problematic due to the reliance on macroscopic variables (Bartelink et al., 2001).

2.3.3: KMA and Qualitative Data

Since these early seminal works regarding kerf marks were relatively lacking in terms of methodology and transparency, researchers began documenting the different qualitative variables in hopes of generating stronger, more reputable methodologies. Lewis (2008) argued kerf marks created by different swords and other bladed weapons could be identified based on the presence or absence of variables such as cut length, shape, feathering, flaking, cracking, breakage, shards, and aspect. Additionally, this work helped standardize the terminology used for kerf marks (Figure 2.1) (Lewis, 2008). Researchers also began implementing other technological approaches to their work, as seen in Thompson and Inglis's (2009) research which used SEM to differentiate non-serrated blades from serrated blades on porcine bone. The conclusions of this work stated serrated blades leave a "y-shaped" mark whereas non-serrated blades leave a "t-shaped" mark (Thompson and Inglis, 2009). Similarly, Sandras et al. (2018) used epifluorescence microscopy to study marks made by 3 non-serrated and 2 serrated knives and learned correct identifications could be made 74-94% of the time, with more accurate identifications being made for serrated knives than non-serrated.

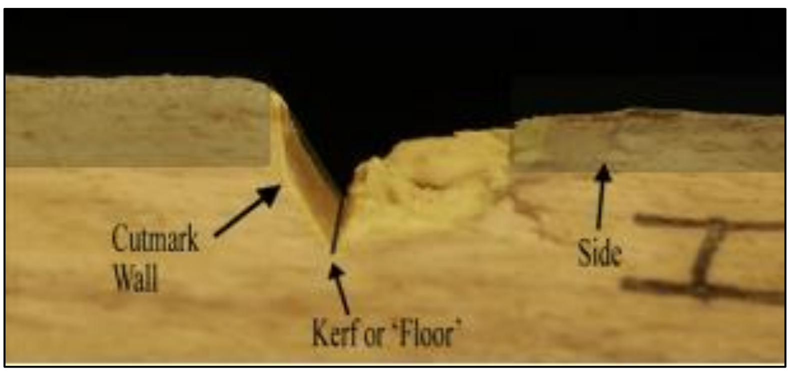

Figure 2.1: Profile of kerf mark demonstrating mark anatomy: base is known as the "floor," walls of the mark are known as "cutmark wall," and unmodified bone surface is known as the "side." Image taken from Lewis (2008).

While the aforementioned studies emphasize the use of different forms of microcopy to better identify kerf marks, the principal trend in KMA was to classify marks made by serrated knives from those made by non-serrated knives (Thompson and Inglis, 2009; Tegtmeyer, 2012; Tennick, 2012; Crowder et al., 2013; Sandras et al., 2018). However, these numerous studies frequently contradict one another, leading to a variety of conclusions. On one hand, some research teams have noted, through macroscopic and microscopic analyses, kerf marks produced by non-serrated and serrated blades are completely distinguishable from one another based on variables like kerf width, shape, and the presence/absence of striations (Tegtmeyer, 2012). Crowder et al. (2013) argued in a collection of 504 kerf marks produced by serrated, partially serrated, and non-serrated blades, marks were easily identified for non-serrated vs serrated blades, however, it was difficult to differentiate marks made by serrated blades from those made by partially serrated blades. Conversely, other research states marks made on bone by the same knife have too much variation in appearance to be accurately identified (Tennick, 2012). Therefore, even though the goals of many KMAs are to identify differences in mark morphology from marks made by serrated and non-serrated knives, there are inconsistencies in the accuracy of these classifications.

As seen above, the history of KMA can be best summarized as the macroscopic and microscopic analysis of qualitative, morphological differences in marks made by non-serrated, partially serrated, and serrated knives. However, one of the principal issues with the aforementioned examples is they all use qualitative methods which have varying error rates. For instance, in a study conducted by Love et al. (2012), blind testing was used to identify 90 cut marks made by a non-serrated blade, a serrated blade with a coarse serration pattern, and a serrated blade with a fine serration pattern. While the researchers were told to document the presence of striations and whether striations followed a "regular" or "irregular" pattern, misclassifications were made at a rate over 65% (Love et al., 2012). When Crowder et al. (2013) evaluated the accuracy of KMA, they studied marks made by 14 knives with a range of non-serrated, partially serrated, and serrated blades. Similar to Love et al. (2012), Crowder's team employed qualitative variables which described the striation patterns, but their error rate was less than 5% (Crowder et al., 2013). Because these error rates – based on qualitative criteria – are so different from one another, and because qualitative identifications are not as replicable, kerf mark analysts have called for studies to implement approaches which favor quantitative data, allowing for more acceptable and replicable results which could be better substantiated in court (Smith, 2014).

2.3.4: KMA and Quantitative Data

Due to the call for more reliable, replicable methods, researchers have begun to implement more quantitative approaches to KMA (Smith, 2014). Although qualitative methods dominated the field into the mid-2010s, the first quantitative KMA began as early as 2001, wherein Bartelink et al. (2001) used SEM to differentiate marks made by three different non-serrated blades (a scalpel, paring knife, and kitchen utility knife). Each kerf mark was produced using a mechanical device that accounted for angle, direction, and force, and results from the study stated kerf mark width was significantly different for all three blades; however there was overlap between knife types (Bartelink et al., 2001). Other quantitative KMAs yielded similar results, such as Cerutti et al. (2014) who noted marks made by different knives in a controlled, mechanical device all exhibited wide overlaps in terms of kerf width, angle, and depth. However, the analysts argue these overlaps were due to measurements being taken from a stereomicroscope (Cerutti et al., 2014). Hence, early quantitative studies took necessary steps toward strengthening the field, but the results oftentimes yielded too much overlap and not enough discriminatory power to be used effectively.

Nevertheless, there has recently been an increase in the number of KMAs which use micro-CT scans as this produces a 3D model which can then be quantified through various measurements. However, there are discrepancies on how valuable the method is at making proper identifications. For example, Norman et al. (2018) used micro-CT to analyze 270 kerf marks made by 8 different tool classes in a controlled environment. The variables measured included minimum toolmark width at floor, wall angle, trough height, trough angle deep, and trough angle shallow. Based on these variables, the research team concluded they made proper identifications 94% of the time, meaning micro-CT was the most appropriate technology for analyzing and identifying kerf marks (Norman et al., 2018). Conversely, micro-CT studies done by Giraudo et al. (2019) – which measured top kerf width, depth, bottom kerf width, angles degrees, and floor width – stated the technology produced high positive predictive values for inter-class analyses whereas intra-class analyses were lacking, concluding the technology should only be used alongside other forms of analysis. Thus, even though KMAs are beginning to transition into incorporating more quantitative approaches, there are still inconsistencies in how effective these approaches are for making proper identifications.

2.3.5:Do KMAs Meet the Daubert Standard?

Although the field of KMA has expanded over the past decade, there are still numerous issues with the current state of the field, particularly with the accuracy of the methods currently being employed. In qualitative studies, some researchers state that qualitative variables are sufficient enough to classify various weapons and toolmarks consistently (Lewis, 2008). Other analysts have stated qualitative methods are only valuable for distinguishing marks made by serrated vs non-serrated blades while others state there is more variation in marks made by the same knife, meaning qualitative assessments are severely lacking (Thompson and Inglis, 2009; Tegtmeyer, 2012; Tennick, 2012; Crowder et al., 2013; Sandras et al., 2018). Moreover, while there have been movements to implement more quantitative approaches, the current state of these studies is also concerning as studies either present contradictory results on the usefulness of the methods or there is too much overlap between measurements (Bartelink et al., 2001; Cerutti et al., 2014; Norman et al., 2018; Giraudo et al., 2019). Finally, different studies have produced severely contradictory error rates, with some research teams stating incorrect identifications were made 65% of the time whereas others say incorrect kerf identifications were made at rates less than 5% (Love et al., 2012; Crowder et al., 2013). While these differences may be due to the experience levels of different research teams, having such contradictory error rates demonstrates there is not an accepted rate within the field, meaning KMAs do not effectively meet the standards outlined by *Daubert* (Love, 2019).

Another issue currently plaguing the field of KMA is the lack of standardization across studies. Some studies state there is more value in qualitative variables whereas others emphasize the use of quantitative data, resulting in a wide variety of approaches that use either qualitative data or quantitative data. Furthermore, when comparing the various kerf mark studies presented in this chapter, almost every research team measured or documented different variables, had different names for the same variables, or did not efficiently explain or present the variables they were measuring (Table 2.1). In terms of qualitative variables, the only ones which appear consistently are kerf shape, striation type, and striation pattern (Lewis, 2008; Thompson and Inglis, 2009; Love et al., 2012; Tegtmeyer, 2012; Crowder et al., 2013; Sandras et al., 2018). Quantitatively, the only consistent variables measured were length and width; profile depth and angle were also measured, but the names for these variables often varied (Bartelink et al., 2001; Lewis, 2008; Thompson and Inglis, 2009; Tegtmeyer, 2012; Love et al., 2012; Cerutti et al., 2014; Norman et al., 2018; Giraudo et al., 2019). Because of the lack of consistency in the variables measured across studies, researchers cannot replicate each other's results, nor can they compare results and error rates (Love, 2019). Therefore, because a known error rate cannot be effectively obtained due to the lack of standardization, KMAs once again do not meet the

Daubert standard, meaning these analyses fall victim to the same scrutiny as numerous other forensic methods (NAS, 2009; Lander and PCAST, 2016).

Table 2.1: List of Qualitative and Quantitative Variables from Numerous KMAs

Research Team	Qualitative Variables	Quantitative Variables	Classification Success Rates
Bonte (1975)	NA	NA	NA
Rao and Hart (1983)	NA	NA	NA
Bartelink et al. (2001)	NA	Maximum cut mark width	NA
Lewis (2008)	Shape, feathering, flaking, cracking, breakage, shards, aspect	Length	NA
Thompson and Inglis (2009)	Shape, kerf damage, fragmentation/fractures	Length, width	NA
Love et al. (2012)	Striations, striation type, striation pattern, cut type	Interstriation distance, mean interstriation distance, width, length, area	45% classification success between serrated and non-serrated blades
Tegtmeyer (2012)	Kerf shape, presence of striations	Width	"100%" classification success between serrated and non-serrated blades
Tennick (2012)	Tip shape, bifurcation, cross-section profile, wall gradient, wall projections, margin regularity, margin definition, margin splitting, lateral ridging, floor definition, floor width, floor splitting, crushing, flaking, size of debris fragment, type of debris	NA	NA
Crowder et al. (2013)	Striation type (fine, coarse, combination of fine and coarse, or none), Striation pattern (patterned, unpatterned, combination, indeterminate), edge bevel	NA	79% classification accuracy when assessing serrated, non-serrated, and partially serrated blades. 96% classification accuracy when only assessing serrated vs. non-serrated blades

Cerutti et al. (2014)	NA	Depth, width, inclination of walls/angle of lesions	NA
Norman et al. (2018)	Edge shape, profile shape	Minimum toolmark width at floor, wall angle, trough height, trough angle deep, trough angle shallow	94% classification success for various saw and knife marks based on toolmark width
Sandras et al. (2018)	Kerf thickness, kerf shape, edges, walls, edge vs. wall angle, profile shape, flakes	NA	92% classification accuracy for observers 1 and 3 when differentiating serrated from non-serrated marks. 74% classification accuracy for observer 2 who was less experienced
Giraudo et al. (2019)	NA	Top kerf width, depth, bottom kerf width, angles degrees, floor width	NA

When looking at the current state of KMA, it can be argued each study only meets the second criteria of *Daubert*, as each study has been peer reviewed and published. However, since there are discrepancies in the error rates presented between studies, there is no clear potential error rate, meaning KMAs do not meet that aspect of the *Daubert* standard (Love et al., 2012; Crowder et al., 2013). Moreover, because various research teams frequently measure different variables when assessing kerf marks, there is no existence/maintenance of standards meaning KMA once again to not meet the *Daubert* criteria. Similarly, because kerf mark methodologies differ so drastically and cross-study comparisons are impossible, the field will continue to be incapable of ever developing a universal error rate (Love, 2019). Additionally, due to the lack of standardization across studies, it is nearly impossible for researchers to replicate or test one another’s work, meaning KMA also does not meet the Daubert criteria which states the theory/methodology can be tested. Finally, because there are such different, unstandardized approaches to analyzing and identifying kerf marks, with different analyses producing vastly different results, it can be argued the method/theory does not exhibit widespread acceptance within its respective community, meaning KMAs, in their current state should not be deemed admissible in court.

2.4: Potential Solutions in Paleoanthropology: A New Approach to KMA?

As noted in the previous section, if KMA is to continue being used in the courtroom, then the field must undergo numerous transitions so the methods employed consistently meet the *Daubert* standard. However, current steps within forensics are failing to make the necessary adjustments as a result of inconsistencies in how *Daubert* is applied in the courtroom (Risinger, 2000; Hans, 2007; Bernstein, 2009; Saks, 2009; Moriarty, 2010; Giannelli, 2013; Epstein, 2018; Hilbert, 2018; Garrett et al., 2021). As mentioned earlier, current advancements in paleoanthropology have been made to implement 3D imaging and quantitative analysis to strengthen analyses in the field. Therefore, this section will outline the current advancements with 3D imaging in paleoanthropology and how they could assist kerf mark analysts in developing a standardized, objective, replicable approach for kerf mark identification.

2.4.1: The Beginnings of 3D Analysis in Paleoanthropology

The first implementation of a 3D scanning method occurred in 2008 when researchers used profilometric microscopy to quantify the differences between cut marks made by metal knives and flint blades; the variables measured included cross-sectional shape, shoulder height, sharpness, cut inclination, and depth (Bello and Soligo, 2008). Since this seminal work, further research using the same methodology has expanded to include marks made by hand axes and marks found on human teeth (Bello et al., 2009; Bello, 2011). Similarly, Boschin and Crezzini (2012) used 3D microscopy to take morphometric measurements like depth, breadth, and opening angles and used them to develop objective methods for identifying the agent responsible for producing different marks. Even as these original 3D analyses helped propel BSM studies forward, there was a lack of reproducibility between research teams, meaning the results of each project could not be adequately retested (Pante et al., 2017; Keevil, 2018).

Other research using 3D approaches in paleoanthropology implemented micro-photogrammetry which operates by combining multiple photos of a mark taken from different angles to create a 3D model of the mark, allowing for quantifiable measurements to be taken like opening angle, width, and depth. (Maté-González et al., 2015). Since the development of this method, numerous research teams have implemented it to compare marks made by various stone tools from different raw materials to marks found in the fossil record (Maté-González et al., 2015; Yravedra et al., 2017). However, like profilometric microscopy, micro-photogrammetry also has issues pertaining to replicability, inter-observer objectivity, and testability. Micro-photogrammetry is limited by the need to take “approximate” measurements which can increase observer bias, plus the method relies on taking central cross-sectional profiles for each measurement which is not representative of the entire mark and is also not easily replicable between researchers (Pante et al., 2017; Keevil, 2018). This method also only creates a 2D cross-sectional profile of each mark, restricting the analyst from measuring any volumetric variables like volume, surface area, and mean depth (Keevil, 2018). Finally, this approach is too time-consuming, taking up to 50 minutes to analyze one mark (Keevil, 2018). Although micro-photogrammetry was a step in the right direction, issues with replicability and inter-observer bias have restricted this approach from becoming more commonplace.

2.4.2: A New Age of Profilometric Microscopy

Because of the need for quantitative analyses and a call for more replicable, testable analyses, 3D studies in paleoanthropology – particularly confocal microscopy – have undergone major advancements in the past 5 years. For instance, Pante et al. (2017) developed a standardized and quantitative protocol for identifying cut marks using 3D reconstruction and measurement of micromorphological features. This new method is also favorable as it allows for both volumetric and profilometric measurements, producing more holistic data for each individual mark. Furthermore, this method has yielded promising results, with cut marks and tooth marks being identified correctly 97.5% of the time (Pante et al. 2017). The replicability of this method has been tested as well, using an inter-observer approach which produced similar results to the original study, demonstrating this current approach produces more accurate results which can be adequately retested (Pante et al., 2017; Keevil, 2018).

Since the development of this method, the protocol has been applied to various other studies. Some of these studies include the classification of tooth marks made by different carnivores, the effects of fluvial action on cut mark morphology, and the identification of cut marks made by different technology types and raw materials (Muttart et al., 2017; Gümrükçü et al., 2018; Gümrükçü and Pante, 2018; Keevil, 2018; Mwakyoma, 2021). Although this new protocol developed by Pante et al. (2017) has only been used in paleoanthropological and archaeological contexts, the method would also be valuable for KMA as the methodology produces results which are objective, quantifiable, standardized, testable, and easily replicable. Therefore, the methodology presented by Pante et al. (2017) should be implemented in forensics to help develop a new standard for identifying kerf marks while also meeting the criteria listed in *Daubert*.

CHAPTER THREE: MATERIALS AND METHODOLOGY

In this study, the main goals are to determine whether a specific knife type or blade class can be identified based solely on a kerf mark's micromorphological features as well as which of those features are most useful for differentiating kerf marks from one another. To achieve these end goals, this study follows the 3D optical metrology analysis technique created by Pante et al. (2017) to analyze and compare kerf marks produced on various diaphyseal segments of bovid long bones. Additionally, since this experiment is exploratory, an emphasis was placed on replicability and generality of results at the expense of realism. The following sections outline the experimental methodology and how data was processed and collected using 3D kerf mark analysis.

3.1: Experimental Bone Sample

Bone samples were sourced by Elle Herner (EH) and Connie Fellmann (CDF) in 2017. Pre-cut bovid long bones were acquired from Beaver's Market in Fort Collins. These 1-2 inch segments of bone were pre-packaged in black Styrofoam and saran wrap and stored in a standard grocery store freezer. Although prior research states porcine bone is more analogous to human osseous tissue, bovine diaphyseal elements were used because of accessibility and cost-effectiveness; bovid long bones provide the user with more surface area to cut, meaning multiple series of kerf marks could be produced on the same bone (Kooi and Fairgrieve, 2013; Miles et al., 2020). A total of 15 bone portions were bought and used to create the collection, but only 13 were recovered for analysis.

3.1.1: Bone Cleaning and Specimen Preparation

While the bovid long bone segments were purchased de-fleshed, the remains still included bone marrow as well as remnants of cartilage. Cleaning of the bone was performed in two separate trials. During the first trial, EH attempted to clean a total of 6 epiphyseal and 3 diaphyseal portions by mixing water with ¼ cup of hydrogen peroxide, heating the mixture on a low heat setting, and submerging the bones in the mix for 8 hours and 40 minutes. However, the process resulted in too much cartilage still attached and some bones were overcooked due to a white, bleached appearance rendering them unusable for the experiment.

During the second trial, EH used the same water, ¼ cup hydrogen peroxide mixture but reduced the time bones were submerged in the mixture to 4 hours and 30 minutes and only used 15 diaphyseal portions. Remains were checked at the 3 and 4 hour marks to guarantee they were not overcooked. Once remains were removed from the water, any additional cartilage was removed using plastic forks to avoid inflicting any trauma on the soft tissue. In the end, the second trial was successful as no remains were overcooked and cartilage had been removed from all cutting surfaces.

3.2: Experimental Knife Collection

The knives used to produce the kerf marks analyzed in this study all belonged to a collection obtained from Chicago Cutlery ™ and consisted of a carbon steel chef's knife, boning knife, steak knife, and bread knife (Figure 3.1). The knife set was purchased new to control for sharpness as a potential confounding factor. Each knife was given its own identification number for analysis: the chef's knife is 1, the boning knife is 2, the steak knife is 3 and 3.5, and the bread knife is 4.

Figure 3.1: Knives used in experiment. From top to bottom knives are chef's knife (1), boning knife (2), steak knife (3, 3.5), and bread knife (4).

The chef's knife was characterized as a large, non-serrated knife, having a blade length of 200 millimeters and a width of 0.7 mm. The boning knife was classified as a small, non-serrated knife with a blade length of 128 mm and a width of 0.8 mm. The steak knife was categorized as a partially serrated blade with the serrated portion at the tip of the knife and the non-serrated portion continuing down to the handle of the knife. The entire steak knife had a length of 123 mm, but the serrated portion was 65 mm long while the non-serrated portion was 55 mm long. The serrated portion of the knife also was 1.1 mm thick whereas the non-serrated portion was 0.8 mm thick. Because this knife had two different blades, it was used in two ways; for marks labeled 3, the entire length of the steak knife's blade was used whereas only the serrated portion was used for marks labeled 3.5. Finally, the bread knife was classified as a large, serrated knife and had a blade length of 261 mm and a width of 1.2 mm (Table 3.1).

Table 3.1: General Information on Knives Used in this Study (measurements in mm)

Knife Type	Blade Class	Knife Length	Blade Length	Blade Width
Chef's	Non-Serrated	329	200	0.7
Boning	Non-Serrated	244	128	0.8
Steak Knife, Full Blade	Partially Serrated	123	55	0.8
Steak Knife, Serrated Portion	Partially Serrated	123	65	1.1
Bread	Serrated	385	261	1.2

3.3: Specimen Cutting Process

Before cutting began, each bone specimen was analyzed to determine the flattest portions of the bone relative to bone curvature to use as the cutting surface. EH was in charge of cutting specimens while CDF labeled each kerf mark and positioned the bones in a table clamp. Only one individual, EH, produced the kerf marks to control for the amount of force applied with each cut and reduce any inter-analyst bias.

Each researcher wore downed blade-resistant gloves and CDF affixed the table clamp to ensure the stability of the bone while cutting. Each bone was fastened in the table clamp with the cutting surface level to the clamp. Once the bone was secured in the table clamp, sets of kerf marks were completed from the right side of the bone to the left with the following knife progression: 1 (chef's knife), 2 (boning knife), 3 (steak knife, full blade), 3.5 (steak knife, just serrated portion), and 4 (bread knife) (Figure 3.2). The cutting surface was penetrated by each knife using a front-to-back motion as perpendicular to the cutting surface as possible rather than following the curvature of the bone. Regardless of knife type, each kerf was ideally created under the same amount of force while keeping the knife as straight as possible.

Figure 3.2: Example of mark series 15DD. Marks were made from right to left following this progression: chef's knife (1), boning knife (2), steak knife full blade (3), steak knife serrated blade only (3.5), bread knife (4).

After each mark was made, CDF labeled the mark with the specific knife label (1, 2, 3 3.5, 4). This process continued until 35 sets of 5 marks had been created, resulting in a total of 175 cut marks (35 marks of each knife type). However, since some bones were missing from the collection when analysis began in 2022, the current data set consists of 28 sets of each mark type for a total of 140 marks. Finally, each set of 5 marks was given an identifying number on the bone (A-II). Therefore, if a kerf mark was made by a chef's knife (knife 1) on bone 1, and was made in the first set of 5 marks, it was coded as 1A.1 (bone 1, mark set A, knife 1).

3.4: Scanning Procedure

Following the production of all cut marks, bones were scanned using the Sensofar non-contact 3D surface metrology scanner and its associated Sensoview® software in the 3D Imaging and Analysis Laboratory at Colorado State University. Kerf marks were scanned according to the methodology created by Pante et al. (2017) as this systematic approach allows for the resulting database to be replicable and comparable for future studies using similar methodologies.

Each bone was manually placed in a position that allowed for the mark to be as level as possible on both the x and y axes. Unlevel marks could prevent the collection of data as areas which are too high or too low relative to the position of the 5x objective lens will not get recorded by the scanner (Pante et al., 2017). Thus, masonry sand was used to create a level surface for the bone so that each kerf mark was level with the scanner's base.

Marks were also oriented along their long axis perpendicular to the x-axis of the scanner. This is done to ensure each profile that comprised the 3D models truly represented a single cross-section throughout the entirety of the mark (Pante et al., 2017). Once the kerf marks were oriented properly, a rectangular area was drawn around each mark using the camera provided by Sensofar, defining the section of the bone to be scanned (Figure 3.3). It was vital to include non-cut marked surfaces around the mark to make sure each scan encapsulated the entirety of the mark for processing and measurement.

3.5: Data Processing

Once the 3D kerf mark models had been completed, they were imported from the Sensoview® software into the Sensomap® (standard edition 7.4) software to be cleaned and processed before taking measurements. With this software, each new studiable produced is a 2D visual representation of the XYZ coordinates for that mark. The first processing step was to remove any outliers within the model using the "remove outliers" 'operator' studiable. The next step was to fill any remaining non-measured points in the 3D models using the "fill in NM" 'operator' studiable; this tool estimates any of the points which were not captured in the scanning process based on neighboring points (Figure 3.4A).

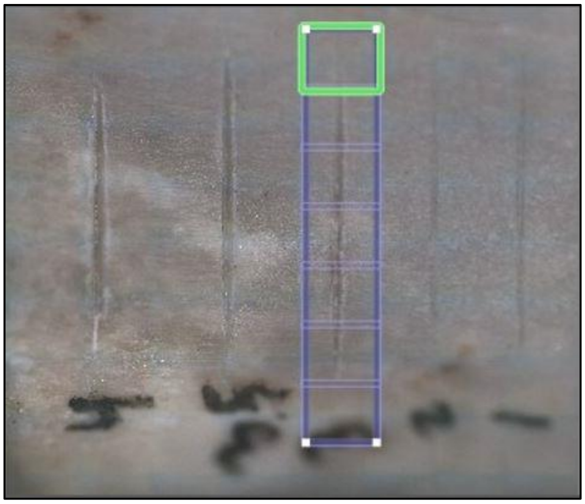

Figure 3.3: Photograph taken by Sensofar camera to define area of bone to be scanned. Note that all marks run perpendicular to the x-axis and within the rectangle there is also non-cut marked bone to guarantee the entirety of the kerf mark is scanned.

After removing outliers and filling non-measured points, the next step was to remove the influence of any bone surface irregularities or curvature on the 3D models while preserving the marks' morphology by using the "remove form" 'operator' studiable set to a polynomial degree of 2 (Figure 3.4B). Although the polynomial degrees can be set from 1-13 depending on the severity of bone surface irregularity, a polynomial degree of 2 was sufficient for this study.

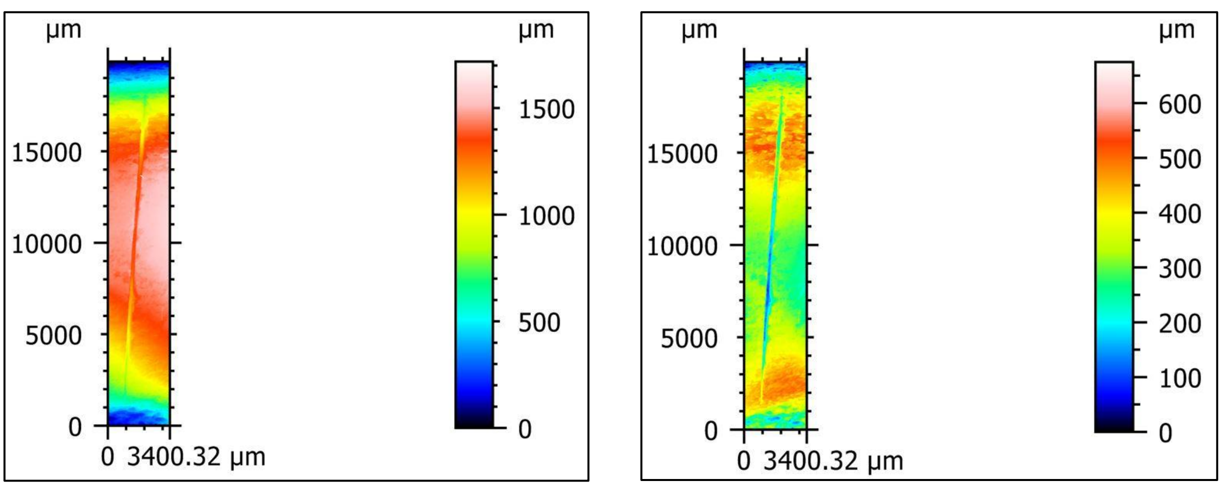

Figures 3.4A and 3.4B: Left image shows 3D kerf mark model (mark 12X.3) after importing from Sensoview, removing outliers, and filling in non-measured points. Right image shows same kerf mark after removing form. Color scales (on right of images) indicate depth.

Following the removal of any bone shape influence on mark shape, the “threshold” ‘operator’ studiable was used to define the extent of the marks’ profile (Figure 3.5A). Additionally, each 3D model that was not perpendicular to the x-axis was rotated using the “rotate” ‘operator’ studiable as slanted marks can reduce the accuracy of any measurements which require the user to trace the boundaries of the mark (Pante et al., 2017; Mwakyoma, 2021) (Figure 3.5B). The final step in processing the 3D kerf mark models was to isolate the mark using the “extract area” ‘operator’ studiable.

3.6: 3D Data Measurement

Similar to data processing, the 3D measurement process followed Pante et al. (2017) protocol and was completed using the Sensomap® software. A total of 6 3D variables were measured including surface area (μm^2), volume (μm^3), maximum depth (μm), mean depth (μm), maximum length (μm), and maximum width (μm).

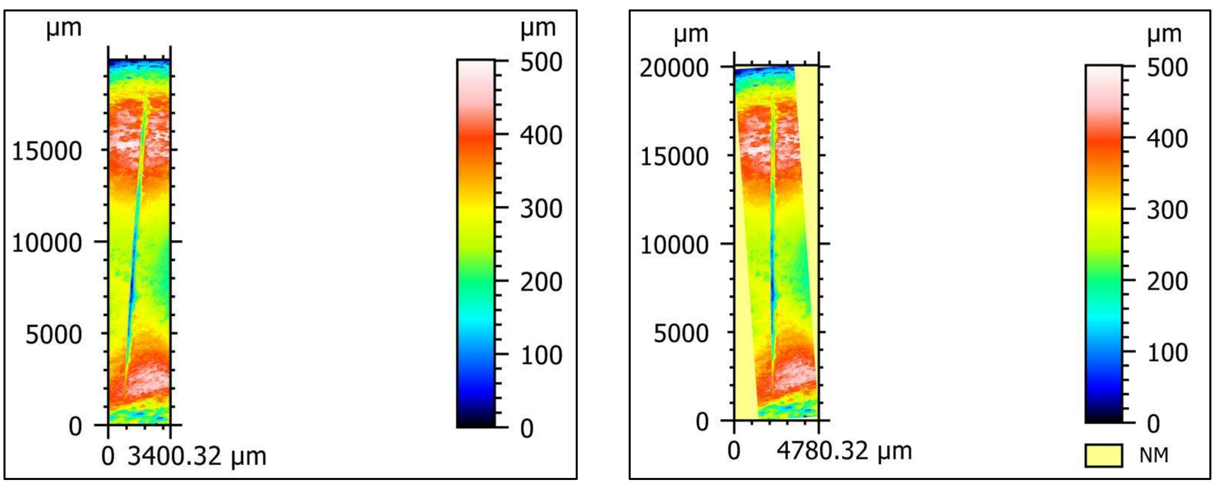

Figures 3.5A and 3.5B: Left image shows 3D kerf mark model (mark 12X3) after setting threshold. Right image shows same mark after being rotated to align perpendicular to the x-axis. Color scales (on right of images) indicate depth.

Surface area, volume, maximum depth, and mean depth were all recorded by using the “volume of a hole” function provided by the software. This function operates by allowing users to manually outline the boundaries of the kerf mark using a series of interconnected points

(Figure 3.6). Once the outline has been established, the function will then implement a least squares method to create a level plane for the kerf mark, estimating the pre-cut bone surface and allowing for three-dimensional volume measurements to be recorded (Pante et al., 2017).

Maximum length and width were recorded using the “distance” function which allows the user to manually measure the length and width with line segments (Figure 3.7). Maximum length was defined as the maximum distance from each end of the mark and was measured using multiple line segments if the mark was not straight. Maximum width was recorded perpendicular to the maximum length measurement and was taken along the widest portion of the entire mark.

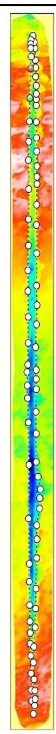

Parameters	Unit	Hole	Peak
Projected area	µm²	3283829	118225
Volume	µm³	461005997	4301208
Max. depth/height	µm	307.786	169.213
Mean depth/height	µm	140.387	36.3815

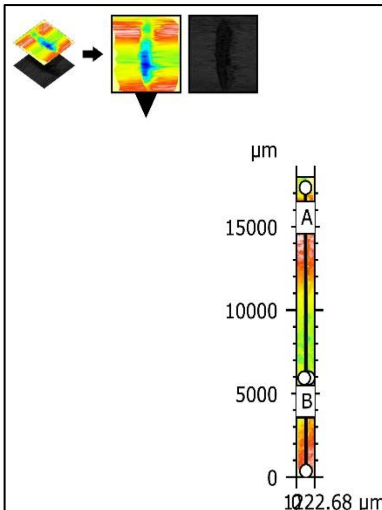

Distances	Unit	A	B
HDist	µm	16974.3	295.004

Figures 3.6 and 3.7: Figure 3.6 (left) depicts the “volume of a hole” function for mark 12X3. Table underneath image contains measurements for surface area, volume maximum depth, and mean depth. Figure 3.7 (right) depicts distance measurements for mark 12X3. Table underneath contains measurements for maximum length (A) and maximum width (B).

3.7: Profile Extraction and Measurement

Once again, following Pante et al. (2017) protocol, a 2D profile was extracted from the 3D kerf mark model using the “extract profile” ‘operator’ studiable. The profile was always taken from the lowest point in the mark as this is the easiest to identify, guarantees consistency, and reduces observer bias. A total of 6 more variables were measured from the resultant profile: these included maximum depth (µm), profile area (µm), maximum width (µm), roughness (Ra), opening angle (degrees), and floor radius (µm).

The “area of a hole” function with the “under the waterline” option was used to measure the maximum depth and profile area for each model (Figure 3.8). The “area of a hole” function operates by allowing the user to identify the leftmost and rightmost edges of the mark, while the “under the waterline” option fills in the mark to the lowermost edges of the kerf, eliminating mark shoulders from influencing the area and depth results.

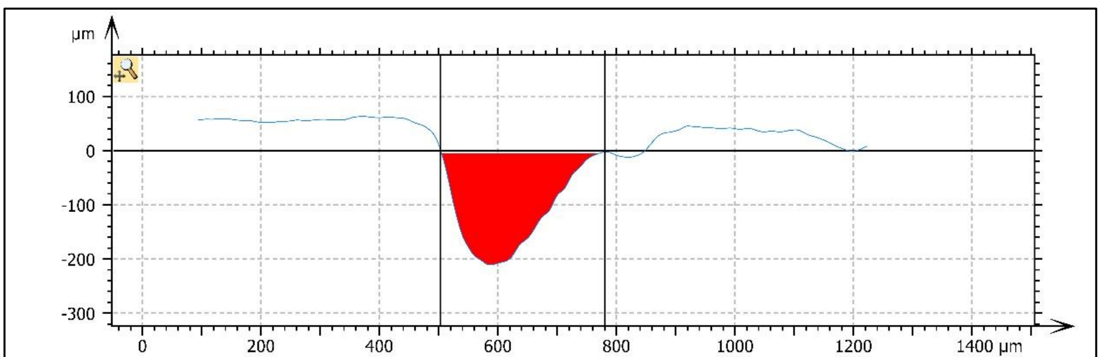

Parameters	Value	Unit
Maximum depth	208.256	µm
Area of the hole	32346.9	µm²

Figure 3.8: Example of “area of a hole” function with “under the waterline” option selected for mark 12X3. The table underneath studiable contains measurements for maximum depth and profile area.

The next four measured variables, maximum width, roughness, opening angle, and floor radius, were taken solely from the portion of the profile that reflects the kerf mark. To do so, the x-coordinates from both edges of the mark taken during the “area of a hole function” were isolated using the “extract area” ‘operator’ studiable, resulting in a new studiable only containing the cross-sectional profile of the kerf mark. Then, the length of this new profile provides the user with the maximum width measurement. Once this new studiable has been created, roughness was measured from the profile by using the “parameters table” function in the software. Roughness can be best defined as the mean deviation from the profile, quantifying the surface texture of the kef floor and walls (Pante et al., 2017; Keevil, 2018).

Finally, the “contour analysis” function was used to obtain the opening angle and floor radius measurements for each profile. Opening angle was measured by drawing two best fit lines – one from the first measured point to the deepest point of the profile and another from the last measured point to the deepest point of the profile – and calculating the angle between them (Figure 3.9). Then, floor radius was measured by drawing an arc between the first and last points of the profile, with the arc itself representing a best fit for all the points within the profile (Pante et al., 2017) (Figure 3.9).

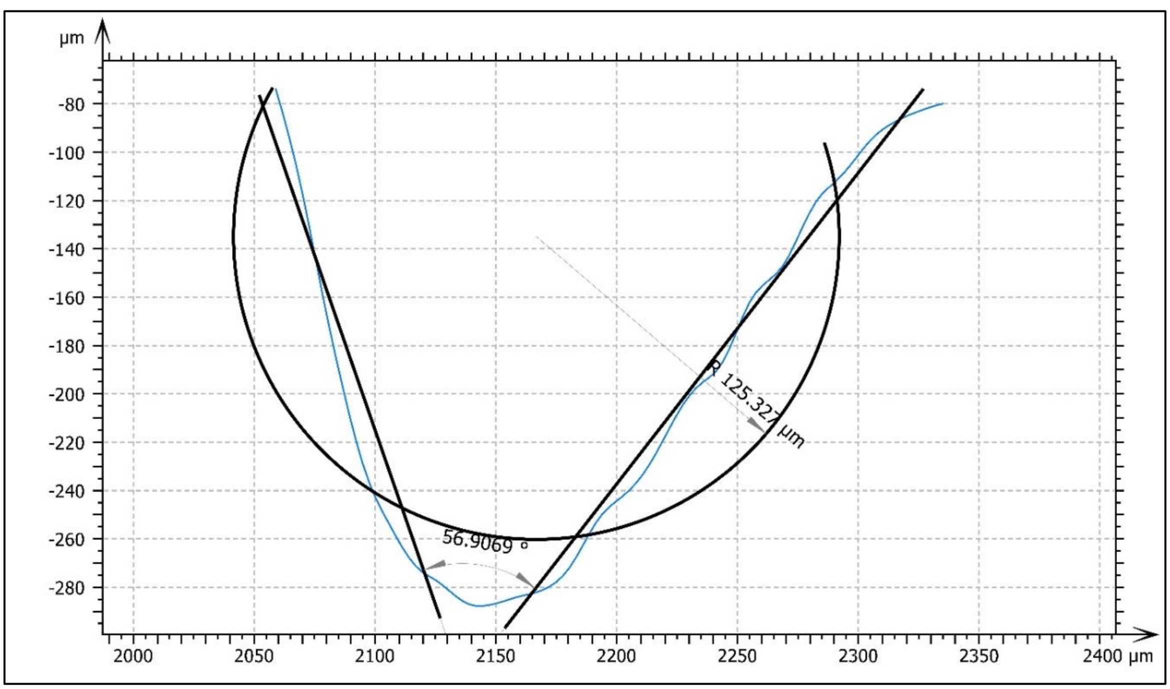

Figure 3.9: Example of opening angle and floor radius measurements for mark 12X3. The blue line represents the kerf mark profile.

3.8: Statistical Analysis

Statistical analyses were performed using PAST – Paleontological Statistics Software Package 4.03 (Hammer et al., 2001) and JMP Pro 15.0.0.

3.8.1: Data Exploration

Shapiro-Wilks tests were first used to determine whether each variable was normally distributed. These tests were conducted using the JMP Pro 15.0.0 software. Measurements indicating the presence of non-normal distributions were then normalized using Box-Cox transformations (Box and Cox, 1964). Optimal lambda values for these transformations were calculated using preprogrammed functions in the PAST 4.03 software.

Following data normalization, predictor screening analysis was conducted to assess the contribution of each variable on making proper mark identifications. Using the predictor screening test in JMP Pro 15.0.0, the software determines which variables most heavily influenced kerf mark classifications as well as which variables carried little weight on mark predictions. Subsequently, this information is beneficial because it helps the user decide which variables should be used when making kerf mark predictions, potentially strengthening the multivariate analyses used in this study and future studies.

3.8.2: Multivariate Analysis

Quadratic discriminate analysis (QDA) was used to assess whether the micromorphological variables for each kerf mark could be used to identify which knife produced the mark. Although linear discriminant analysis (LDA) was originally used in the Pante et al. (2017) protocol, QDA was currently used in this study because the data does not meet the assumptions of LDA, particularly the assumption that all covariances are equal (Büyüköztürk and Çokluk-Bökeoğlu, 2008). Equality of covariance was assessed using Box's M Test (1949) and revealed numerous variables exhibited unequal variance. Therefore, because this dataset violated some of the assumptions necessary for LDA, QDA was implemented as the assumptions for QDA are more relaxed.

QDA operates by modeling the likelihood of each knife type/class as a Gaussian distribution, then uses the posterior distributions to estimate the class for any given test point (Srivastava et al., 2007). However, for QDA to operate properly, all the data must follow a normal distribution (McLachlan, 2005). Therefore, all the data was normalized using Box-Cox transformations prior to analysis due to some variables not following a normal distribution. In total, four QDA models were created using JMP Pro 15.0.0.

The first two QDA models were conducted to compare each knife type (chef, boning, steak full blade, steak serrated portion, and bread) to one another. The first QDA model used every variable whereas the second QDA model only used variables deemed significant by predictive screening; the three least influential variables were excluded from the second model. The final two QDA models were structured to compare blade class (non-serrated, partially serrated, and fully serrated) against one another rather than knife type. Similar to the first two models, the third QDA model used all of the variables whereas the fourth only used significant variables, excluding the three least influential variables. Finally, in all four QDA models a 75% training and 25% testing split with specified priors proportional to occurrence was implemented to cross-validate the models' accuracy. However, marks on one bone will be more similar to marks on that same bone than marks on another, presenting a non-independence issue which could bias the QDA models. To alleviate this problem, training and testing sets were hand-picked so that all marks on an individual bone were either in the testing or training set. Therefore, all the testing set marks (35 in total) came from bones 2, 7, and 12.

CHAPTER FOUR: RESULTS

4.1: Qualitative Description of Results

While one of the principal goals of this research is to develop an easily replicable, quantifiable method for KMA, a brief, qualitative description of each kerf mark has been included to visualize some of the differences between marks made by the four knife types. When comparing marks made by the chef, boning, steak knife (full blade), steak knife (just serrated portion), and bread knife, there are relatively clear distinctions between the marks in terms of width and depth. For instance, marks made by the chef's knife tended to appear the thinnest and shallowest. Marks made by the boning knife were still quite shallow, but deeper than those made by the chef's knife (Figure 4.1A). Marks made by the steak knife – regardless of whether the full blade or just the serrated portion was used – were deeper and wider than any of the marks made by the two non-serrated knives, but marks made by the bread knife were consistently deeper and wider than marks made by any other knife type (Figure 4.1B).

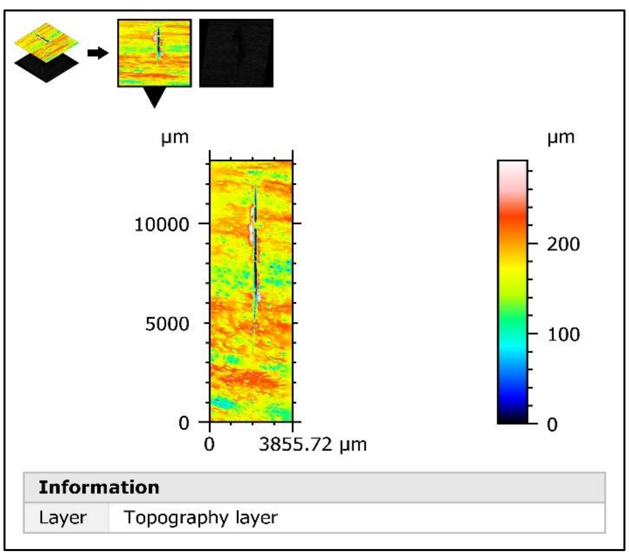

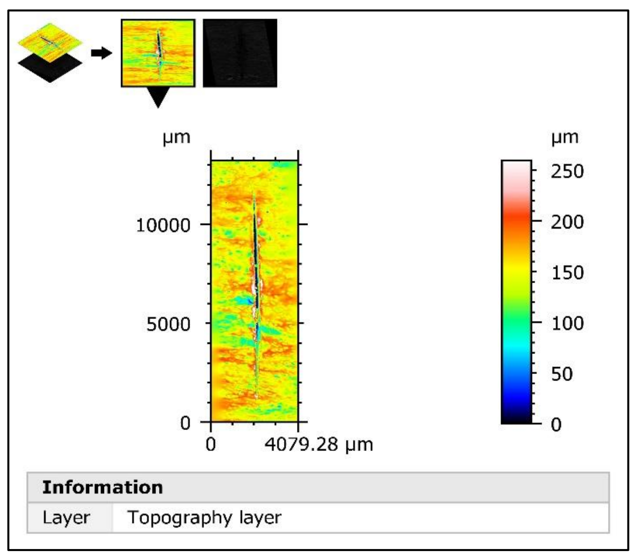

Figure 4.1A: Kerf marks made by chef's knife (left) and boning knife (right) from mark series 13Z. Note how chef's mark is quite shallow and thin whereas boning knife exhibits a slightly greater width and depth (depth denoted by scales to right of images).

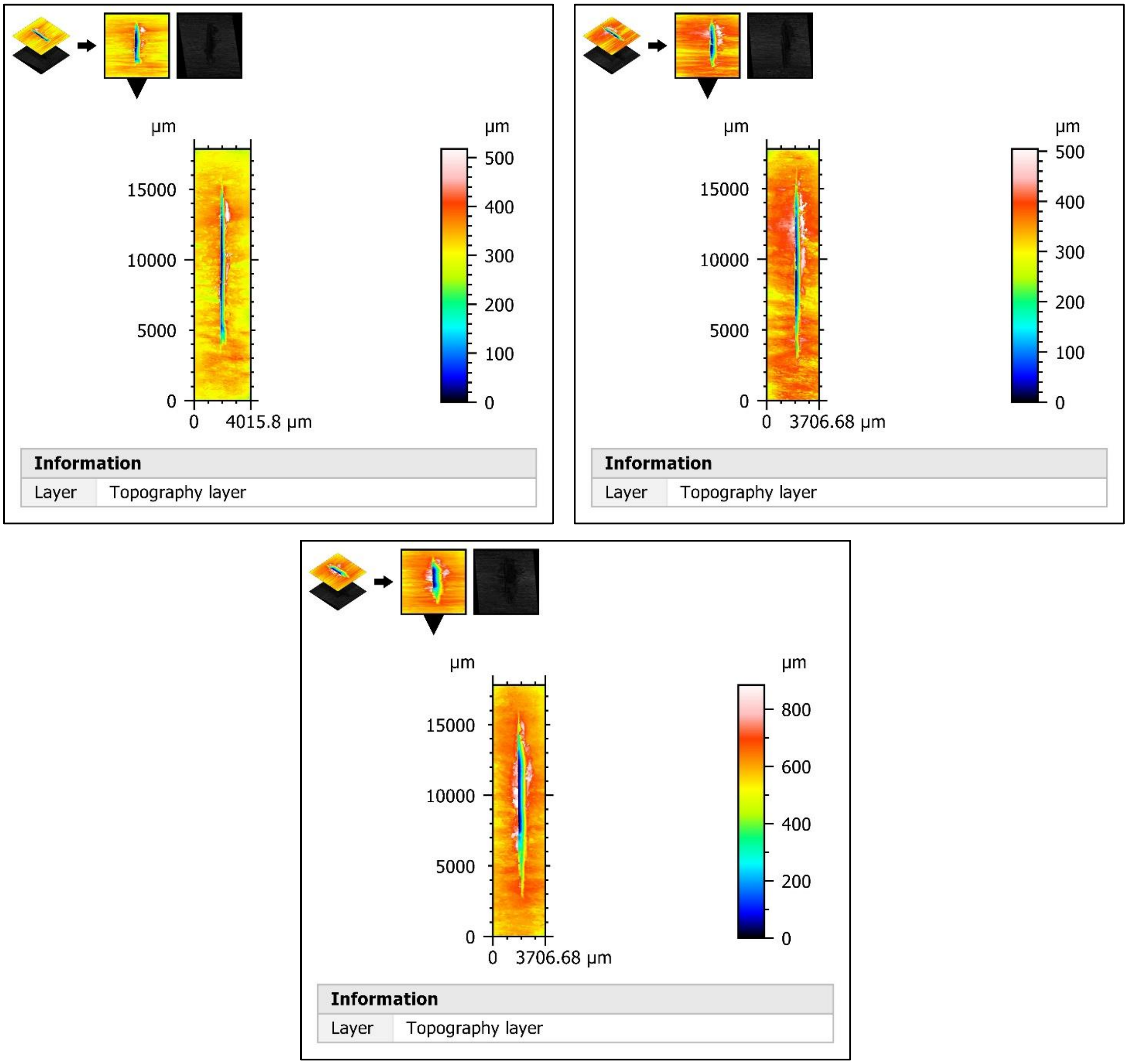

Figure 4.1B: Kerf marks made by the steak knife, full blade (top left), steak knife, serrated portion only (top right), and bread knife (bottom center) from mark series 13Z. Note how all three marks are deeper and wider than those in Figure 4.1A, but kerf marks made by the bread knife are the deepest and widest (depth denoted by scale to right of images).

Additionally, while similar trends relating to width and depth were also visible in profile view, the cross-sectional profiles of each mark exhibited additional diagnostic information. For the chef and boning knives, both kerf mark walls were angled inward towards the kerf floor (Figure 4.2A). However, when observing the mark profiles for kerf marks made by the steak knife and bread knife, the right kerf wall is angled towards the kerf floor at a more gradual angle whereas the left kerf wall drops more steeply towards the floor. More specifically, marks created by the bread knife exhibit an almost 90 degree angle from the left kerf wall to the kerf floor (Figure 4.2B). In other words, marks made by serrated and partially serrated blades have a steeper kerf wall on one side that is almost cliff-like whereas marks made by non-serrated blades angle inwards at both walls. Therefore, when generally assessing the kerf marks in this study qualitatively, there appear to be differences in terms of kerf width, depth, and profile morphology which could assist in mark identification. However, even though these qualitative identifiers may be useful, they cannot stand on their own as they are relatively subjective and must be assessed quantitatively to corroborate these distinctions and generate more replicable results.

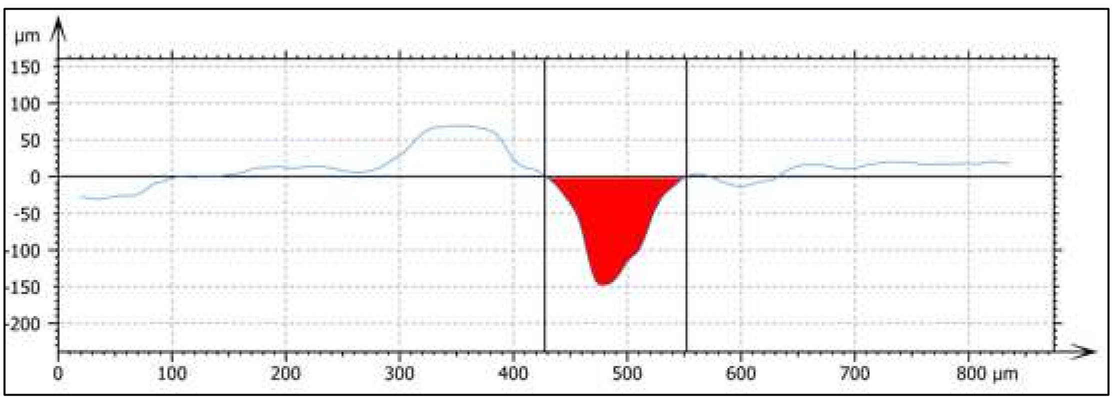

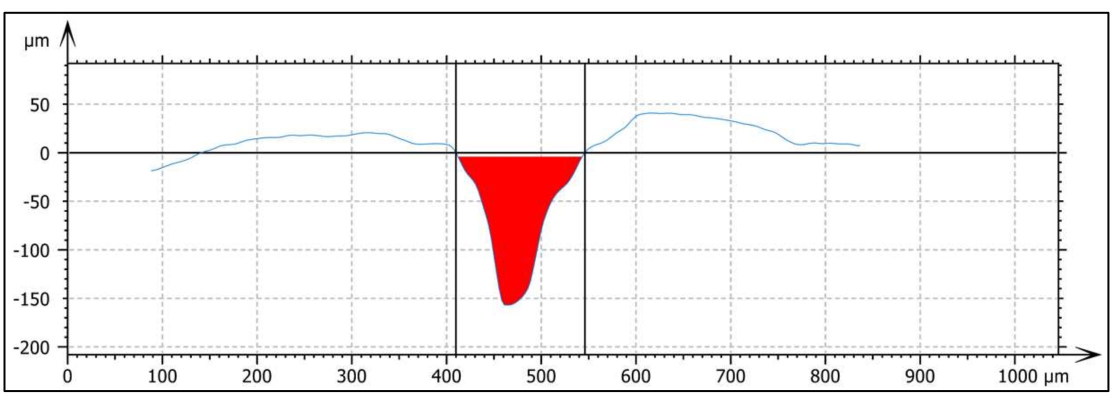

Figure 4.2A: Cross-sectional profiles of kerf marks made by a chef's knife (top) and boning knife (bottom) from mark series 13Z. Note how the left and right kerf walls angle in towards the kerf floor.

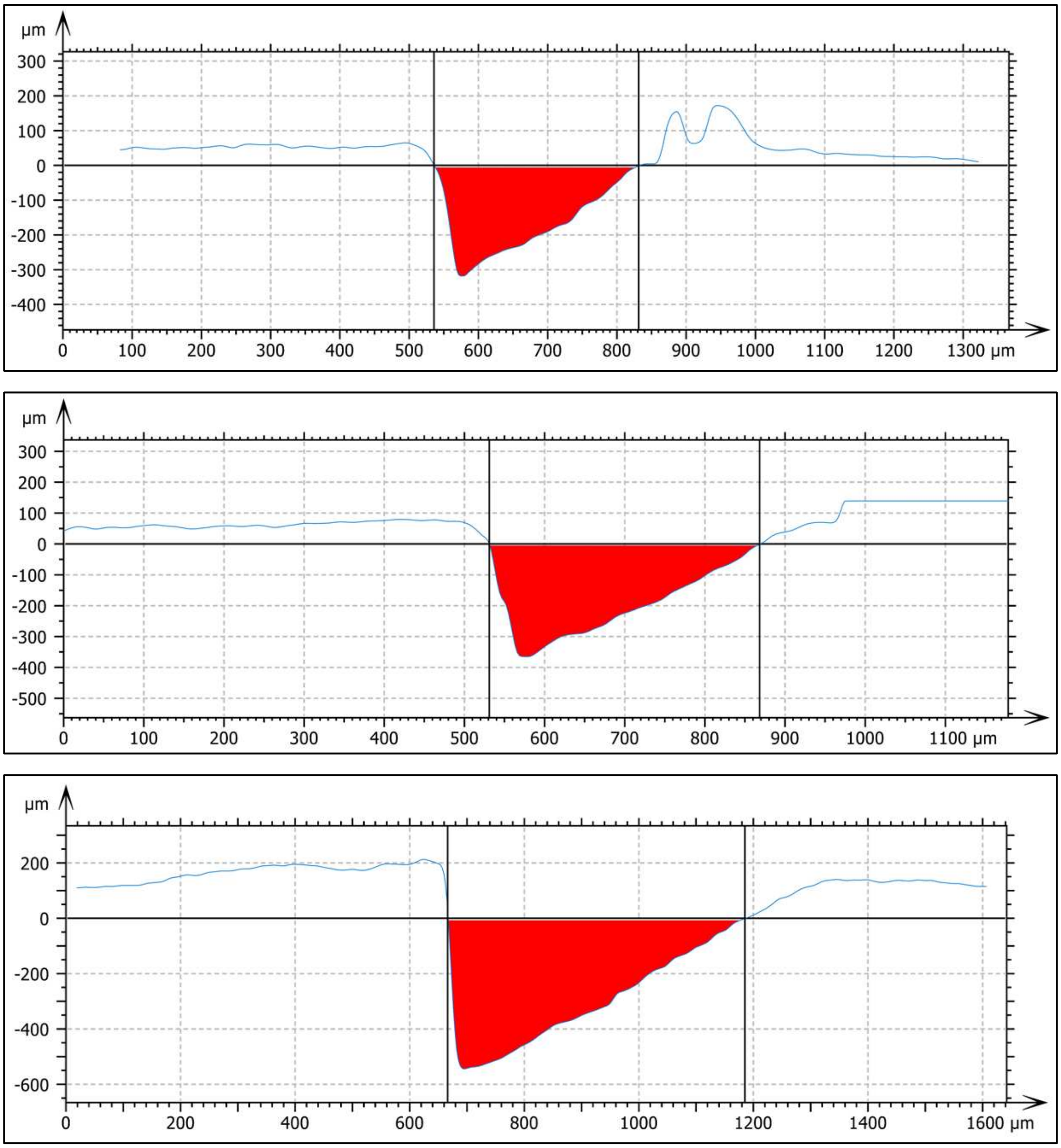

Figure 4.2B: Cross-sectional profiles of kerf marks made by a steak knife, full blade (top), steak knife, just serrated portion (middle), and bread knife (bottom) from mark series 13Z. Note how besides differences in width and depth, all three marks exhibit a sharper angle for the left kerf wall and a more gradual angle for the right kerf wall. This differs from marks made by non-serrated blades in Figure 4.2A which exhibit more gracile angles for both kerf walls.

4.2: Data Exploration Results

4.2.1: Normalization

Shapiro-Wilk tests as well as histograms were produced for each variable to assess normality (Appendix A and B). Results from these tests and distributions revealed numerous measurements were not normally distributed. Therefore, Box-Cox transformations were conducted on each variable to achieve as close to a normal distribution as possible so quadratic discriminant analysis (QDA) could be performed. The optimal lambda values for each transformation were calculated using Paleontological Statistics Software (PAST) (Table 4.1).

Table 4.1: Optimal Lambda Values Applied to Each Measurement for Box-Cox Transformations

Measurement	Optimal Lambda	Log Likelihood
Surface Area (3D)	0.38162	-2012.11
Volume (3D)	0.18434	-2766.90
Maximum Depth (3D)	0.26272	-713.21
Mean Depth (3D)	0..29343	-616.14
Maximum Length (3D)	1.02426	-1136.81
Maximum Width (3D)	0.15388	-704.79
Area (Profile)	0.12270	-1447.44
Maximum Depth (Profile)	0.27091	-682.13
Maximum Width (Profile)	0.25245	-680.39
Roughness (Profile)	0.26600	-109.69
Opening Angle (Profile)	-1.06743	-329.44
Floor Radius (Profile)	0.04817	-600.89

4.2.2: Descriptive Statistics

All comprehensive results including distribution, quantile range, and summary statistics for each variable in relation to knife type are attached at the end of this study (Appendix C). Similarly, box plots were generated to depict the distributions for each measurement in relation to knife type, revealing any outliers in the dataset.

4.2.3: Predictor Screening Analyses

In total, two predictor screening analyses were conducted before beginning multivariate analyses. These tests were done to explore the contribution of each measurement on mark estimation. When conducting predictor screening for each variable in relation to knife type, the last three variables were deemed to be the least influential: these three variables included maximum length (3D), opening angle (profile), and roughness (profile). The three most influential variables were surface area (3D), volume (3D), and area (profile) (Table 4.2). When conducting predictor screening for each variable in relation to blade class, the three least influential variables were once again maximum length (3D), roughness (profile), and opening angle (profile). The most influential measurements were volume (3D), surface area (3D), and area (profile) (Table 4.3).

Table 4.2: Predictor Screening for Measurements in Relation to Knife Type

Predictor	Contribution	Portion		Rank
Surface Area (3D)	38.5747	0.2379		1
Volume (3D)	26.2623	0.1619		2
Area (Profile)	25.5461	0.1575		3
Maximum Width (3D)	15.8572	0.0978		4
Maximum Depth (Profile)	14.3485	0.0885		5
Floor Radius (Profile)	13.4380	0.0829		6
Maximum Depth (3D)	10.8768	0.0671		7
Mean Depth (3D)	7.2961	0.0450		8
Maximum Width (Profile)	6.5958	0.0407		9
Maximum Length (3D)	1.7429	0.0107		10
Opening Angle (Profile)	1.0032	0.0062		11
Roughness (Profile)	0.6255	0.0039		12

Table 4.3: Predictor Screening for Measurements in Relation to Blade Class

Predictor	Contribution	Portion		Rank
Volume (3D)	32.7805	0.2263		1
Surface Area (3D)	31.5797	0.2180		2
Area (Profile)	17.0415	0.1176		3
Floor Radius (Profile)	15.5792	0.1075		4
Maximum Depth (Profile)	14.4711	0.0999		5
Maximum Width (3D)	10.9486	0.0756		6
Maximum Depth (3D)	9.9476	0.0687		7
Maximum Width (Profile)	5.5554	0.0383		8
Mean Depth (3D)	5.3371	0.0368		9
Maximum Length (3D)	0.8358	0.0058		10
Roughness (Profile)	0.4523	0.0031		11
Opening Angle (Profile)	0.3304	0.0023		12

4.3: Multivariate Analysis: Quadratic Discriminant Analysis (QDA)

In total, 4 QDA models were constructed using JMP Pro 15.0.0 to test whether various, quantifiable, micromorphological measurements could be used to discriminate between kerf marks made by different knife types/classes. Two models were created to test knife type, with one model using all the variables while the other model only used variables deemed influential by predictor screening; maximum length (3D), opening angle (profile), and roughness (profile) were considered the least influential and thus removed for this second QDA model (Table 4.2). Two additional models were also generated to test blade class, with one model using all the variables and the other using variables deemed useful by predictor screening; the least influential variables were once again maximum length (3D), roughness (profile), and opening angle (profile) (Table 4.3).

Furthermore, since there were two variables which measured maximum depth – one from the 3D scan and one from the cross-sectional profile – using both variables in the QDA models could potentially bias the model due to the use of redundant variables. Therefore, since the 3D measurement for maximum depth was deemed less influential by predictor screening, this measurement was omitted from all 4 QDA models to reduce any biases in the models. In the following sections, the results from each of the 4 QDA models are presented, including the accuracy percentages and discriminant scores for the testing datasets. Discriminant scores for all the training sets have also been attached at the end of this study (Appendix D-G). Accuracy percentages were presented as they indicate how effective the models are at classifying new data in the testing set that was not present in the original dataset (Molinaro et al., 2005).

4.3.1: QDA for Knife Type Including All Variables

When using all the variables and testing knife type (chef, boning, steak full blade, steak serrated portion, bread), correct classifications in the testing set were made 51.43% of the time (Table 4.4). Marks made by the bread knife had the highest classification accuracy in the model, with these marks being accurately identified 85.7% of the time. However, marks made by the boning and chef's knives were commonly misclassified as one another, with accurate identifications only being made for these two knife types in the testing set 42.9% of the time. Similarly, marks made by the full steak blade and those made by just the steak knife's serrated portion were misidentified as one another 50% of the time in the testing set (table 4.6).

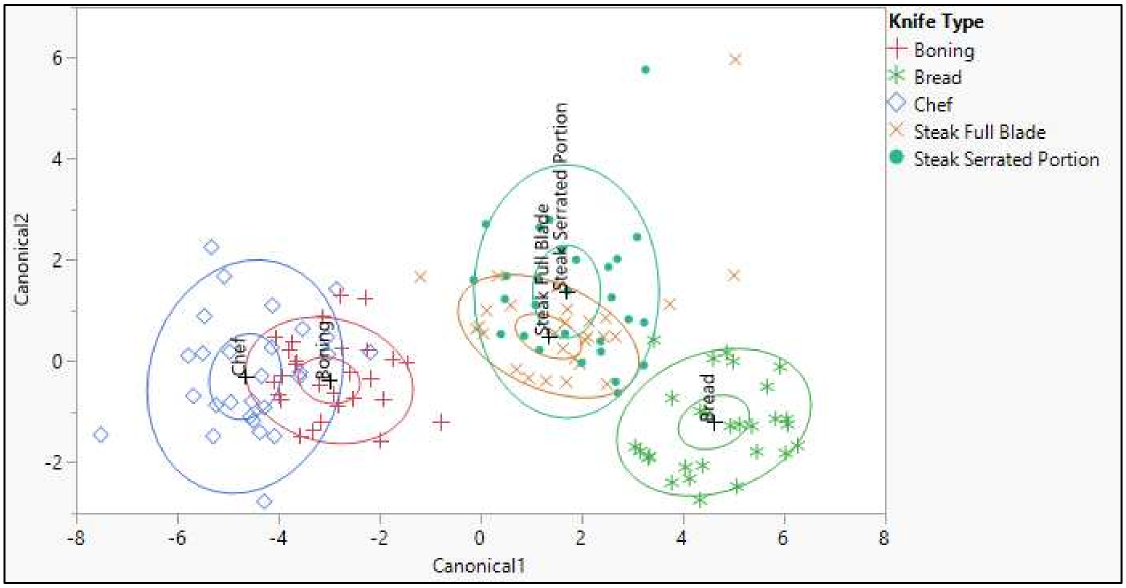

Figure 4.3: QDA Canonical Plot showing classifications and distributions of kerf marks in relation to knife type when using all measurements.

Table 4.4: Score Summaries for Knife Type QDA Model Using All Variables

Source	Count	Number Misclassified	Percent Misclassified	Entropy RSquare	-2LogLikelihood
Training	105	7	6.6667	0.9394	20.4753
Testing	35	17	48.5714	-2.4822	

Table 4.5: Confusion Matrix for Knife Type QDA Model Using All Variables (Training Set)

Actual	Predicted Count				
Knife Type	**Boning**	**Bread**	**Chef**	**Steak Full Blade**	**Steak Serrated Portion**
Boning	19	0	2	0	0
Bread	0	21	0	0	0
Chef	1	0	20	0	0
Steak Full Blade	0	0	0	20	1
Steak Serrated Portion	0	0	0	3	18

Table 4.6: Confusion Matrix for Knife Type QDA Model Using All Variables (Testing Set)

Actual	Predicted Count				
Knife Type	**Boning**	**Bread**	**Chef**	**Steak Full Blade**	**Steak Serrated Portion**
Boning	3	0	4	0	0
Bread	0	6	0	0	1
Chef	4	0	3	0	0
Steak Full Blade	0	1	0	2	4
Steak Serrated Portion	0	0	0	3	4

Table 4.7: Discriminant Scores for Knife Type QDA Model Using All Variables (Testing Set)

Row	Actual	Predicted	Prob(Pred)	Others
1	Boning	Chef	0.9711	
2	Boning	Boning	0.6342	Chef 0.37
3	Boning	Boning	0.9661	
4	Boning	Chef	1.0000	
5	Boning	Boning	0.7587	Chef 0.24
6	Boning	Chef	0.9999	
7	Boning	Chef	0.5410	
8	Bread	Bread	0.9996	
9	Bread	Bread	1.0000	
10	Bread	Bread	1.0000	
11	Bread	Bread	1.0000	
12	Bread	Bread	1.0000	
13	Bread	Bread	0.8792	Steak Serrated Portion 0.12
14	Bread	Steak Serrated Portion	0.9988	
15	Chef	Boning	0.9501	
16	Chef	Chef	0.9855	
17	Chef	Boning	0.9959	
18	Chef	Chef	0.9977	
19	Chef	Chef	0.9977	
20	Chef	Boning	0.9912	
21	Chef	Boning	1.0000	
22	Steak Full Blade	Steak Serrated Portion	0.6049	
23	Steak Full Blade	Steak Serrated Portion	0.9746	
24	Steak Full Blade	Steak Full Blade	0.9638	
25	Steak Full Blade	Steak Serrated Portion	1.0000	
26	Steak Full Blade	Bread	0.9956	
27	Steak Full Blade	Steak Serrated Portion	0.9955	
28	Steak Full Blade	Steak Full Blade	0.5450	Steak Serrated Portion 0.45
29	Steak Serrated Portion	Steak Full Blade	0.9863	
30	Steak Serrated Portion	Steak Serrated Portion	1.0000	
31	Steak Serrated Portion	Steak Serrated Portion	0.9510	
32	Steak Serrated Portion	Steak Serrated Portion	0.9900	
33	Steak Serrated Portion	Steak Serrated Portion	0.9959	
34	Steak Serrated Portion	Steak Full Blade	0.8760	
35	Steak Serrated Portion	Steak Full Blade	0.9397	

4.3.2: QDA for Knife Type Excluding Non-Influential Variables

When excluding the three least influential variables as stated by predictor screening, the QDA model worsens, with accurate identifications only being made 45.71% of the time (Table 4.8). Marks made by the bread knife once again had the most accurate classification rate of

85.7%. Kerf marks made by the chef and boning knife were misidentified as one another at a higher rate than the first QDA model, with accurate identifications for both knife types only being made 21.4% of the time. Likewise, marks made by the full steak knife blade and just the serrated portion of the steak knife were misclassified as one another 35.7% of the time, with correct classifications only being made 50% of the time (Table 4.10).

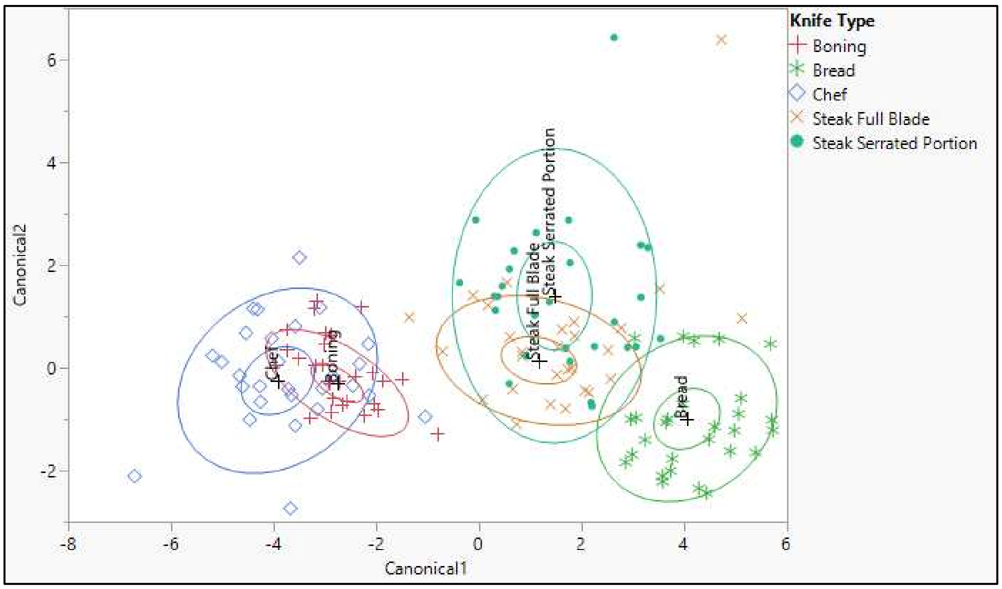

Figure 4.4: QDA Canonical Plot showing classification and distribution of kerf marks in relation to knife type when only using influential measurements.

Table 4.8: Score Summaries for Knife Type QDA Model Using Influential Variables

Source	Count	Number Misclassified	Percent Misclassified	Entropy RSquare	-2LogLikelihood
Training	105	10	9.5238	0.8566	48.4587
Testing	35	19	54.2857	-0.7437	

Table 4.9: Confusion Matrix for Knife Type QDA Model Using Influential Variables (Training Set)

Actual	Predicted Count				
Knife Type	Boning	Bread	Chef	Steak Full Blade	Steak Serrated Portion
Boning	19	0	2	0	0
Bread	0	21	0	0	0
Chef	2	0	19	0	0
Steak Full Blade	0	0	0	19	2
Steak Serrated Portion	0	0	0	4	17

Table 4.10: Confusion Matrix for Knife Type QDA Model Using Influential Variables (Testing Set)

Actual	Predicted Count				
Knife Type	**Boning**	**Bread**	**Chef**	**Steak Full Blade**	**Steak Serrated Portion**
Boning	2	0	5	0	0
Bread	0	6	0	0	1
Chef	6	0	1	0	0
Steak Full Blade	0	2	0	3	2
Steak Serrated Portion	0	0	0	3	4

Table 4.11: Discriminant Scores for Knife Type QDA Model Using Influential Variables (Testing Set)

Row	Actual	Predicted	Prob(Pred)	Others
1	Boning	Chef	0.6296	
2	Boning	Chef	0.7841	
3	Boning	Boning	0.8159	Chef 0.18
4	Boning	Chef	0.5499	
5	Boning	Boning	0.8364	Chef 0.16
6	Boning	Chef	0.9993	
7	Boning	Chef	0.9496	
8	Bread	Bread	0.9996	
9	Bread	Bread	0.9958	
10	Bread	Bread	0.9999	
11	Bread	Bread	0.9993	
12	Bread	Bread	0.9983	
13	Bread	Bread	0.9999	
14	Bread	Steak Serrated Portion	0.9310	
15	Chef	Boning	0.8587	
16	Chef	Boning	0.5815	
17	Chef	Boning	0.9977	
18	Chef	Chef	0.9966	
19	Chef	Boning	0.9961	
20	Chef	Boning	0.9295	
21	Chef	Boning	0.9903	
22	Steak Full Blade	Steak Full Blade	0.9216	
23	Steak Full Blade	Steak Full Blade	0.5645	Steak Serrated Portion 0.44
24	Steak Full Blade	Steak Serrated Portion	0.5459	Bread 0.11
25	Steak Full Blade	Steak Serrated Portion	0.9386	
26	Steak Full Blade	Bread	0.9995	
27	Steak Full Blade	Bread	0.9153	
28	Steak Full Blade	Steak Full Blade	0.6690	Steak Serrated Portion 0.33
29	Steak Serrated Portion	Steak Full Blade	0.7876	
30	Steak Serrated Portion	Steak Serrated Portion	0.9994	
31	Steak Serrated Portion	Steak Serrated Portion	0.9906	
32	Steak Serrated Portion	Steak Serrated Portion	0.9877	

Row	Actual	Predicted	Prob(Pred)	Others
33	Steak Serrated Portion	Steak Serrated Portion	0.9173	
34	Steak Serrated Portion	Steak Full Blade	0.7987	
35	Steak Serrated Portion	Steak Full Blade	0.7041	Bread 0.19

4.3.3: QDA for Blade Class Including All Variables

When using all the variables and testing blade class (non-serrated, partially serrated, serrated), correct classifications were made at much higher rates in the testing set at 97.14% (Table 4.12). In other words, this model was much more accurate as there was only one misclassification in the testing set, with one kerf mark produced by a serrated knife being misclassified as partially serrated (table 4.14).

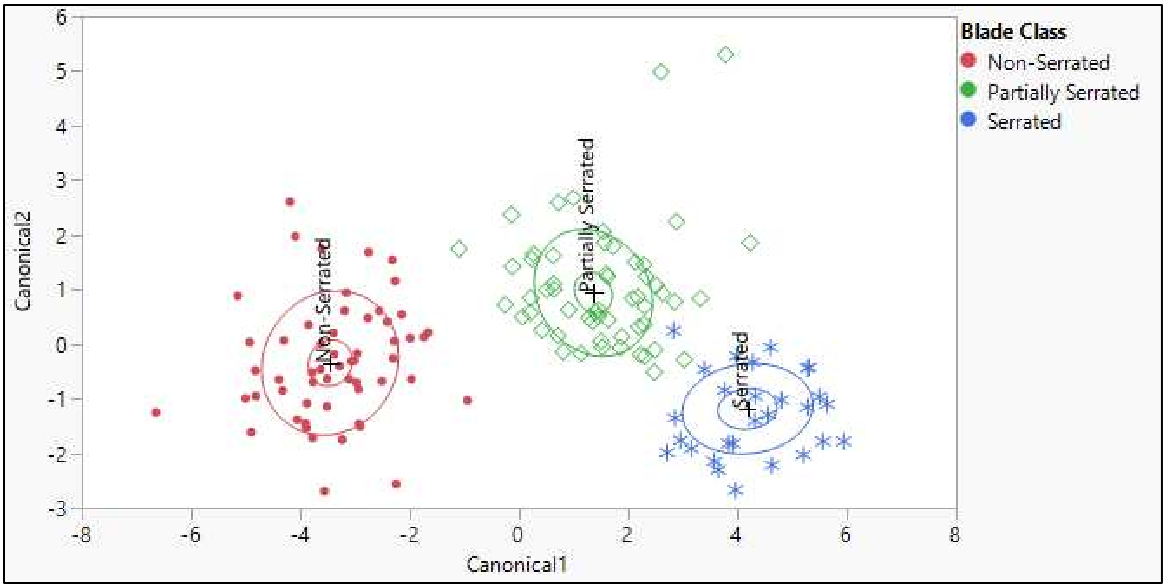

Figure 4.5: QDA Canonical Plot showing classification and distribution of kerf marks in relation to blade class when using all measurements.

Table 4.12: Score Summaries for Blade Class QDA Model Using All Variables

Source	Count	Number Misclassified	Percent Misclassified	Entropy RSquare	-2LogLikelihood
Training	105	0	0.00000	0.9995	0.0913
Validation	35	1	2.8571	0.8574	

Table 4.13: Confusion Matrix for Blade Class QDA Model Using All Variables (Training Set)

Actual	Predicted Count		
Blade Class	**Non-Serrated**	**Partially Serrated**	**Serrated**
Non-Serrated	42	0	0
Partially Serrated	0	42	0
Serrated	0	0	21

Table 4.14: Confusion Matrix for Blade Class QDA Model Using All Variables (Testing Set)

Actual	Predicted Count		
Blade Class	**Non-Serrated**	**Partially Serrated**	**Serrated**
Non-Serrated	14	0	0
Partially Serrated	0	14	0
Serrated	0	1	6

Table 4.15: Discriminant Scores for Blade Class QDA Model Using All Variables (Testing Set)

Row	Actual	Predicted	Prob(Pred)	Others
1	Non-Serrated	Non-Serrated	1.0000	
2	Non-Serrated	Non-Serrated	1.0000	
3	Non-Serrated	Non-Serrated	0.9971	
4	Non-Serrated	Non-Serrated	1.0000	
5	Non-Serrated	Non-Serrated	1.0000	
6	Non-Serrated	Non-Serrated	1.0000	
7	Non-Serrated	Non-Serrated	1.0000	
8	Serrated	Serrated	0.9964	
9	Serrated	Serrated	0.9999	
10	Serrated	Serrated	0.9998	
11	Serrated	Serrated	1.0000	
12	Serrated	Serrated	0.9998	
13	Serrated	Serrated	0.9273	
14	Serrated	Partially Serrated	0.9944	
15	Non-Serrated	Non-Serrated	1.0000	
16	Non-Serrated	Non-Serrated	1.0000	
17	Non-Serrated	Non-Serrated	1.0000	
18	Non-Serrated	Non-Serrated	1.0000	
19	Non-Serrated	Non-Serrated	1.0000	
20	Non-Serrated	Non-Serrated	1.0000	
21	Non-Serrated	Non-Serrated	1.0000	
22	Partially Serrated	Partially Serrated	1.0000	
23	Partially Serrated	Partially Serrated	1.0000	
24	Partially Serrated	Partially Serrated	1.0000	
25	Partially Serrated	Partially Serrated	0.9991	

Row	Actual	Predicted	Prob(Pred)	Others
26	Partially Serrated	Partially Serrated	0.9961	
27	Partially Serrated	Partially Serrated	1.0000	
28	Partially Serrated	Partially Serrated	0.9999	
29	Partially Serrated	Partially Serrated	1.0000	
30	Partially Serrated	Partially Serrated	1.0000	
31	Partially Serrated	Partially Serrated	1.0000	
32	Partially Serrated	Partially Serrated	1.0000	
33	Partially Serrated	Partially Serrated	1.0000	
34	Partially Serrated	Partially Serrated	1.0000	
35	Partially Serrated	Partially Serrated	0.9994	

4.3.4: QDA for Blade Class Excluding Non-Influential Variables

When using only the influential variables as dictated by predictor screening and testing blade class, the QDA model once again worsens, but less severely with accurate identifications being made 91% of the time (Table 4.16). While all non-serrated kerf marks were identified accurately by the QDA model, there were a total of 3 misclassifications wherein partially serrated and fully serrated marks were misclassified as one another 14.2% of the time (Table 4.18).

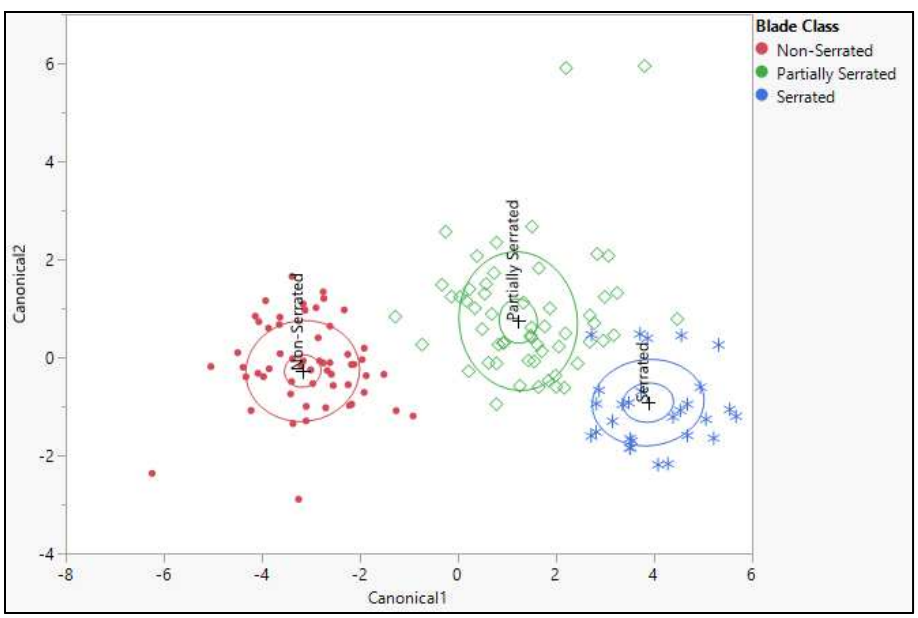

Figure 4.6: QDA Canonical Plot showing classification and distribution of kerf marks in relation to blade class when only using influential measurements.

Table 4.16: Score Summaries for Blade Class QDA Model Using Influential Variables

Source	Count	Number Misclassified	Percent Misclassified	Entropy RSquare	-2LogLikelihood
Training	105	0	0.0000	0.9902	2.1612
Validation	35	3	8.5714	0.6774	

Table 4.17: Confusion Matrix for Blade Class QDA Model Using Influential Variables (Training Set)

Actual	Predicted Count		
Blade Class	Non-Serrated	Partially Serrated	Serrated
Non-Serrated	42	0	0
Partially Serrated	0	42	0
Serrated	0	0	21

Table 4.18: Confusion Matrix for Blade Class QDA Model Using Influential Variables (Testing Set)

Actual	Predicted Count		
Blade Class	Non-Serrated	Partially Serrated	Serrated
Non-Serrated	14	0	0
Partially Serrated	0	12	2
Serrated	0	1	6

Table 4.19: Discriminant Scores for Blade Class QDA Model Using Influential Variables (Testing Set)

Row	Actual	Predicted	Prob(Pred)	Others
1	Non-Serrated	Non-Serrated	0.9999	
2	Non-Serrated	Non-Serrated	0.9997	
3	Non-Serrated	Non-Serrated	0.9942	
4	Non-Serrated	Non-Serrated	1.0000	
5	Non-Serrated	Non-Serrated	0.9997	
6	Non-Serrated	Non-Serrated	0.9994	
7	Non-Serrated	Non-Serrated	0.9999	
8	Serrated	Serrated	0.9993	
9	Serrated	Serrated	0.9969	
10	Serrated	Serrated	0.9999	
11	Serrated	Serrated	0.9993	
12	Serrated	Serrated	0.9989	
13	Serrated	Serrated	0.9999	
14	Serrated	Partially Serrated	0.6466	
15	Non-Serrated	Non-Serrated	1.0000	
16	Non-Serrated	Non-Serrated	0.9997	
17	Non-Serrated	Non-Serrated	0.9979	
18	Non-Serrated	Non-Serrated	0.9998	
19	Non-Serrated	Non-Serrated	0.9919	

Row	Actual	Predicted	Prob(Pred)	Others
20	Non-Serrated	Non-Serrated	0.9980	
21	Non-Serrated	Non-Serrated	1.0000	
22	Partially Serrated	Partially Serrated	1.0000	
23	Partially Serrated	Partially Serrated	1.0000	
24	Partially Serrated	Partially Serrated	0.9617	
25	Partially Serrated	Partially Serrated	0.7393	Serrated 0.26
26	Partially Serrated	Serrated	0.9997	
27	Partially Serrated	Serrated	0.8460	
28	Partially Serrated	Partially Serrated	0.9999	
29	Partially Serrated	Partially Serrated	0.9998	
30	Partially Serrated	Partially Serrated	1.0000	
31	Partially Serrated	Partially Serrated	1.0000	
32	Partially Serrated	Partially Serrated	1.0000	
33	Partially Serrated	Partially Serrated	0.7919	Serrated 0.21
34	Partially Serrated	Partially Serrated	1.0000	
35	Partially Serrated	Partially Serrated	0.7077	Serrated 0.29

CHAPTER FIVE: DISCUSSION

5.1: Identifying Knife Type and Blade Class from Kerf Mark Micromorphology

The primary objective of this research was to test whether variations in 3D micromorphological measurements can be used to identify the knife type or blade class responsible for producing certain kerf marks. This research suggests knife type cannot currently be classified from kerf marks, but it is possible to identify blade class. The following sections will further detail how these distinctions were made and their importance for KMA.

5.1.1: Qualitative Trends for Mark Identification

While not the main focus of this study, qualitative assessments of mark morphology yielded some interesting trends in relation to blade class. Generally, the larger and more serrated the knife blade, the deeper and wider the cut. However, profile shape exhibited more diagnostic trends for differentiating serrated from non-serrated marks. Non-serrated blades – the chef and boning knives – displayed both kerf walls being angled inwards towards the kerf floor whereas serrated and partially serrated blades – the steak and bread knifes – had a steep left kerf wall and a more gradually angled right kerf wall (Figures 4.1A and 4.1B). This trend has been seen previously in research conducted by Thompson and Inglis (2009) wherein they realized kerf marks made by non-serrated blades produced a “y-shaped” pattern whereas serrated blades created a “t-shaped” pattern (Figure 5.1). While Thompson and Inglis (2009) found these patterns by stabbing directly into the cortical bone surface, the stab wounds still were characteristic of blade profile and matched marks made by the non-serrated, partially serrated and fully serrated blades in this study. Since the cross-sectional profiles in their study and this study corroborate one another, it can be argued profile shape helps with identifying serrated from non-serrated blades, but this cannot be used to differentiate serrated from partially serrated blades.

		Shape	Length (mm)	Width (mm)	Kerf damage	Fragmentation / fractures
Serrated Blade	**Rib**		3.43	0.88	3	Ruffling and some fragmentation of kerf
	Radius epiphysis		5.53	1.02	3	Kerf gouged out to the left of the mark
	Radius diaphysis		1.81	0.65	2	—
	Scapula		18.54	0.73	2	Fragmentation of other side
	Vertebra		3.65	0.72	2	Small fractures at top causing Y shape
	Carpal		1.23	0.50	3	Fracture of the mark's tail and fragmentation of kerf
	Mean		5.94	0.75	2.5	—
Non-serrated blade	**Rib**		3.87	0.66	2	2 fractures either side of top giving a T shape. 1 fracture on bottom left of tail
	Radius epiphysis		2.53	0.88	3	Kerf gouged out to the left of the mark
	Radius diaphysis		1.54	0.73	1	—
	Scapula		9.09	1.38	3	Ruffling of kerf and several small fractures. Fragmentation of back
	Vertebra		2.71	0.78	3	Small fragmentation of kerf
	Carpal		3.14	0.60	2	—
	Mean		3.81	0.84	2.3	—

Figure 5.1: Stab mark wounds from serrated and non-serrated blades when viewed through low-power microscopy by Thompson and Inglis (2009). Note how the serrated blades leave a "t-shaped" profile, matching those in this study where one kerf wall is steep whereas the other is more gradual. Similarly, the non-serrated blades leave behind a "y-shaped" profile where each kerf wall is angled in towards the kerf floor, matching kerf mark profiles made by non-serrated blades in this study.

However, it could also be argued that this finding based on profile shapes is more informative about knife edge than blade class. For instance, in this study both non-serrated blades were double edged meaning they were angled on both the left and right sides. On the other hand, the partially serrated and fully serrated blades were only angled on the right side where the serrations are present. The left side of these knives have no edge, instead dropping down at an almost 90-degree angle (Figure 5.2). These patterns – double edged vs. single edged – are also consistent with the kerf mark cross-sectional profiles in this study, meaning profile shape may be more diagnostic of knife edge than knife type of class. Nevertheless, this is still important information as it can tell forensic analysts whether they have a single- or double-edged knife and if single-edged, which side is sharpened helping narrow down the characteristics of the knife used.

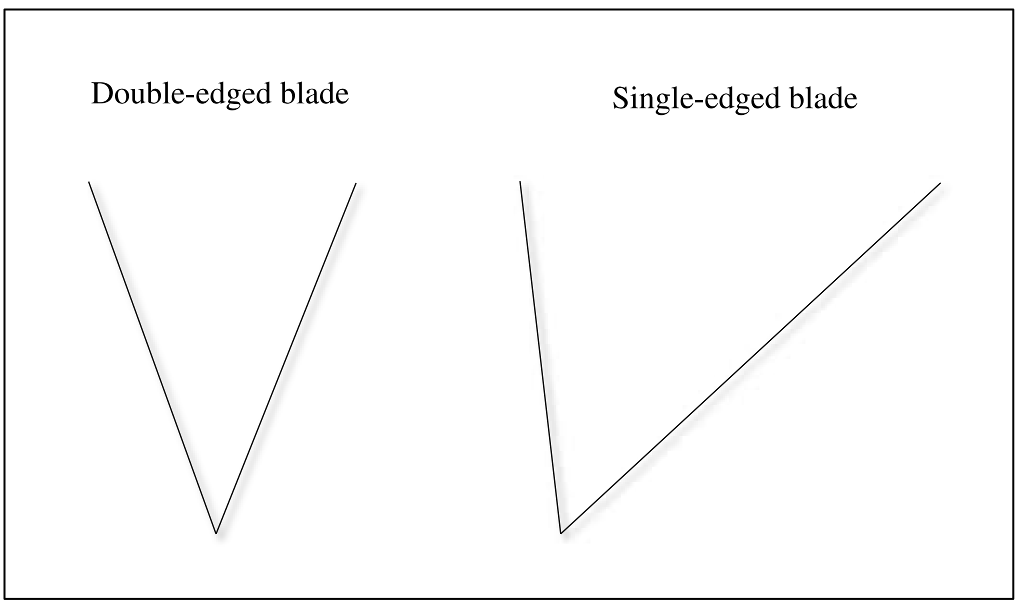

Figure 5.2: Diagram depicting knife edges. In this research, the non-serrated blades – chef and boning knives – were defined as double-edged whereas partially and fully serrated blades – steak and bread knives – were defined as single-edged. Note now these types of blades roughly match the kerf mark profiles in Figures 4.1A and 4.1B.

5.1.2: Trends and Accuracy of Knife Type Identifications

In short, knife type could not be accurately surmised from the data in this study. When using the more accurate QDA model that implemented all measurements, accurate identifications were only made 51.43% of the time (Table 4.4). In canonical space, marks made by the chef and boning knives severely overlapped with one another while marks made by the steak knife – full blade and just serrated portion – overlapped as well (Figure 4.3). Similarly, in the testing set marks made by the chef and boning knifes were misclassified as one another 57% of the time while marks made by the steak knife – full blade and just serrated portion – were misclassified as one another 50% of the time (Table 4.6).

Kerf marks produced by non-serrated blades were likely indiscernible from one another because both knives were made by the company, Chicago Cutlery. Because of this, the production process for the blades was likely synonymous for both knives, meaning resultant mark morphology would be increasingly similar. Thus, there is the possibility that future studies of non-serrated knives could exhibit more diagnostic differences if not produced by the same company. Additionally, kerf marks created by just the serrated portion of the steak knife as well as the full blade were likely comparable to one another because the serrated portion was always the final segment of the blade cutting the bone, overshadowing any influence the non-serrated portion had on the marks' morphology. In other words, this QDA model does not effectively discriminate mark classifications based on knife type because there is too much overlap between certain knives. In turn, this means the level of specificity necessary to identify a singular knife cannot be achieved using this model, matching findings of previous KMAs (Bartelink et al., 2001; Thompson and Inglis, 2009; Love et al., 2012; Tegtmeyer, 2012; Tennick, 2012; Crowder et al., 2013; Sandras et al., 2018).

5.1.3: Trends and Accuracy of Blade Class Identifications

Due to the severe overlap in mark identifications made for knife type, blade class was also tested and yielded more promising results. When comparing marks made by non-serrated, partially serrated and fully serrated blades, there was minimal to no overlap between blade classes in the canonical plot (Figure 4.5). Moreover, correct classifications were made in the testing set 97.14% of the time, with only one serrated mark being misidentified as partially serrated; the error rate for this QDA was 2.86% (Table 4.14). Hence, blade class was consistently classified correctly resulting in the identification of kerf marks made not only by serrated and non-serrated blades but also partially serrated blades.

Previous KMAs frequently struggled with identifying kerf marks made by partially serrated vs. fully serrated blades, with conclusions solely differentiating serrated marks from non-serrated marks (Thompson and Inglis, 2009; Tegtmeyer, 2012; Crowder et al., 2013; Feldman, 2015; Sandras et al., 2018). However, because the technology and methodology used in this study produces quantifiable data, slight differences between partially and fully serrated blades – which were previously unobservable through qualitative or quantitative methods – could be calculated and used to make more accurate classifications. Therefore, even though this study was not able to classify the specific knives used, being able to differentiate blade class and distinctly classify marks made by partially serrated blades from fully serrated blades is a step in the right direction when trying to specify the knife used in SFT cases.

5.2: Variable Selection for Kerf Mark Identification

The second objective of this study was to identify which micromorphometric measurements are the most useful when making kerf mark identifications. Although predictor screening was implemented to try and assist in variable section, QDA analyses demonstrated the use of all measurements presented in this study, specifically volume (3D), surface area (3D), and area (profile), was necessary to make the most accurate mark classifications possible. This section will detail which variables were the most useful for kerf mark identification and their implications for the field of KMA.

5.2.1: Predictor Screening and Variable Selection

To reiterate, predictor screening was employed to best estimate which variables were the most influential for mark classifications and help determine which measurements should be included in the QDA models and which should be removed. For both knife type and blade class, the least three influential measurements were maximum length (3D), opening angle (profile), and roughness (profile). Similarly, for both knife type and blade class the most influential measurements were volume (3D), surface area (3D), and area (profile) (Tables 4.2 and 4.3).

Interestingly, the three most influential measurements – according to predictor screening – were all variables which were not being measured in previous quantified KMAs (Bartelink et al., 2001; Thompson and Inglis, 2008; Love et al., 2012; Tegtmeyer, 2012; Cerutti et al., 2014; Norman et al., 2018; Sandras et al., 2018; Giraudo et al., 2019). Taking volumetric measurements like surface area and volume is crucial to KMA as this study reveals they are the most discriminatory variables in terms of mark classification as they allow researchers to differentiate between non-serrated, partially serrated, and fully serrated marks. In other words, since this research relies on variables not being measured previously and also yields more specific identifications than seen in previous works, KMAs should place more emphasis on collecting volumetric data.

5.2.2: Conflicts Between Predictor Screening and QDA

In theory, the removal of non-influential variables like maximum depth (3D), opening angle (profile), and roughness (profile) should strengthen the QDA models and yield more accurate classification rates. However, the opposite reigned true in this research. For example, the QDA model using all measurements in relation to knife type was accurate 51.43% of the time, but when omitting "non-influential" variables, the QDA model was only accurate 45.71% of the time. Again, even though the QDA models for blade class were significantly more accurate than those for knife type, blade class QDA models were weakened when omitting "non-significant" variables, going from 97.14% accuracy to 91%.

Although predictor screening suggests maximum length (3D), opening angle (profile), and roughness profile) should not help with mark classification, in practice their inclusion still strengthens the QDA models and should be implemented in KMAs. Therefore, by seeing all the variables are necessary for making accurate mark identifications, future research should include all the measurements used in this study as this will not only allow for better results but also more replicable studies as forensic analysts will know which measurements to take.

5.3: Limitations and Future Research

Although this study yielded promising results for KMA, there were numerous limitations to the work which should be transparently presented and resolved before ever applying this method in a court of law. The following sections will explain the limitations of this study regarding a lack realism, sample size concerns, and affordability as well as how these limitations could be fixed in the future to produce better research.

5.3.1: Lack of Realism

To begin, there is a prominent lack of realism within this study. In any scientific research, there are trade-offs pertaining to how realistic, precise, of general a project will be and no experiment can fully embody all three of these goals (Levins and Lewontin, 1985). Therefore, researchers must weigh the costs and benefits of favoring one goal over the other. In this case, realism was sacrificed for generality and precision in hopes of creating an easily replicable method. Furthermore, it is important to note the method used in this analysis has been fruitful in paleoanthropology (Muttart et al., 2017; Pante, 2017; Gümrükçü et al., 2018; Gümrükçü and Pante, 2018; Keevil, 2018; Mwakyoma, 2021). However, all the aforementioned research was in relation to tooth marks and cut marks made by lithic tools; the methodology used in those studies was never used to analyze kerf marks made by knives. Thus, prioritizing generality and precision in this research was necessary to test and evaluate the method's value for KMA. Now that it is known this method provides researchers with more information than previous KMAs, more realistic studies can be conducted to see if the method holds up.

One of the primary critiques of this study is how bovine bones were used for the analysis. When the kerf mark collection was originally created by CF and EH in 2017, the decision to use bovid bones was made to increase the number of cutting surfaces and decrease the overall cost. However, in forensic analyses porcine bone is typically used as a viable proxy for human remains because pigs have a similar body mass to humans, the soft tissue surrounding porcine bone breaks down in ways which parallel human remains, and porcine bone is similar in hardness to humans (Miles et al., 2020; Bonney and Goodman, 2021; Waltenberger et al., 2021). Therefore, since bovid remains are denser and harder than human bone, they should be replaced by porcine bone in future analyses as pig bones better parallel human remains and may produce more realistic results to what is found in SFT cases.

Additionally, while long bones were used in this study, it is important to note the majority of fatal SFT occurs to the abdomen and thoracic cavity (Swann et al., 1985; Ormstad et al., 1986; Hunt and Cowling, 1991; Rouse, 1994; Webb et al., 1999; Rodge et al., 2000; Banasr et al., 2003; Henderson et al., 2005; Schmidt and Pollack, 2006). Because of this, future research should also account for mark locality and produce kerf marks on the ribs and sternum to better parallel the bones in which fatal SFT is more frequently present.

Similarly, in this study bones were defleshed by CF and EH prior to kerf mark production. While this was done to ensure all kerf marks were readily visible and present for analysis, it is relatively unrealistic as flesh and musculature would be present in real world cases (Merritt, 2012; Lynn and Fairgrieve, 2009a; Lynn and Fairgrieve, 2009b). Thus, future studies should produce kerf marks on fleshed, porcine ribs/bones so that the resultant kerf marks best parallel those seen in actual SFT cases.

Another realism concern related to this analysis pertains to having one individual create all the kerf marks. Common in KMAs, the individual producing kerfs is controlled for by either having one individual or a machine produce all the kerf marks as to regulate the angle, force, and impact applied for each kerf (Bartelink et al., 2001; Thompson and Inglis, 2009; Tegtmeyer, 2012; Tennick, 2012; Cerutti et al., 2014; Norman et al., 2018; Sandras et al., 2018; Giraudo et al., 2019). However, like previous research, this study does not account for real-world variation in terms of who made the marks as differing statures and experience levels with knives may influence the kerf marks left behind on bone (Puentes and Cardoso, 2013). Hence, future experiments should not control for the agent responsible when producing kerf marks and instead test whether differences in kerf marks are truly due to blade class or if they are the result of the individual variation between agents.

Finally, while this study accounts for kerf marks on defleshed, unaltered bone, future research can also account for other real-world factors that may influence the morphology of a kerf mark. For instance, fabric can change the shape and depth of kerf marks as it directly interacts with the knife, altering the force and speed in which a knife will interact with the underlying flesh and bone (Kemp et al., 2009; Daroux et al., 2010; Ferllini, 2013; Feldman, 2015; Miles et al., 2020). Furthermore, since many remains are burned to conceal a crime, some studies have examined whether the morphology of kerf marks is altered in response to burning (Kooi and Fairgrieve, 2013; Vegh and Rando, 2017; Vachirawongsakorn et al., 2022). Thus, future research could implement the same method used in this study but test real-world factors like the influence of fabric and burning on kerf mark morphology.

5.3.2: Sample Size Issues

Unfortunately, the overall sample size in this study was reduced because some bones went missing between the time of mark creation by CF and EH in 2017 and data collection in 2022. Moreover, when this project was originally devised by CF and EH the only focus was knife type, not blade class, meaning there were an even number of marks made by the 5 knife types in this analysis but not an even number for blade class. Because of this, there was an imbalance in the number of non-serrated, partially serrated, and serrated marks in the testing set. Therefore, future analyses should ensure there is an even number of marks made by each blade class.

Additionally, this study only tested a total of four knifes all from the same Chicago Cutlery ™ kitchen set. This set was chosen because it generally accounts for the different knife types one would see in an individual household. However, testing a wider variety of knives from various brands may reveal different trends in relation to blade class as knives from different sets/companies may exhibit a wider range of variation which could produce kerf marks with differing morphologies from those seen in this study. Thus, creating a larger sample size using more knives will test for more variability amongst blade classes, either strengthening or weakening the findings of this study and helping progress KMAs forward.

5.3.3: Affordability and Cost-Effectiveness

One final limitation to this study's forensic application is the technology used to conduct this research is expensive. A used SENSOFAR® S Neox non-contact 3D optical profilometer costs $150,000. Expensive technologies are frequently inaccessible to crime labs because they are often underfunded and understaffed (Giannelli, 2013). Even though the results of this study are beneficial to KMA as a whole, the implementation of this technology could be problematic due to the monetary expenses associated with this scanner.

While this technology is expensive, the process of using the scanner can be learned quickly as the protocol for scanning, processing, and measuring a mark are clearly delineated in this research and previous works (Muttart et al., 2017; Pante, 2017; Gümrükçü et al., 2018; Keevil, 2018; Mwakyoma, 2021). Moreover, this scanner works quicker than previous technologies with scans only taking minutes to process instead of hours (Keevil, 2018). Therefore, even though this scanner is expensive, the results it can produce and the time saved through the use of this technology far outweigh the monetary price.

CHAPTER SIX: CONCLUSION

The implementation of the *Daubert* standard was meant to help judges and juries determine whether certain forensic practices should be considered as evidence in court. While *Daubert* has led to the criticism of most forensic sciences besides DNA, this standard has not been consistently upheld in courtrooms across America, with inadmissible forensic evidence still finding its way into numerous court cases. Due to the discrepancies regarding *Daubert's* application, it has now become the job of forensic analysts to be critical of their own fields and adjust accordingly so their analyses and methods are scientifically valid.

Like many other forensic practices, KMAs suffer from varying criticisms, particularly regarding differing error rates, minimal standardization of methods in the field, and a lack of general acceptance amongst analysts. Therefore, new approaches to KMA are mandatory to ensure the methods used are replicable and that they produce reliable, replicable results that are not only scientifically acceptable but also adhere to *Daubert*.

To resolve the issues currently impacting KMA, this research had two primary objectives. First, this thesis tested whether variations in 3D micromorphological measurements can be used to identify the knife type or blade class responsible for producing certain kerf marks. Through the use of 3D, volumetric measurements and QDA modeling it became known that knife type – chef, boning, steak, and bread – cannot be identified accurately with consistency. However, blade class – non-serrated, partially serrated and serrated – was consistently and accurately classified with an error rate of only 2.86%.

Second, this research asked which mircomorphometric variables are the most useful when making mark identifications. Although predictor screening stated certain measurements like maximum length (3D), opening angle (profile), and roughness (profile) were not useful, omittance of any variables weakened the accuracy of QDA models for both knife type and blade class, revealing all measurements used in this study are necessary for making the most accurate kerf mark identifications possible. Predictor screening also stated the most valuable measurements were volume (3D), surface area (3D), and area (profile); these measurements were not previously being taken by other quantifiable KMAs.

When taking into account the results of this analysis, it becomes apparent the method used can considerably benefit the field of KMA. To begin, this study generated novel results unseen previously by other KMAs as this research effectively discriminated between non-serrated, partially serrated, and fully serrated kerf marks whereas other KMAs only differentiate marks from serrated and non-serrated knifes. Furthermore, the scanner and method used in this analysis were capable of taking volumetric measurements that were previously unmeasurable, allowing for more accurate classifications to be made. Finally, since this analysis makes kerf mark identifications through machine learning and QDA modeling, any observer biases are removed from identifications resulting in more reliable mark classifications. Therefore, taking volumetric measurements allows for more accurate, unbiased blade class identifications to be made, demonstrating the value of optical profilometry and machine learning for KMA.

Additionally, the primary goal of this study was to not only develop and test a new method for KMA but also ensure the methodology meets the *Daubert* standard. While certain criteria – like widespread acceptance – can only come with time and further testing, this research lays a prominent foundation for a new, more admissible era of KMA. For instance, this research demonstrates the Pante et al. (2017) methodology can be tested and generate more promising results than previous KMAs. However, further testing is necessary to ensure this method holds up when accounting for more real-world circumstances. Moreover, this method produces an error rate for blade class identifications of 2.86%. Although this error rate may fluctuate in future studies, the method standardization in this analysis makes future works measuring similar variables comparable to one another. Similarly, since this work clearly outlines the protocol used and dictates which quantifiable measurements generate the most optimal results, a new easily maintainable scientific standard can be created for future analyses. Therefore, this research is a step in the right direction for KMA as the method used produces a known error rate and constructs a new standard based on quantifiable data that can be easily maintained if this protocol becomes more commonplace. While future research must account for more realistic factors to test the validity of this study's results, this research still demonstrates KMAs can develop further to better adhere to the *Daubert* standard and be considered as reliable, admissible forensic evidence.

REFERENCES

Banasr, A., de la Grandmaison, G.L., and Durigon, M. (2003). Frequency of Bone/Cartilage Lesions in Stab and Incised Wounds Fatalities. *Forensic Science International*, 131, 131-133.

Bartelink, E.J., Wiersema, J.M., and Demaree, R. (2001). Quantitative Analysis of Sharp-Force Trauma: An Application of Scanning Electron Microscopy in Forensic Anthropology. *Journal of Forensic Sciences,* 46, 1288-1293.

Bello, S.M. and Soligo, C. (2008). A New Method for the Quantitative Analysis of Cutmark Micromorphology. *Journal of Archaeological Science*, 35, 1542-1552.

Bello, S. M., Parfitt, S. A., and Stringer, C. (2009). Quantitative Micromorphological Analyses of Cut Marks Produced by Ancient and Modern Handaxes. *Journal of Archaeological Science*, 36(9), 1869-1880.

Bello, S.M. (2011). New Results from the Examination of Cut-Marks Using Three-Dimensional Imaging. *Developments in Quaternary Science*, 14, 249-262.

Bernstein, D. E. (2000). Frye, Frye, Again: The Past, Present, and Future of the General Acceptance Test. *Jurimetrics*, 41, 385-407.

Bernstein, D.E. (2009). The Unfinished *Daubert* Revolution. *Engage*, 10(1), 35-38.

Billauer, B. P. (2016). Daubert Debunked: A History of Legal Retrogression and the Need to Reassess Scientific Admissibility. *Suffolk Journal of Trial and Appellate Advocacy*, 21(1), 1-57.

Blumenschine, R.J. and Selvaggio, M.M. (1988). Percussion Marks on Bone Surfaces as a New Diagnostic of Hominid Behaviour. *Nature,* 333, 763-765.

Blumenschine, R.J., Marean, C.W., and Capaldo, S.D. (1996). Blind Tests of Inter-Analyst Correspondence and Accuracy in the Identification of Cut Marks, Percussion Marks, and Carnivore Tooth Marks on Bone Surfaces. *Journal of Archaeological Science*, 23, 493-507.

Bohnert, M., Hüttemann, H., and Schmidt, U. (2006). Homicides by Sharp Force. In M. Tsokos (Ed.), *Forensic Pathology Reviews* (pp. 65-89). Humana Press.

Bonney, H., and Goodman, A. (2021). Validity of the Use of Porcine Bone in Forensic Cut Mark Studies. *Journal of Forensic Sciences*, 66(1), 278-284.

Bonte, W. (1975). Tool Marks in Bone and Cartilage. *Journal of Forensic Sciences*, 20, 315-325.

Boschin, F. and Crezzini, J. (2012). Morphometrical Analysis on Cut Marks Using a 3D Digital Microscope. *International Journal of Osteoarchaeology*, 22(5), 549-562.

Box, G. E. (1949). A General Distribution Theory for a Class of Likelihood Criteria. *Biometrika*, 36(3/4), 317-346.

Box, G.E.P. and Cox, D.R. (1964). An Analysis of Transformations. *Journal of the Royal Statistical Society. Series B (Methodological)*, 26(2), 211-252.

Bunn, H.T. (1981). Archaeological Evidence for Meat-Eating by Plio-Pleistocene Hominids from Koobi Fora and Olduvai Gorge. *Nature,* 291, 574-577.

Burd, D.Q. and Kirk, P.L. (1942). Tool Marks: Factors Involved in their Comparison and Use as Evidence. *Journal of Criminal Law, Criminology, and Police Science*, 32, 679-686.

Büyüköztürk, Ş., and Çokluk-Bökeoğlu, Ö. (2008). Discriminant Function Analysis: Concept and Application. *Eurasian Journal of Education Research*, 33, 73-92.

Cates, P., Dominguez, I., Pierce, E., and Kortan, M. P. (2015). *FBI Testimony on Microscopic Hair Analysis Contained Errors in at Least 90 Percent of Cases in Ongoing Review*. [Press release].

Cerutti, E., Magli, F., Porta, D., Gibelli, D., and Cattaneo, C. (2014). Metrical Assessment of Cutmarks on Bone: Is Size Important? *Legal Medicine*, 16, 208–213

Crowder, C., Rainwater, C.W., and Fridie, J.S. (2013). Microscopic Analysis of Sharp Force Trauma in Bone and Cartilage: A Validation Study. *Journal of Forensic Sciences*, 58, 1119-1126.

Daubert v. Merrell Dow Pharmaceuticals Inc., 509 U.S. 579 (1993).

Daroux, F.Y., Carr, D.J., Kieser, J., Niven, B.E., Taylor, M.C. (2010). Effect of Laundering on Blunt Force Impact Damage in Fabrics. *Forensic Science International*, 197, 21-29.

Dillon, J. R. (2017). Expertise on Trial. *Columbia Science Technology and Law Review*, 19, 247-312.

Efremov, I.A. (1940). Taphonomy: A New Branch of Paleontology. *Pan American Geologist*, 74, 81-93.

Eggen, J. M. (1993). Toxic Torts, Causation, and Scientific Evidence After Daubert. *University of Pittsburg Law Review*, 55, 889-953.

Epstein, J. (2018). The National Commission on Forensic Science: Impactful or Ineffectual. *Seton Hall Law Review*, 48, 743-769.

Faigman, D. L., Porter, E., and Saks, M. J. (1993). Check your Crystal Ball at the Courthouse Door, Please: Exploring the Past, Understanding the Present, and Worrying About the Future of Scientific Evidence. *Cardozo Law Review*, 15, 1799-1834.

Feldman, A.D. (2015). *From Trauma to Trial: Proposing New Methods for Examining the Variability of Sharp Force Trauma on Bone* [Doctoral dissertation, San Jose State University]. ProQuest Dissertations Publishing.

Ferllini, R. (2012). Macroscopic and Microscopic Analysis of Knife Stab Wounds on Fleshed and Clothed Ribs. *Journal of Forensic Sciences*, 57, 683-690.

Fisher, J.W. (1995). Bone Surface Modifications in Zooarchaeology. *Journal of Archaeological Method and Theory*, 2, 7-68.

Frye v United States, 293 F. 1013 (1923).

Garrett, B. L. and Neufeld, P. J. (2009). Invalid Forensic Science Testimony and Wrongful Convictions. *Virginia Law Review*, 95(1), 1-97.

Garrett, B.L., Gardner, B.O., Murphy, E., and Grimes, P. (2021). Judges and Forensic Science Education: A National Survey. *Forensic Science International*, 321, 1-7.

Giannelli, P. C. (1993). Daubert: Interpreting the Federal Rules of Evidence. *Cardozo Law Review.*, 15, 1999-2026.

Giannelli, P. C. (2006). Daubert Challenges to Fingerprints. *Criminal Law Bulletin Boston*, 42(5), 624-642.

Giannelli, P. C. (2013). Regulating DNA Laboratories: The New Gold Standard. *NYU Annual Survey of American Law*., 69, 617-637.

Giraudo, C., Montisci, M., Giorgetti, A., Martinuzzo, L., Bisceglia, M., Moschi, S., Fais, P., Weber, M., Quaia, E., Viel, G., and Cecchetto, G. (2019). Intra-Class and Inter-Class Tool Discrimination Through Micro-CT Analysis of False Starts on Bone. *International Journal of Legal Medicine*, 134, 1023-1032.

Gottesman, M. H. (1998). From Barefoot to Daubert to Joiner: Triple Play or Double Error. *Arizona Law Review*, 40, 753-780.

Grivas, C.R. and Komar, D.A. (2008). Kumho, Daubert, and the Nature of Scientific Inquiry: Implications for Forensic Anthropology. *Journal of Forensic Science*, 53(4), 771-776.

Gümrükçü, M. and Pante, M. C. (2018). Assessing the Effects of Fluvial Abrasion on Bone Surface Modifications Using High-Resolution 3-D Scanning. *Journal of Archaeological Science: Reports*, 21, 208-221.

Gümrükçü, M., Pante, M., Glantz, M., and Lacy, M. (2018). *Assessing the Effects of Fluvial Abrasion on Bone Surface Modifications Using High-Resolution 3-D Scanning* [Master's thesis, Colorado State University]. ProQuest Dissertations Publishing.

Hammer, Ø., Harper, D.A.T., Ryan, P.D. 2001. PAST: Paleontological Statistics Software Package for Education and Data Analysis. *Palaeontologia Electronica*, 4, 1-9.

Hans, V.P. (2007). Judges, Juries, and Scientific Evidence. *Journal of Law and Policy,* 16(1), 3-27.

Henderson, J.P., Morgan, S.E., Patel, F., and Tiplady, M.E. (2005). Patterns of Non-Firearm Homicide. *Journal of Clinical Forensic Medicine*, 12(3), 128-132.

Hilbert, J. (2018). The Disappointing History of Science in the Courtroom: Frye, Daubert, and the Ongoing Crisis of Junk Science in Criminal Trials. *Oklahoma Law Review*, 71, 759-804.

Hunt, A.C. and Cowling, R.J. (1991). Murder by Stabbing. *Forensic Science International*, 52, 107-112.

Keevil, T. L. (2018*). Inferring Early Stone Age Tool Technology and Raw Material from Cut Mark Micromorphology Using High-Resolution 3-D Scanning with Applications to Middle Bed II, Olduvai Gorge, Tanzania* [Master's thesis, Colorado State University]. ProQuest Dissertations Publishing.

Kemp, S.E., Carr, D.J., Kieser, J., Niven, B.E., and Taylor, M.C. (2009). Forensic Evidence in Apparel Fabrics Due to Stab Events. *Forensic Science International*, 191, 86-96.

Kirk, P. L. and Kirk, P. L. (1953). *Crime Investigation: Physical Evidence and the Police Laboratory.* Interscience Publishers, New York.

Kooi, R. J., and Fairgrieve, S. I. (2013). SEM and Stereomicroscopic Analysis of Cut Marks in Fresh and Burned Bone. *Journal of Forensic Sciences*, 58(2), 452-458.

Lander, E. S. and PCAST Working Group. (2016). Forensic Science in Criminal Courts: Ensuring Scientific Validity of Feature-Comparison Methods. Baker Institute for Public Policy, Rice University.

Lander, E. S. (2018). Fixing rule 702: The PCAST Report and Steps to Ensure the Reliability of Forensic Feature-Comparison Methods in the Criminal Courts. *Fordham Law Review*, 86, 1661-1679.

Levins, R. and Lewontin, R.C. (1985). *The Dialectical Biologist*. Harvard University Press, Cambridge.

Lewis, J.E. (2008). Identifying Sword Marks on Bone: Criteria for Distinguishing Between Cut Marks Made by Different Classes of Bladed Weapons. *Journal of Archaeological Sciences*, 35, 2001-2008.

Love, J.C., Derrick, S.M., Wiersems, J.M., and Peters, C. (2012). Validation of Tool Mark Analysis on Cut Costal Cartilage. *Journal of Forensic Science*, 57(2), 306-311.

Love, J. C. (2019). Sharp Force Trauma Analysis in Bone and Cartilage: A Literature Review. *Forensic Science International*, 299, 119-127.

Lupo, K.D. and O'Connell, J.F. (2002). Cut and Tooth Mark Distributions on Large Animal Bones: Ethnoarchaeological Data from the Hadza and Their Implications for Current Ideas About Early Human Carnivory. *Journal of Archaeological Science*, 29, 85-109.

Lyman, R.L. and Lyman, C. (1994). *Vertebrate Taphonomy*. Cambridge University Press.

Lynn, K.S. and Fairgreave, S.I. (2009a). Macroscopic Analysis of Axe and Hatchet Trauma in Fleshed and Defleshed Mammalian Long Bones. *Journal of Forensic Science*, 54(4), 786-792.

Lynn, K.S. and Fairgreave, S.I. (2009b). Microscopic Indicators of Axe and Hatchet Trauma in Fleshed and Defleshed Mammalian Long Bones. *Journal of Forensic Science*, 54(4), 793-797.

Maté-González, M.Á., Yravedra, J., González-Aguilera, D., Palomeque-González, J.F., and Domínguez-Rodrigo, M. (2015). Micro-Photogrammetric Characterization of Cut Marks on Bones. *Journal of Archaeological Science,* 62, 128-142.

McLachlan, G. J. (2005). *Discriminant Analysis and Statistical Pattern Recognition*. John Wiley and Sons.

Merritt, S. R. (2012). Factors Affecting Early Stone Age Cut Mark Cross-Sectional Size: Implications from Actualistic Butchery Trials. *Journal of Archaeological Science*, 39(9), 2984-2994.

Miles, K.L., Finaughty, D.A., and Gibbon, V.E. (2020). A Review of Experimental Design in Forensic Taphonomy: Moving Towards Forensic Realism. *Forensic Sciences Research*, 5(3), 249-259.

Mistek, E., Fikiet, M. A., Khandasammy, S. R., and Lednev, I. K. (2018). Toward Locard's Exchange Principle: Recent Developments in Forensic Trace Evidence Analysis. *Analytical Chemistry*, 91(1), 637-654.

Mnookin, J. L. (2008). Expert Evidence, Partisanship, and Epistemic Competence. *Brooklyn Law Review,* 73, 1009-1033.

Molinaro, A. M., Simon, R., and Pfeiffer, R. M. (2005). Prediction Error Estimation: A Comparison of Resampling Methods. *Bioinformatics*, 21(15), 3301-3307.

Moreno, J.A. (2003). Einstein on the Bench? Exposing What Judges Do Not Know About Science and Using Child Abuse Cases to Improve How Courts Evaluate Scientific Evidence. *Ohio State Law Journal*, 64, 531-584.

Moriarty, J. C. (2010). Will History Be Servitude: The NAS Report of Forensic Science and the Role of the Judiciary. *Utah Law Review*, 299-326.

Muttart, M., Pante, M., Boone, R., and LaBelle, J. (2017). *Taxonomic Distinctions in the 3D Micromorphology of Tooth Marks with Application to Feeding Traces from Middle Bed II, Olduvai Gorge, Tanzania.* [Master's thesis, Colorado State University]. ProQuest Dissertations Publishing.

Mwakyoma, I. F. (2021). *New Insights into Pleistocene Hominin Butchery and Tool Choice from a 0.9 Ma Fossil Assemblage from the Heb Site, Olduvai Gorge, Tanzania* [Master's thesis, Colorado State University]. ProQuest Dissertations Publishing.

National Research Council. (2009). *Strengthening Forensic Science in the United States: A Path Forward*. National Academies Press.

Norman, D.G., Baier, W., Watson, D.G., Burnett, B., Painter, M., and Williams, M.A. (2018). Micro-CT for Saw Mark Analysis on Human Bone. *Forensic Science International*, 293, 91-100.

Ormstad, K., Karlsson, T., Enkler, L., Law, B., and Rajs, J. (1986). Patterns in Sharp-Force Fatalities: A Comprehensive Forensic Study. *Journal of Forensic Science*, 31(2):529-542.

Pante, M. C., Muttart, M. V., Keevil, T. L., Blumenschine, R. J., Njau, J. K., and Merritt, S. R. (2017). A New High-Resolution 3-D Quantitative Method for Identifying Bone Surface Modifications with Implications for the Early Stone Age Archaeological Record. *Journal of Human Evolution,* 102, 1-11.

Posin, D. Q. (1995). Silicone Breast Implant Litigation and My Father-in-Law: A Neo-Coasean Analysis. *Tulane Law Review*, 70, 2565-2582.

Potts, R. and Shipman, P. (1981). Cutmarks Made by Stone Tools on Bones from Olduvai Gorge, Tanzania. *Nature*, 291(5816), 577-580.

Puentes, K. and Cardoso, H.F.V. (2013). Reliability of Cut Mark Analysis in Human Costal Cartilage: The Effects of Blade Penetration Angle and Intra- and Inter-Individual Differences. *Forensic Science International,* 231, 244-248.

Rainwater, C. (2015). Three Modes of Dismemberment: Disarticulation Around the Joints, Transection of Bone Via Chopping, and Transection of Bone Via Sawing, In N.V. Passalacqua, C.W. Rainwater (Eds.), *Skeletal Trauma Analysis: Case Studies in Context* (pp. 222-245)., John Wiley and Sons Ltd.

Rao, V.J. and Hart, R. (1983). Tool Mark Determination in Cartilage of Stabbing Victim. *Journal of Forensic Science*, 28(3), 794-799.

Risinger, D. M. (2000). Navigating expert reliability: Are Criminal Standards of Certainty Being Left on the Dock. *Albany Law Review*, 64, 99-149.

Rodge, S., Hougen, H.P., and Poulsen, K. (2000). Homicide by Sharp Force in Two Scandinavian Capitals. *Forensic Science International*, 109, 135-145.

Rouse, D.A. (1994). Patterns of Stab Wounds: A Six Year Study. *Medicine, Science, and the Law*, 34, 67-71.

Saks, M. J. (2009). Judging admissibility. *Journal of Corporation Law*, 35, 135-155.

Sandras, A., Guilbeau-Frugier, C., Savall, F., Telmon, N., and Capuani, C. (2018). Sharp Bone Trauma Diagnosis: A Validation Study Using Epifluorescence Microscopy. *International Journal of Legal Medicine*, 133(2), 521-528.

Schmidt, U. and Pollak, S. (2006). Sharp Force Injuries in Clinical Forensic Medicine: Findings in Victims and Perpetrators. *Forensic Science International*, 159, 113-118.

Seaman, J. A. (2012). A Tale of Two Dauberts. *Georgia Law Review*, 47, 889-922.

Shipman, P. and Rose, J. (1983). Early Hominid Hunting, Butchering, and Carcass-Processing Behaviors: Approaches to the Fossil Record. *Journal of Anthropological Archaeology*, 2(1), 57-98.

Smith, A.C. (2014). The Effects of Sharp-Force Thoracic Trauma on the Rate and Pattern of Decomposition. *Journal of Forensic Sciences*, 49, 319-326.

Srivastava, S., Gupta, M. R., and Frigyik, B. A. (2007). Bayesian Quadratic Discriminant Analysis. *Journal of Machine Learning Research*, 8(6), 1277-1305.

Swann, I. J., MacMillan, R., and Watson, A. A. (1985). A Study of Stab Wounds. *Emergency Medicine Journal*, *2*(1), 31-36.

Symes, S. A., Williams, J. A., Murray, E. A., Hoffman, J. M., Holland, T. D., Saul, J. M., ... and Pope, E. J. (2002). Taphonomic Context of Sharp-Force Trauma in Suspected Cases of Human Mutilation and Dismemberment. In W.D. Haglund and M.H. Sorg (Eds.), *Advances in Forensic Taphonomy: Method, Theory, and Archaeological Perspectives*, (pp. 403-436). CRC Press.

Tegtmeyer, C. (2012). *A Comparative Analysis of Serrated and Nonserrated Sharp Force Trauma to Bone* [Unpublished master's thesis]. Texas State University-San Marcos.

Tennick, C. (2012). *The Identification and Classification of Sharp Force Trauma on Bone Using Low Power Microscopy* [Unpublished doctoral dissertation]. University of Central Lancashire.

Thompson, T. J., and Inglis, J. (2009). Differentiation of Serrated and Non-serrated Blades from Stab Marks in Bone. *International Journal of Legal Medicine*, *123*(2), 129-135.

Ubelaker, D. H. (1997). Taphonomic Applications in Forensic Anthropology. In M.H. Sorg and W.D. Haglund (Eds.), *Forensic Taphonomy: The Postmortem Fate of Human Remains*, (pp. 1-14). CRC Press.

United Nations Office of Drugs and Crime. (2019). *Global Study on Homicide: Understanding Homicide*. United Nations.

United States Department of Justice. (2020). Uniform Crime Report: Crime in the United States, 2015.

Vachirawongsakorn, V., Painter, J., and Márquez-Grant, N. (2022). Knife Cut Marks Inflicted by Different Blade Types and the Changes Induced by Heat: A Dimensional and Morphological Study. *International Journal of Legal Medicine*, 136(1), 329-342.

Vegh, E.I. and Rando, C. (2017). Effects of Heat as a Taphonomic Agent on Kerf Dimensions. *Archaeological and Environmental Forensic Science*, 1(2), 105-118.

Webb, E., Wyatt, J.P., Henry, J. and Busuttil, A. (1999). A Comparison of Fatal with Non-Fatal Knife Injuries in Edinburgh. *Forensic Science International*, 99(3), 179-187.

APPENDIX A: DISTRIBUTIONS FOR VARIABLES BEFORE BOX-COX TRANSFOMRATIONS

Surface Area (3D) Distribution

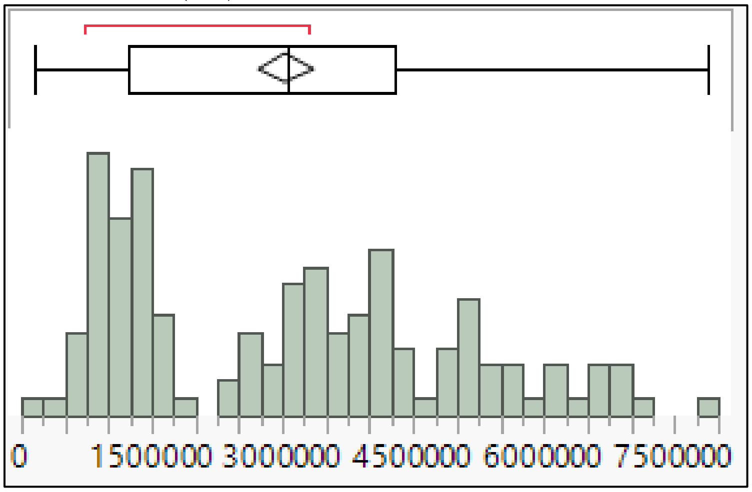

Surface Area (3D) Quantiles

100.0%	Maximum	7868592.000
99.5%		7868592.000
97.5%		6951244.800
90.0%		5584280.600
75.0%	Quartile	4289931.500
50.0%	Median	3046905.000
25.0%	Quartile	1233808.750
10.0%		830667.900
2.5%		578820.000
0.5%		140366.000
0.0%	Minimum	140366.000

Surface Area (3D) Summary Statistics

Mean	3035176.100
Standard Deviation	1896026.600
Standard Error Mean	160243.490
Upper 95% Mean	3352006.000
Lower 95% Mean	2718346.200
N	140

Volume (3D) Distribution

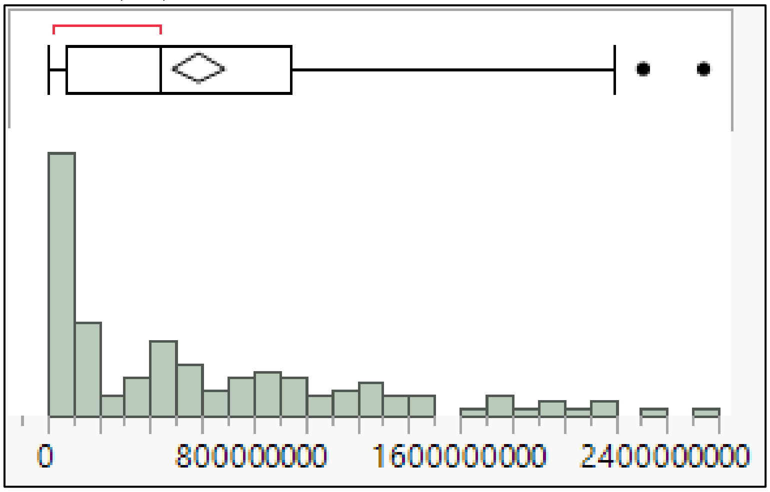

Volume (3D) Quantiles

100.0%	Maximum	2542507845.000
99.5%		2542507845.000
97.5%		2154601646.775
90.0%		1424638725.200
75.0%	Quartile	944149578.500
50.0%	Median	432477515.500
25.0%	Quartile	77226160.500
10.0%		36268608.300
2.5%		22707163.700
0.5%		1752288.000
0.0%	Minimum	1752288.000

Volume (3D) Summary Statistics

Mean	584801732.000
Standard Deviation	601439735.000
Standard Error Mean	50830935.000
Upper 95% Mean	685303524.000
Lower 95% Mean	484299939.000
N	140

Maximum Depth (3D) Distribution

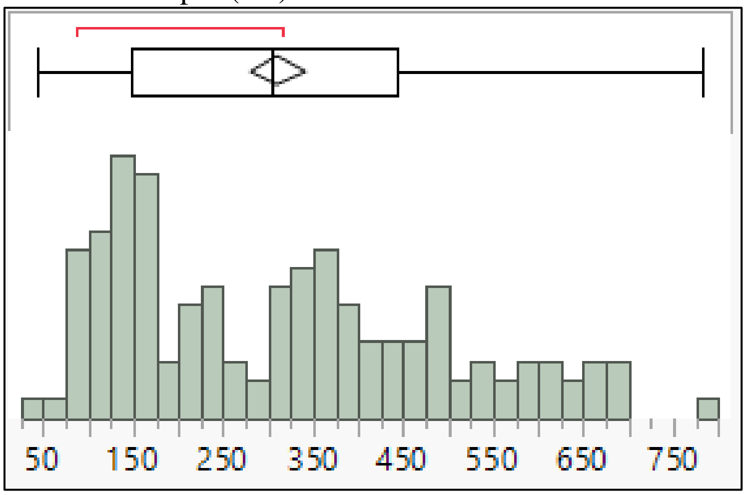

Maximum Depth (3D) Quantiles

100.0%	Maximum	780.775
99.5%		780.775
97.5%		686.044
90.0%		579.546
75.0%	Quartile	442.879
50.0%	Median	302.589
25.0%	Quartile	147.667
10.0%		109.665
2.5%		82.550
0.5%		41.970
0.0%	Minimum	41.970

Maximum Depth (3D) Summary Statistics

Mean	310.789
Standard Deviation	178.290
Standard Error Mean	15.068
Upper 95% Mean	340.682
Lower 95% Mean	280.996
N	140

Mean Depth (3D) Distribution

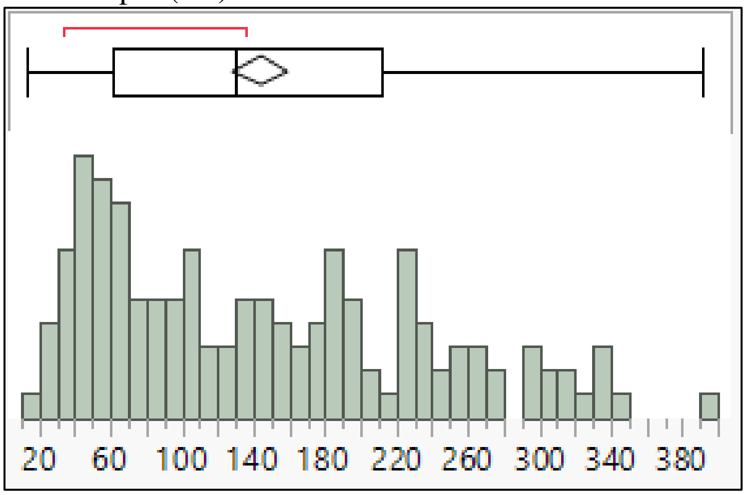

Mean Depth (3D) Quantiles

100.0%	Maximum	391.315
99.5%		391.315
97.5%		336.733
90.0%		272.841
75.0%	Quartile	210.855
50.0%	Median	129.830
25.0%	Quartile	61.854
10.0%		41.505
2.5%		28.531
0.5%		12.484
0.0%	Minimum	12.484

Mean Depth (3D) Summary Statistics

Mean	143.908
Standard Deviation	90.762
Standard Error Mean	7.671
Upper 95% Mean	159.074
Lower 95% Mean	128.741
N	140

Maximum Length (3D) Distribution

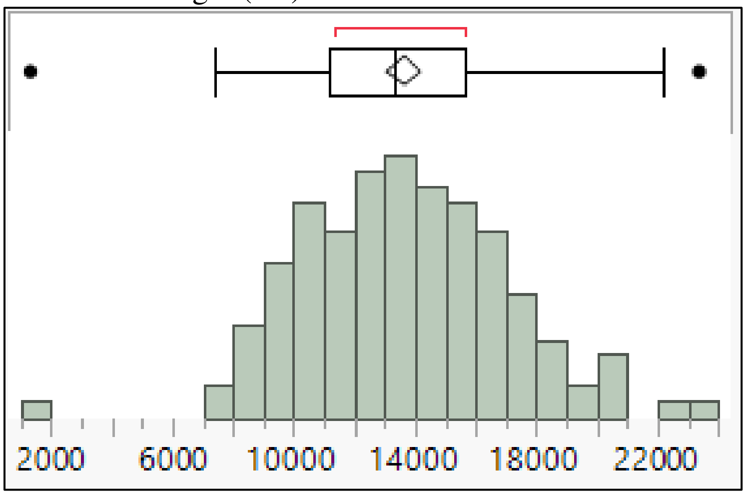

Maximum Length (3D) Quantiles

100.0%	Maximum	23372.300
99.5%		23372.300
97.5%		20849.301
90.0%		17849.270
75.0%	Quartile	15653.835
50.0%	Median	13312.000
25.0%	Quartile	11180.075
10.0%		9745.687
2.5%		8115.340
0.5%		1311.500
0.0%	Minimum	1311.500

Maximum Length (3D) Summary Statistics

Mean	13645.322
Standard Deviation	3361.469
Standard Error Mean	284.096
Upper 95% Mean	14207.030
Lower 95% Mean	13083.614
N	140

Maximum Width (3D) Distribution

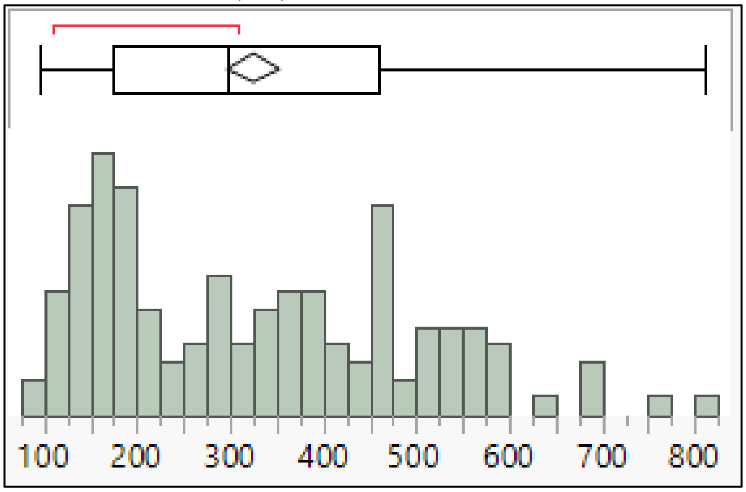

Maximum Width (3D) Quantiles

100.0%	Maximum	811.823
99.5%		811.823
97.5%		692.171
90.0%		556.024
75.0%	Quartile	460.678
50.0%	Median	298.284
25.0%	Quartile	172.822
10.0%		137.922
2.5%		109.349
0.5%		94.496
0.0%	Minimum	94.496

Maximum Width (3D) Summary Statistics

Mean	324.951
Standard Deviation	167.042
Standard Error Mean	14.118
Upper 95% Mean	352.864
Lower 95% Mean	297.038
N	140

Area (Profile) Distribution

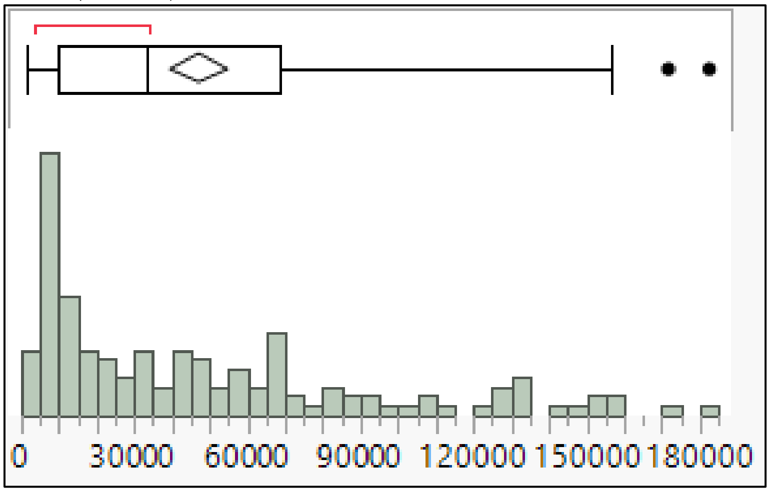

Area (Profile) Quantiles

100.0%	Maximum	182484.000
99.5%		182484.000
97.5%		156255.500
90.0%		126989.000
75.0%	Quartile	68372.000
50.0%	Median	33364.350
25.0%	Quartile	9714.735
10.0%		5542.878
2.5%		3618.808
0.5%		1480.140
0.0%	Minimum	1480.140

Area (Profile) Summary Statistics

Mean	47007.185
Standard Deviation	44609.234
Standard Error Mean	3770.168
Upper 95% Mean	54461.478
Lower 95% Mean	39552.892
N	140

Maximum Depth (Profile) Distribution

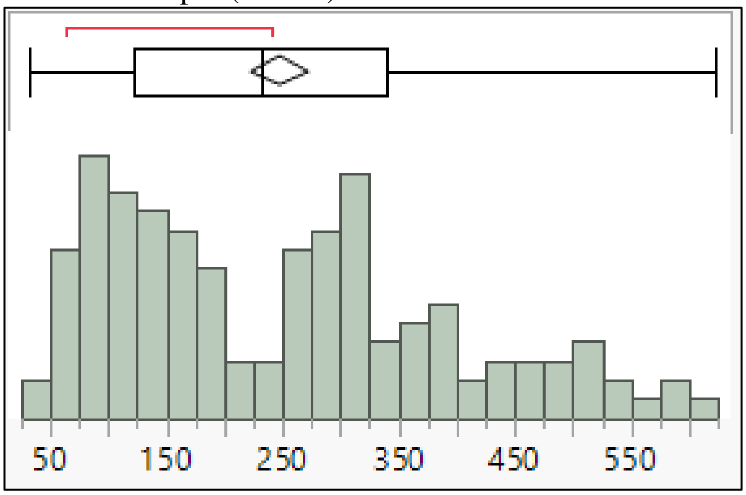

Maximum Depth (Profile) Quantiles

100.0%	Maximum	621.850
99.5%		621.850
97.5%		575.897
90.0%		473.335
75.0%	Quartile	339.861
50.0%	Median	232.025
25.0%	Quartile	121.197
10.0%		87.012
2.5%		64.269
0.5%		32.879
0.0%	Minimum	23.879

Maximum Depth (Profile) Summary Statistics

Mean	247.106
Standard Deviation	143.898
Standard Error Mean	12.162
Upper 95% Mean	271.152
Lower 95% Mean	223.061
N	140

Maximum Width (Profile) Distribution

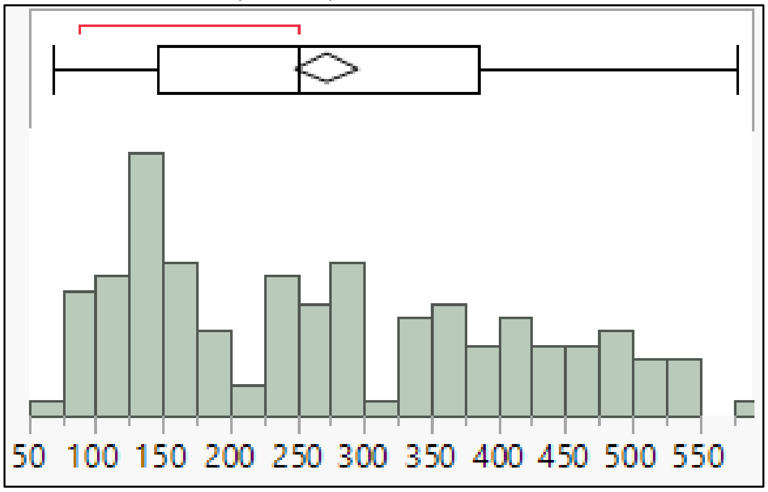

Maximum Width (Profile) Quantiles

100.0%	Maximum	576.840
99.5%		576.840
97.5%		535.164
90.0%		482.724
75.0%	Quartile	384.330
50.0%	Median	251.160
25.0%	Quartile	146.280
10.0%		110.400
2.5%		89.769
0.5%		69.000
0.0%	Minimum	69.000

Maximum Width (Profile) Summary Statistics

Mean	272.530
Standard Deviation	137.326
Standard Error Mean	11.606
Upper 95% Mean	295.478
Lower 95% Mean	249.583
N	140

Roughness (Profile) Distribution

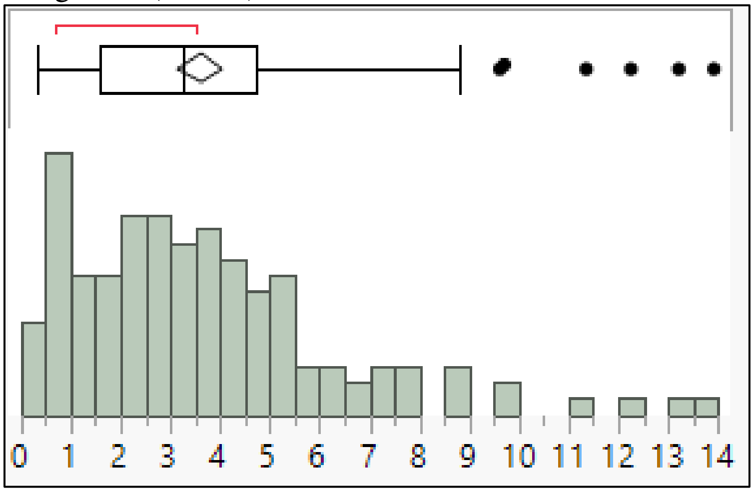

Roughness (Profile) Quantiles

100.0%	Maximum	13.917
99.5%		13.917
97.5%		11.781
90.0%		7.478
75.0%	Quartile	4.736
50.0%	Median	3.244
25.0%	Quartile	1.578
10.0%		0.718
2.5%		0.447
0.5%		0.332
0.0%	Minimum	0.332

Roughness (Profile) Summary Statistics

Mean	3.614
Standard Deviation	2.681
Standard Error Mean	0.227
Upper 95% Mean	4.062
Lower 95% Mean	3.166
N	140

Opening Angle (Profile) Distribution

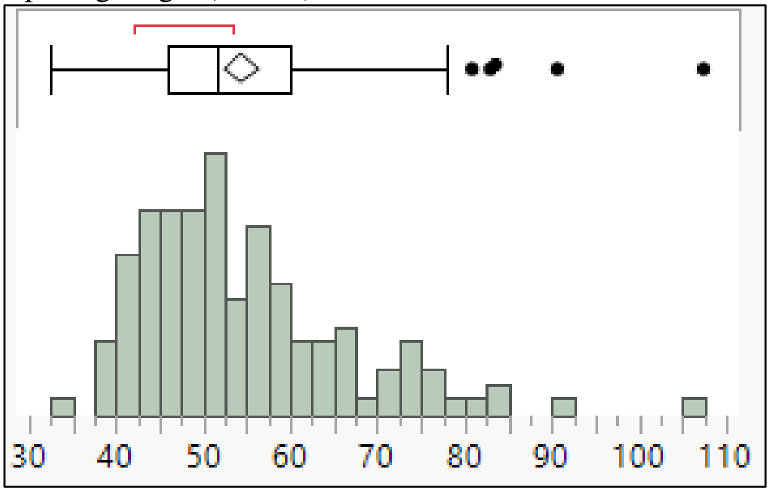

Opening Angle (Profile) Quantiles

100.0%	Maximum	107.372
99.5%		107.372
97.5%		83.193
90.0%		72.698
75.0%	Quartile	59.872
50.0%	Median	51.454
25.0%	Quartile	46.020
10.0%		42.056
2.5%		38.721
0.5%		32.504
0.0%	Minimum	32.504

Opening Angle (Profile) Summary Statistics

Mean	54.383
Standard Deviation	11.887
Standard Error Mean	1.001
Upper 95% Mean	56.362
Lower 95% Mean	52.404
N	140

Floor Radius (Profile) Distribution

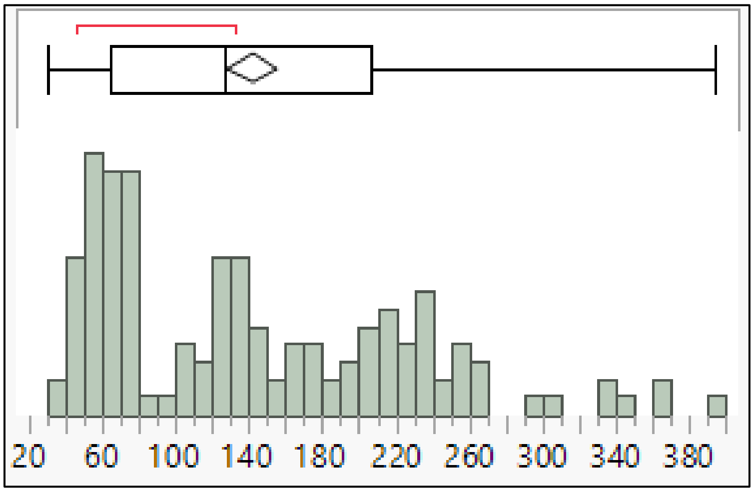

Floor Radius (Profile) Quantiles

100.0%	Maximum	393.691
99.5%		393.691
97.5%		351.874
90.0%		253.213
75.0%	Quartile	207.067
50.0%	Median	127.423
25.0%	Quartile	64.459
10.0%		55.003
2.5%		42.077
0.5%		30.217
0.0%	Minimum	30.217

Floor Radius (Profile) Summary Statistics

Mean	141.954
Standard Deviation	83.981
Standard Error Mean	7.098
Upper 95% Mean	155.987
Lower 95% Mean	127.920
N	140

APPENDIX B: DISTRIBUTIONS FOR VARIABLES AFTER BOX-COX TRANSFOMRATIONS

Surface Area (3D) Distribution

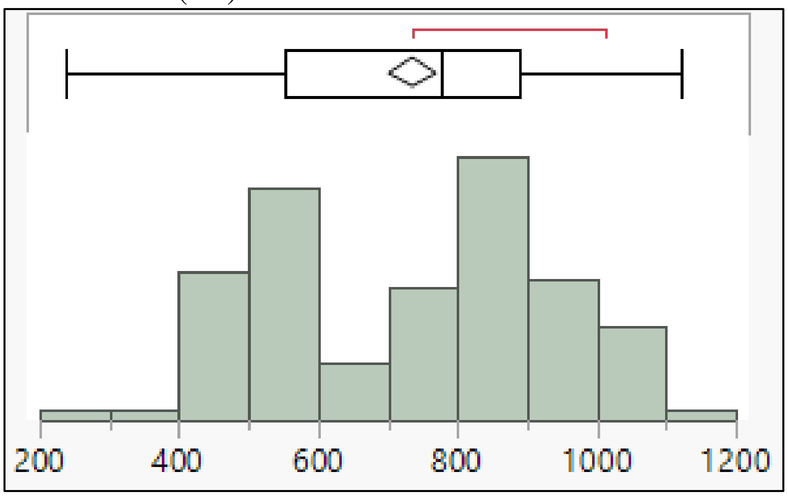

Surface Area (3D) Quantiles

100.0%	Maximum	1119.345
99.5%		1119.345
97.5%		1067.506
90.0%		981.719
75.0%	Quartile	887.477
50.0%	Median	778.535
25.0%	Quartile	550.580
10.0%		473.086
2.5%		411.827
0.5%		238.740
0.0%	Minimum	238.740

Surface Area (3D) Summary Statistics

Mean	736.431
Standard Deviation	199.2127
Standard Error Mean	16.837
Upper 95% Mean	769.721
Lower 95% Mean	703.141
N	140

Volume (3D) Distribution

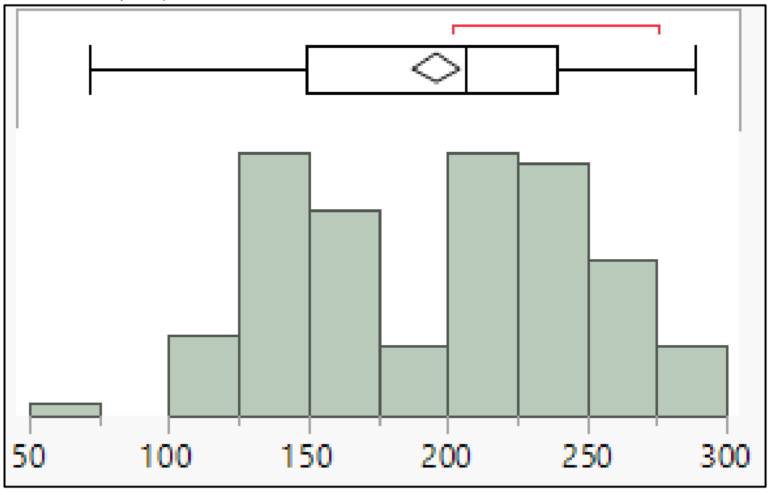

Volume (3D) Quantiles

100.0%	Maximum	288.449
99.5%		288.449
97.5%		279.611
90.0%		258.687
75.0%	Quartile	239.394
50.0%	Median	206.580
25.0%	Quartile	148.890
10.0%		128.825
2.5%		117.658
0.5%		71.371
0.0%	Minimum	71.371

Volume (3D) Summary Statistics

Mean	195.824
Standard Deviation	50.725
Standard Error Mean	4.287
Upper 95% Mean	204.300
Lower 95% Mean	187.348
N	140

Maximum Depth (3D) Distribution

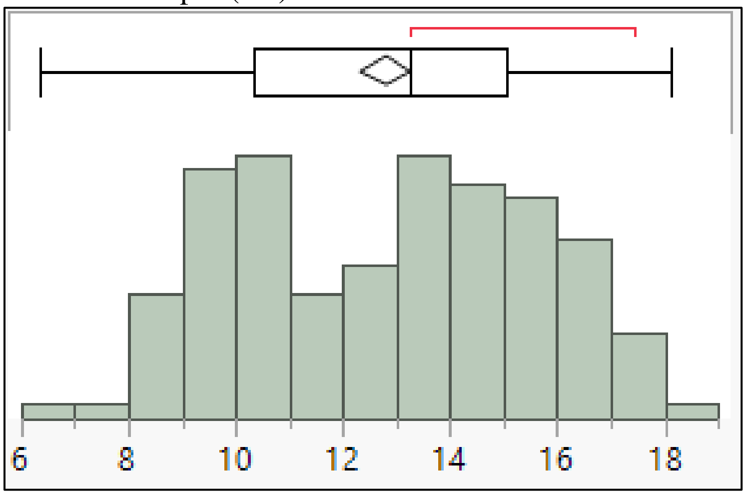

Maximum Depth (3D) Quantiles

100.0%	Maximum	18.093
99.5%		18.093
97.5%		17.361
90.0%		16.444
75.0%	Quartile	15.062
50.0%	Median	13.265
25.0%	Quartile	10.332
10.0%		9.269
2.5%		8.327
0.5%		6.353
0.0%	Minimum	6.353

Maximum Depth (3D) Summary Statistics

Mean	12.796
Standard Deviation	2.717
Standard Error Mean	0.230
Upper 95% Mean	13.250
Lower 95% Mean	12.342
N	140

Mean Depth (3D) Distribution

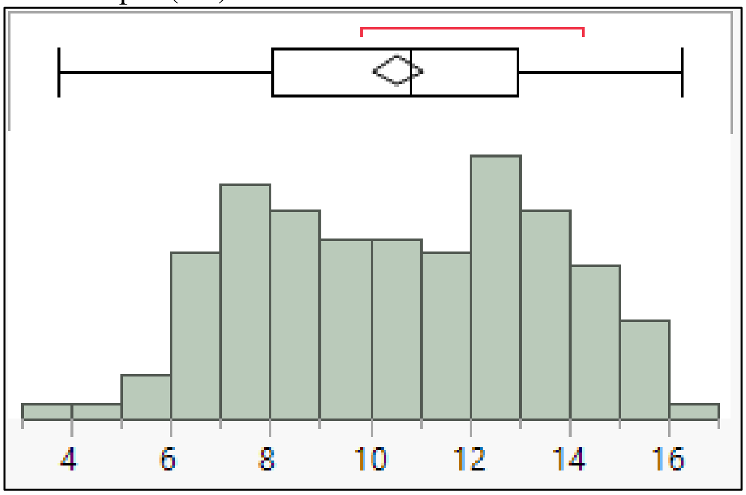

Mean Depth (3D) Quantiles

100.0%	Maximum	16.236
99.5%		16.236
97.5%		15.389
90.0%		14.263
75.0%	Quartile	12.976
50.0%	Median	10.803
25.0%	Quartile	8.024
10.0%		6.761
2.5%		5.702
0.5%		3.740
0.0%	Minimum	3.740

Mean Depth (3D) Summary Statistics

Mean	10.575
Standard Deviation	2.872
Standard Error Mean	0.243
Upper 95% Mean	11.055
Lower 95% Mean	10.095
N	140

Maximum Length (3D) Distribution

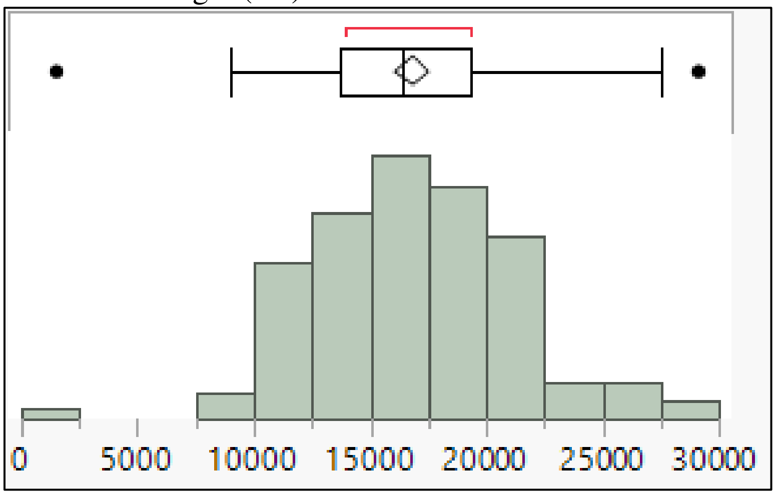

Maximum Length (3D) Quantiles

100.0%	Maximum	29124.695
99.5%		29124.695
97.5%		25908.735
90.0%		22097.107
75.0%	Quartile	19317.464
50.0%	Median	16362.940
25.0%	Quartile	13684.184
10.0%		11888.722
2.5%		9855.858
0.5%		1523.059
0.0%	Minimum	1523.059

Maximum Length (3D) Summary Statistics

Mean	16796.917
Standard Deviation	4230.835
Standard Error Mean	357.571
Upper 95% Mean	17502.898
Lower 95% Mean	16088.936
N	140

Maximum Width (3D) Distribution

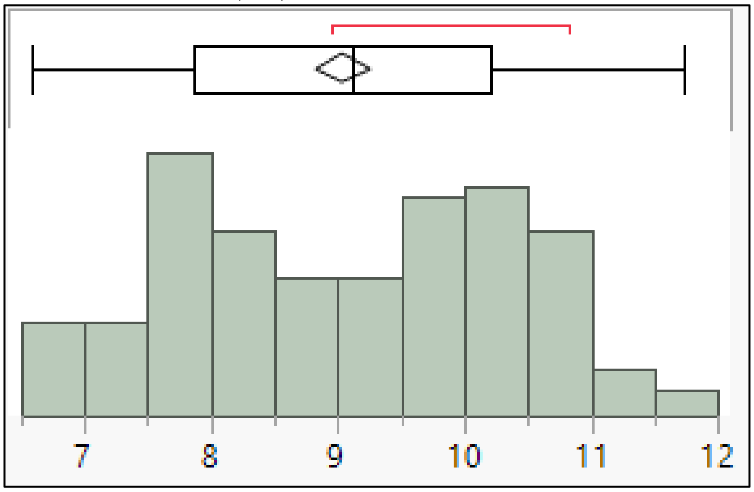

Maximum Width (3D) Quantiles

100.0%	Maximum	11.720
99.5%		11.720
97.5%		11.279
90.0%		10.690
75.0%	Quartile	10.199
50.0%	Median	9.119
25.0%	Quartile	7.861
10.0%		7.371
2.5%		6.884
0.5%		6.587
0.0%	Minimum	6.587

Maximum Width (3D) Summary Statistics

Mean	9.042
Standard Deviation	1.296
Standard Error Mean	0.110
Upper 95% Mean	9.259
Lower 95% Mean	8.826
N	140

Area (Profile) Distribution

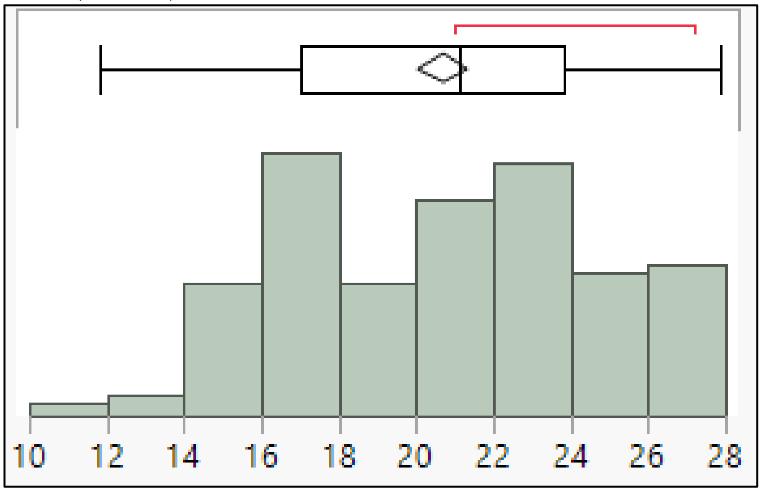

Area (Profile) Quantiles

100.0%	Maximum	27.883
99.5%		27.883
97.5%		27.203
90.0%		26.315
75.0%	Quartile	23.794
50.0%	Median	21.102
25.0%	Quartile	16.993
10.0%		15.319
2.5%		14.120
0.5%		11.809
0.0%	Minimum	11.809

Area (Profile) Summary Statistics

Mean	20.684
Standard Deviation	3.945
Standard Error Mean	0.333
Upper 95% Mean	21.343
Lower 95% Mean	20.025
N	140

Maximum Depth (Profile) Distribution

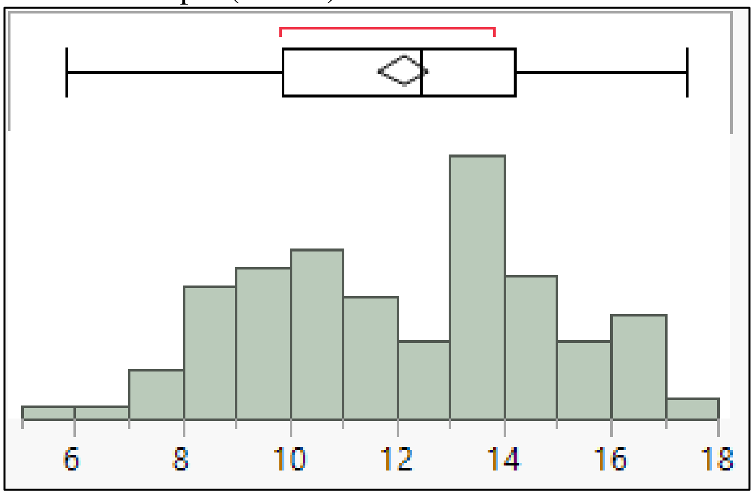

Maximum Depth (Profile) Quantiles

100.0%	Maximum	17.396
99.5%		17.396
97.5%		16.962
90.0%		15.893
75.0%	Quartile	12.211
50.0%	Median	12.452
25.0%	Quartile	9.849
10.0%		8.686
2.5%		7.710
0.5%		5.817
0.0%	Minimum	5.817

Maximum Depth (Profile) Summary Statistics

Mean	12.145
Standard Deviation	2.700
Standard Error Mean	0.228
Upper 95% Mean	12.597
Lower 95% Mean	11.694
N	140

Maximum Width (Profile) Distribution

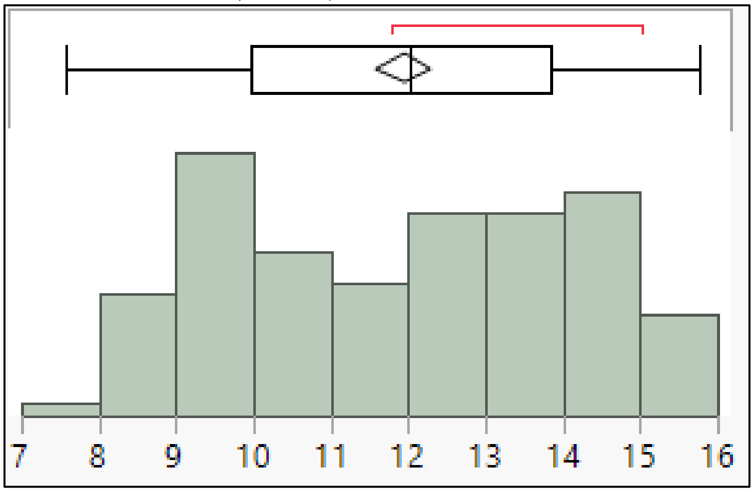

Maximum Width (Profile) Quantiles

100.0%	Maximum	15.757
99.5%		15.757
97.5%		15.387
90.0%		14.890
75.0%	Quartile	13.835
50.0%	Median	12.023
25.0%	Quartile	9.984
10.0%		9.028
2.5%		8.367
0.5%		7.575
0.0%	Minimum	7.575

Maximum Width (Profile) Summary Statistics

Mean	11.939
Standard Deviation	2.165
Standard Error Mean	0.183
Upper 95% Mean	12.301
Lower 95% Mean	11.578
N	140

Roughness (Profile) Distribution

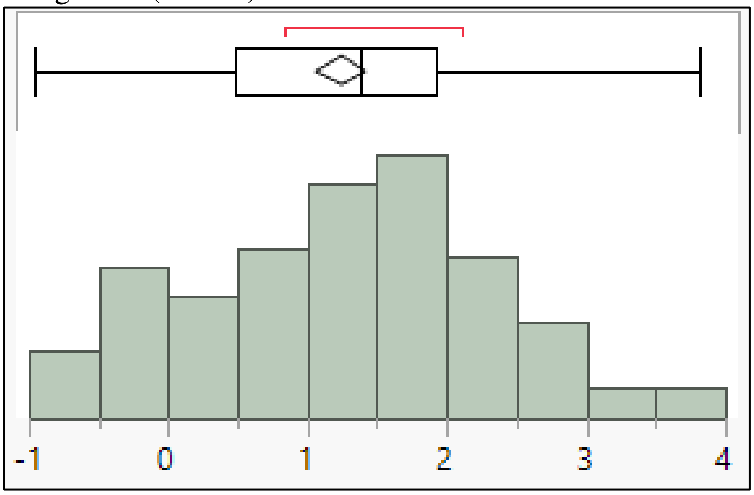

Roughness (Profile) Quantiles

100.0%	Maximum	3.816
99.5%		3.816
97.5%		3.487
90.0%		2.662
75.0%	Quartile	1.923
50.0%	Median	1.382
25.0%	Quartile	0.485
10.0%		-0.317
2.5%		-0.726
0.5%		-0.955
0.0%	Minimum	-0.995

Roughness (Profile) Summary Statistics

Mean	1.244
Standard Deviation	1.063
Standard Error Mean	0.090
Upper 95% Mean	1.422
Lower 95% Mean	1.067
N	140

Opening Angle (Profile) Distribution

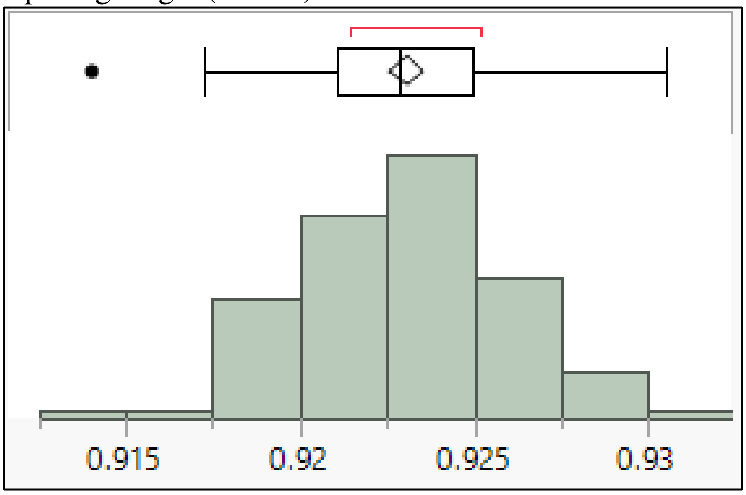

Opening Angle (Profile) Quantiles

100.0%	Maximum	0.930
99.5%		0.930
97.5%		0.928
90.0%		0.927
75.0%	Quartile	0.925
50.0%	Median	0.923
25.0%	Quartile	0.921
10.0%		0.920
2.5%		0.918
0.5%		0.914
0.0%	Minimum	0.914

Opening Angle (Profile) Summary Statistics

Mean	0.923
Standard Deviation	0.003
Standard Error Mean	0.0002
Upper 95% Mean	0.924
Lower 95% Mean	0.923
N	140

Floor Radius (Profile) Distribution

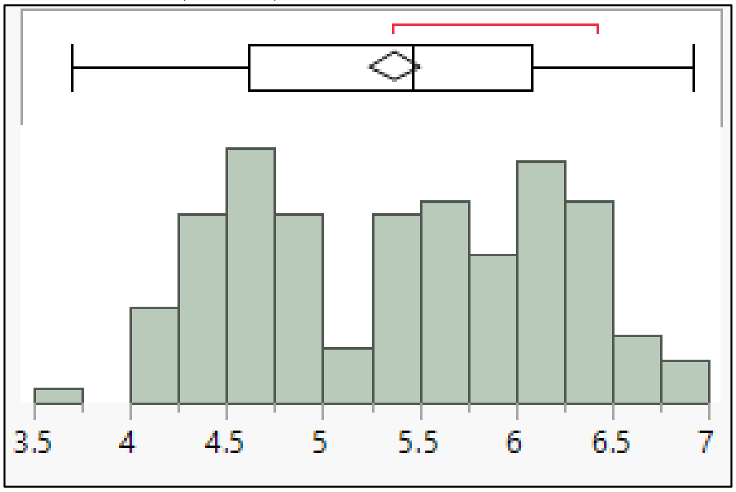

Floor Radius (Profile) Quantiles

100.0%	Maximum	6.924
99.5%		6.924
97.5%		6.775
90.0%		6.342
75.0%	Quartile	6.081
50.0%	Median	5.460
25.0%	Quartile	4.613
10.0%		4.420
2.5%		4.097
0.5%		3.704
0.0%	Minimum	3.704

Floor Radius (Profile) Summary Statistics

Mean	5.379
Standard Deviation	0.777
Standard Error Mean	0.066
Upper 95% Mean	5.509
Lower 95% Mean	5.250
N	140

APPENDIX C: BOX PLOTS AND DESCRIPTIVE STATISTICS FOR BOX-COX TRANSFORMED DATA IN RELATION TO KNIFE TYPE

Box Plot for Surface Area (3D)

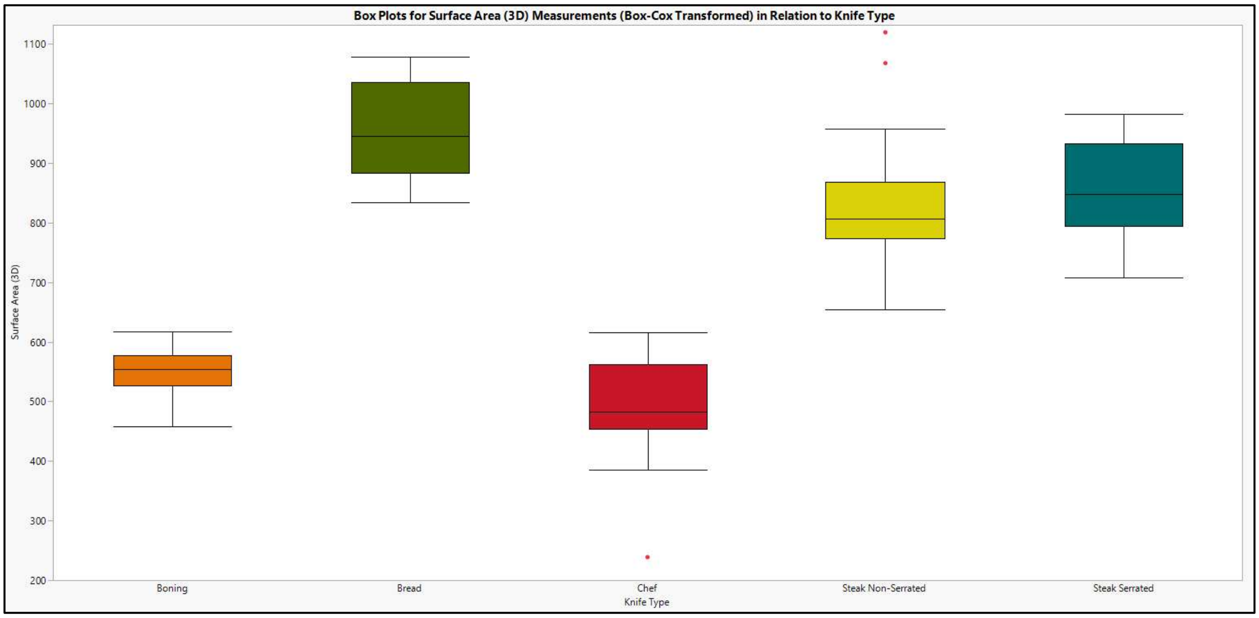

Descriptive Statistics for Surface Area (3D)

Knife Type	Mark Count	Mean	Standard Deviation	Standard Error Mean	Lower 95%	Upper 95%
Chef	28	489.725	79.616	15.046	458.854	520.597
Boning	28	549.954	43.410	8.204	533.121	566.786
Steak Non-Serrated	28	828.533	100.726	19.035	789.476	867.590
Steak Serrated	28	854.194	78.739	14.880	823.662	884.726
Bread	28	959.750	75.311	14.232	930.547	988.952

Box Plot for Volume (3D)

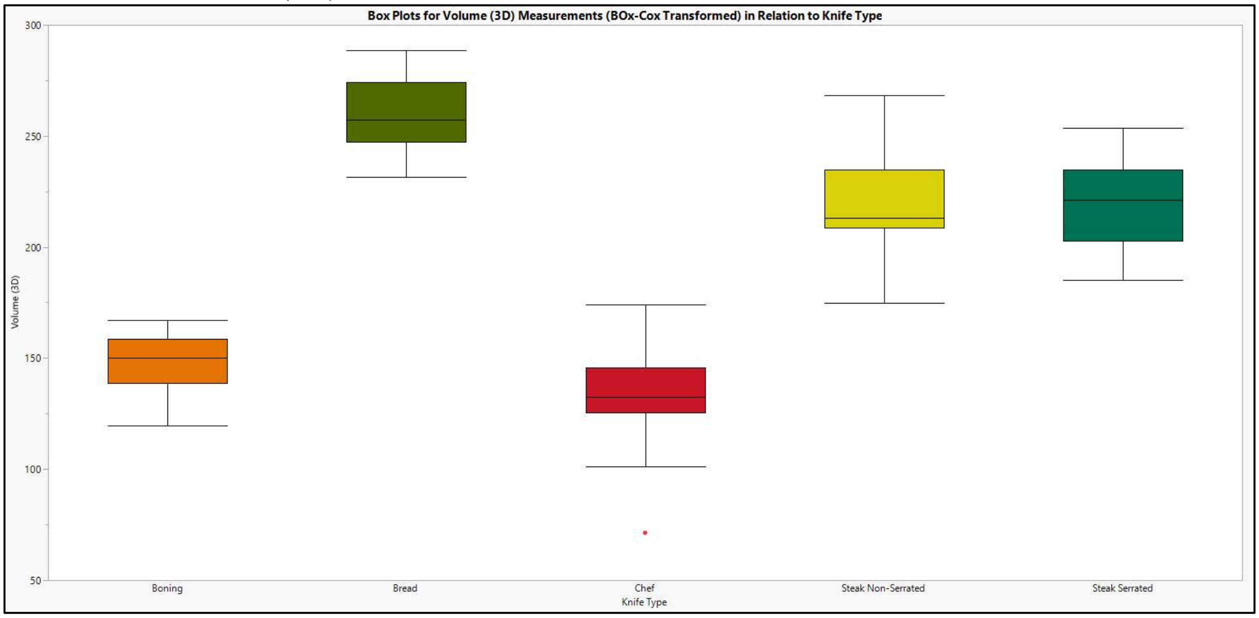

Descriptive Statistics for Volume (3D)

Knife Type	Mark Count	Mean	Standard Deviation	Standard Error Mean	Lower 95%	Upper 95%
Chef	28	134.347	20.340	3.844	126.460	142.234
Boning	28	147.815	13.267	2.507	142.671	152.960
Steak Non-Serrated	28	218.639	21.203	4.007	210.417	226.861
Steak Serrated	28	219.253	19.705	3.724	211.613	226.894
Bread	28	259.065	15.886	3.002	252.904	265.225

Box Plot for Maximum Depth (3D)

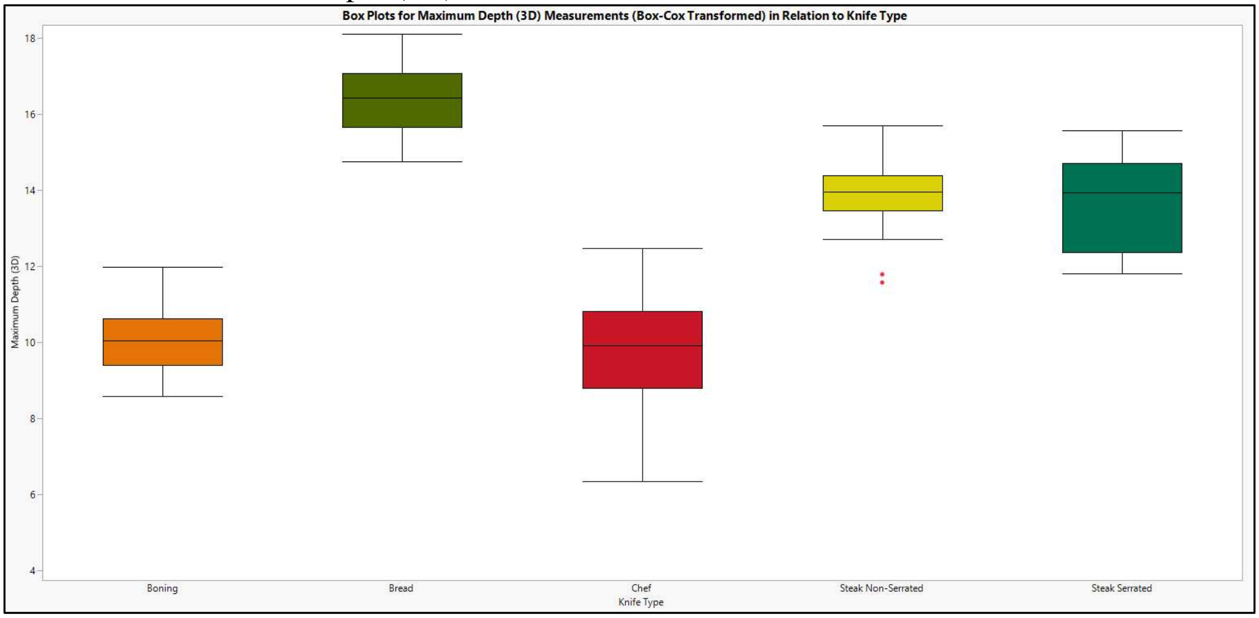

Descriptive Statistics for Maximum Depth (3D)

Knife Type	Mark Count	Mean	Standard Deviation	Standard Error Mean	Lower 95%	Upper 95%
Chef	28	9.807	1.350	0.255	9.284	10.330
Boning	28	10.117	0.884	0.167	9.774	10.460
Steak Non-Serrated	28	13.931	1.008	0.190	13.540	14.322
Steak Serrated	28	13.740	1.157	0.219	13.291	14.188
Bread	28	16.386	0.845	0.160	16.058	16.714

Box Plot for Mean Depth (3D)

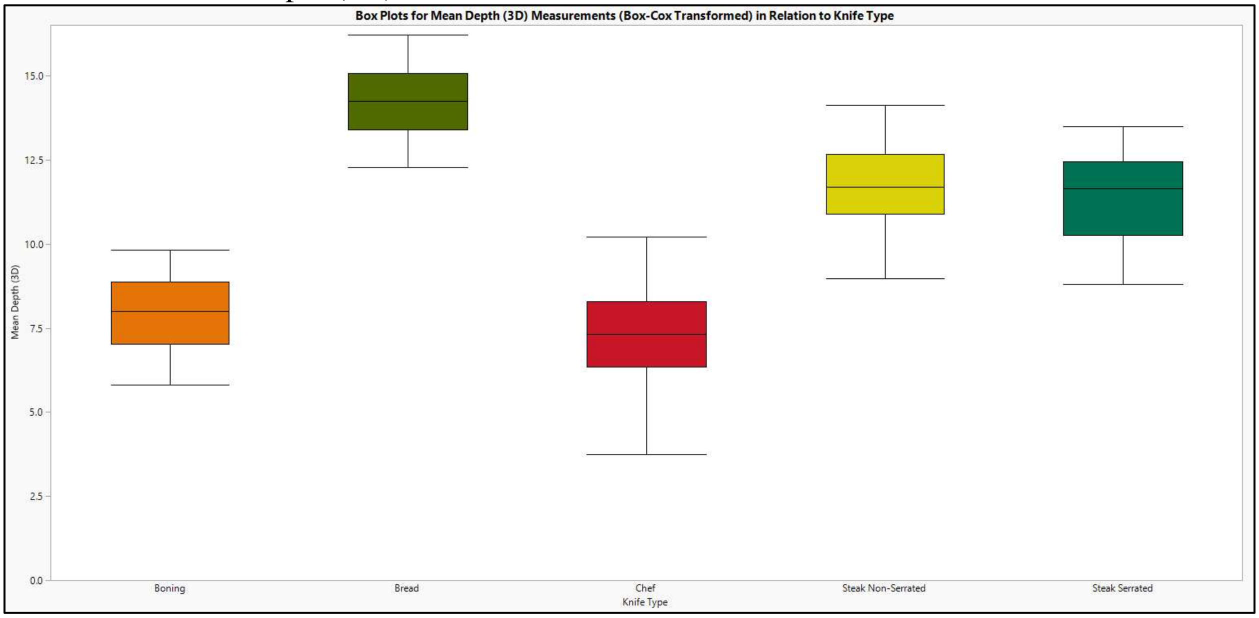

Descriptive Statistics for Mean Depth (3D)

Knife Type	Mark Count	Mean	Standard Deviation	Standard Error Mean	Lower 95%	Upper 95%
Chef	28	7.322	1.463	0.276	6.755	7.889
Boning	28	7.958	1.095	0.207	7.533	8.382
Steak Non-Serrated	28	11.806	1.289	0.244	11.307	12.306
Steak Serrated	28	11.509	1.313	0.248	11.000	12.018
Bread	28	14.279	0.974	0.184	13.901	14.657

Box Plot for Maximum Length (3D)

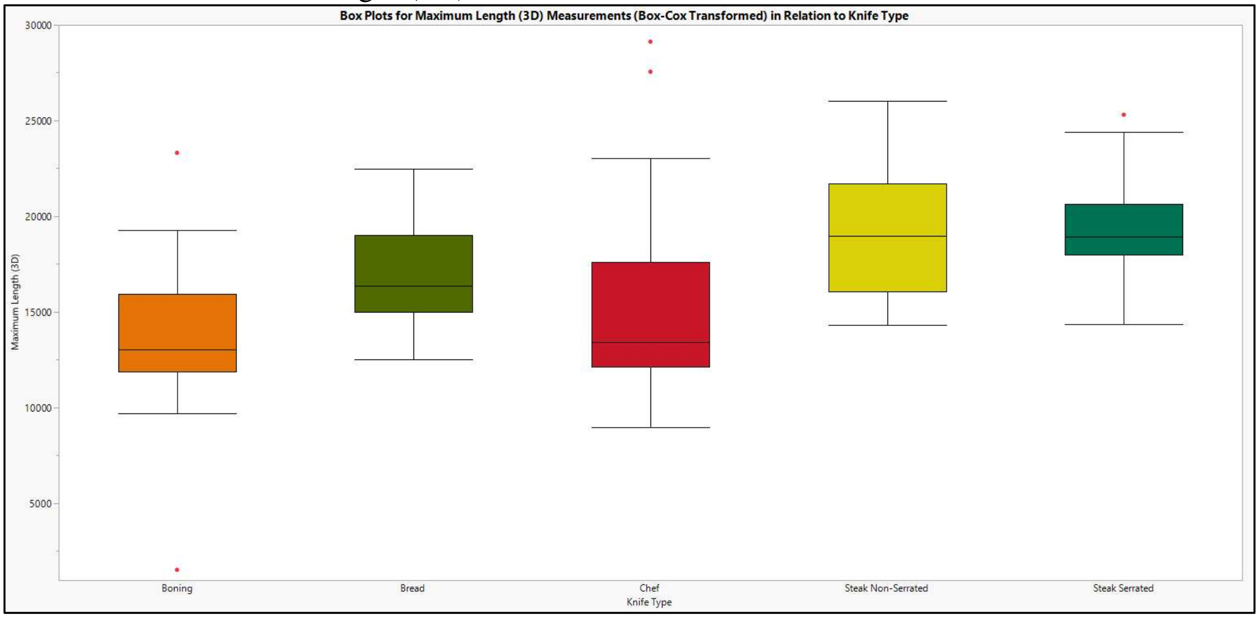

Descriptive Statistics for Maximum Length (3D)

Knife Type	Mark Count	Mean	Standard Deviation	Standard Error Mean	Lower 95%	Upper 95%
Chef	28	15144.617	5045.781	953.563	13188.067	17101.166
Boning	28	13444.482	3806.361	719.335	11968.529	14920.435
Steak Non-Serrated	28	19158.553	3496.205	660.721	17802.866	20514.239
Steak Serrated	28	19305.132	2440.082	461.132	18358.967	20251.297
Bread	28	16926.802	2685.915	507.590	15885.313	17968.291

Box Plot for Maximum Width (3D)

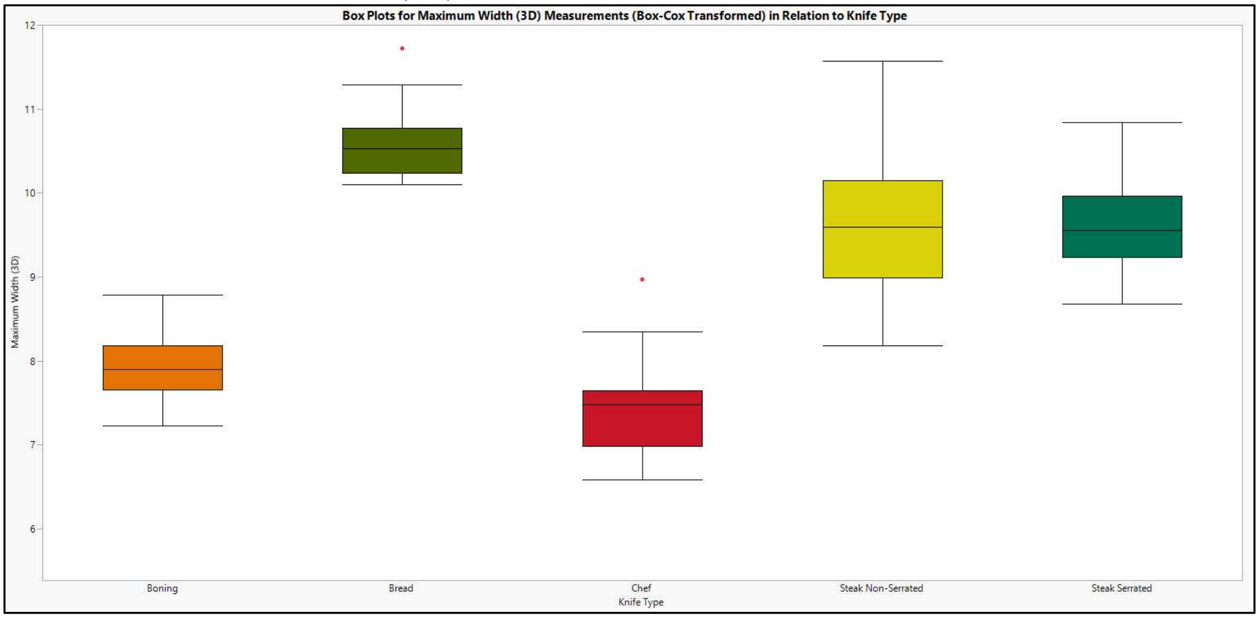

Descriptive Statistics for Maximum Width (3D)

Knife Type	Mark Count	Mean	Standard Deviation	Standard Error Mean	Lower 95%	Upper 95%
Chef	28	7.449	0.539	0.102	7.240	7.658
Boning	28	7.914	0.347	0.066	7.779	8.048
Steak Non-Serrated	28	9.624	0.785	0.128	9.320	9.928
Steak Serrated	28	9.638	0.565	0.107	9.418	9.857
Bread	28	10.587	0.539	0.074	10.436	10.740

Box Plot for Area (Profile)

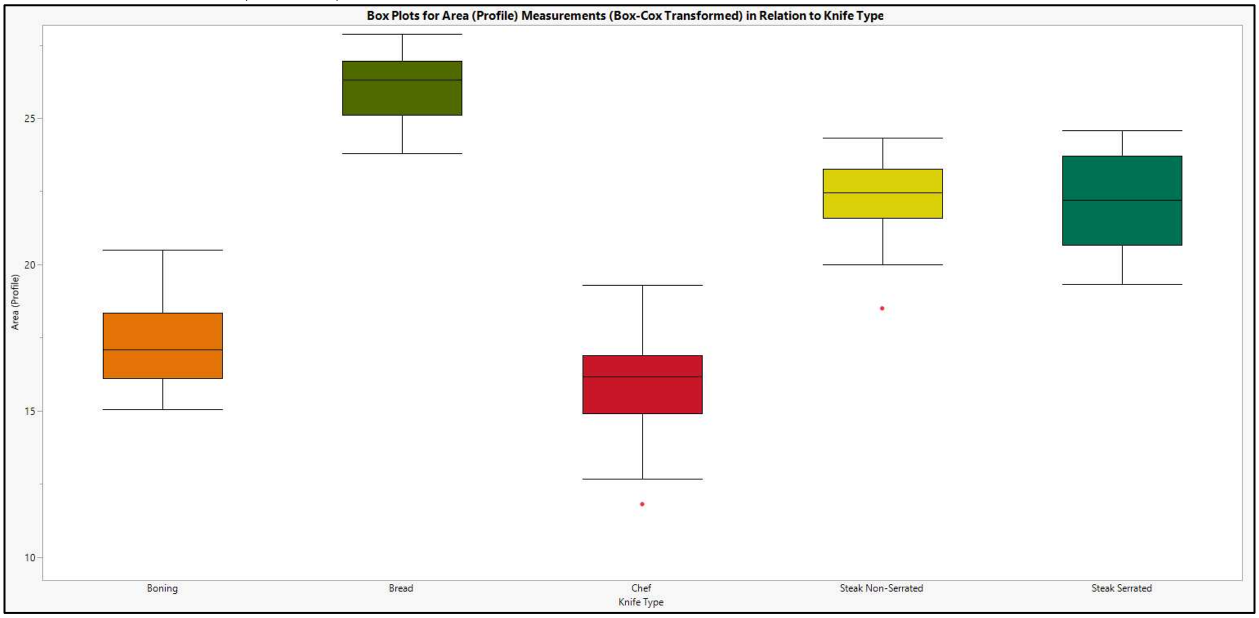

Descriptive Statistics for Area (Profile)

Knife Type	Mark Count	Mean	Standard Deviation	Standard Error Mean	Lower 95%	Upper 95%
Chef	28	16.022	1.677	0.317	15.372	16.672
Boning	28	17.083	1.375	0.260	16.550	17.616
Steak Non-Serrated	28	22.218	1.333	0.252	21.702	22.735
Steak Serrated	28	22.064	1.562	0.295	21.458	22.670
Bread	28	26.035	1.046	0.198	25.629	26.440

Box Plot for Maximum Depth (Profile)

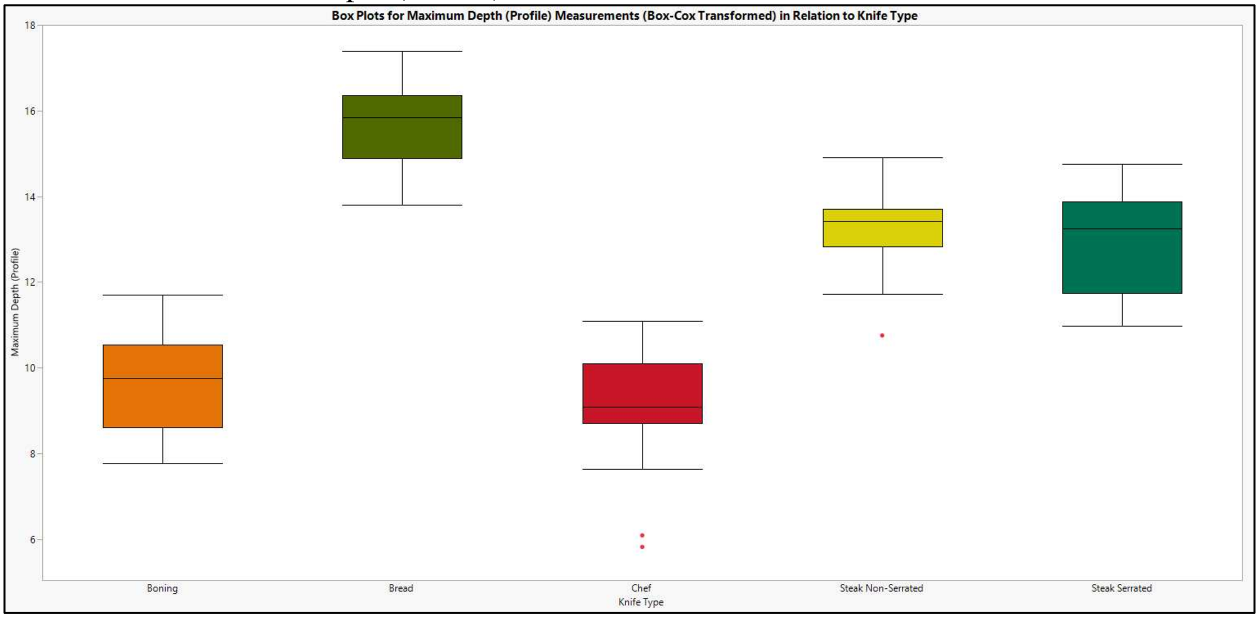

Descriptive Statistics for Maximum Depth (Profile)

Knife Type	Mark Count	Mean	Standard Deviation	Standard Error Mean	Lower 95%	Upper 95%
Chef	28	9.145	1.267	0.239	8.654	9.637
Boning	28	9.598	1.112	0.210	9.167	10.030
Steak Non-Serrated	28	13.199	0.891	0.168	12.853	13.544
Steak Serrated	28	13.013	1.196	0.226	12.549	13.477
Bread	28	15.772	0.911	0172	15.418	16.125

Box Plot for Maximum Width (Profile)

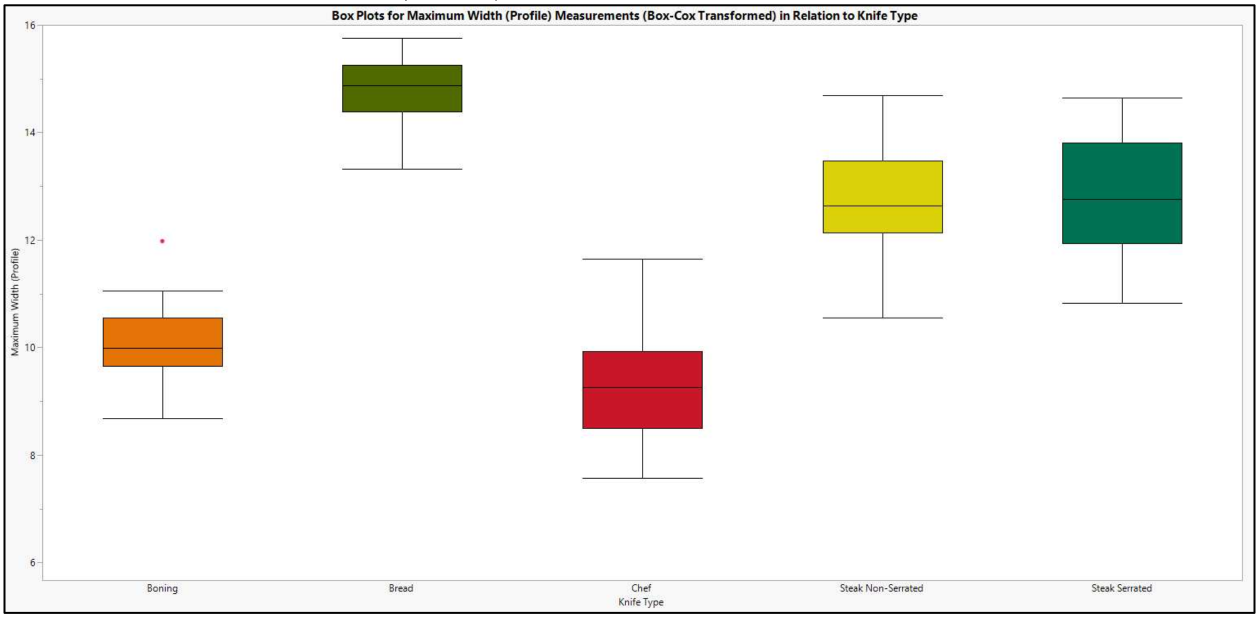

Descriptive Statistics for Maximum Width (Profile)

Knife Type	Mark Count	Mean	Standard Deviation	Standard Error Mean	Lower 95%	Upper 95%
Chef	28	9.311	0.923	0.174	8.953	9.669
Boning	28	10.051	0.700	0.132	9.780	10.322
Steak Non-Serrated	28	12.751	0.953	0,180	12.381	13.120
Steak Serrated	28	12.847	0.993	0.188	12.462	13.233
Bread	28	14.737	0.609	0.115	14.501	14.973

Box Plot for Roughness (Profile)

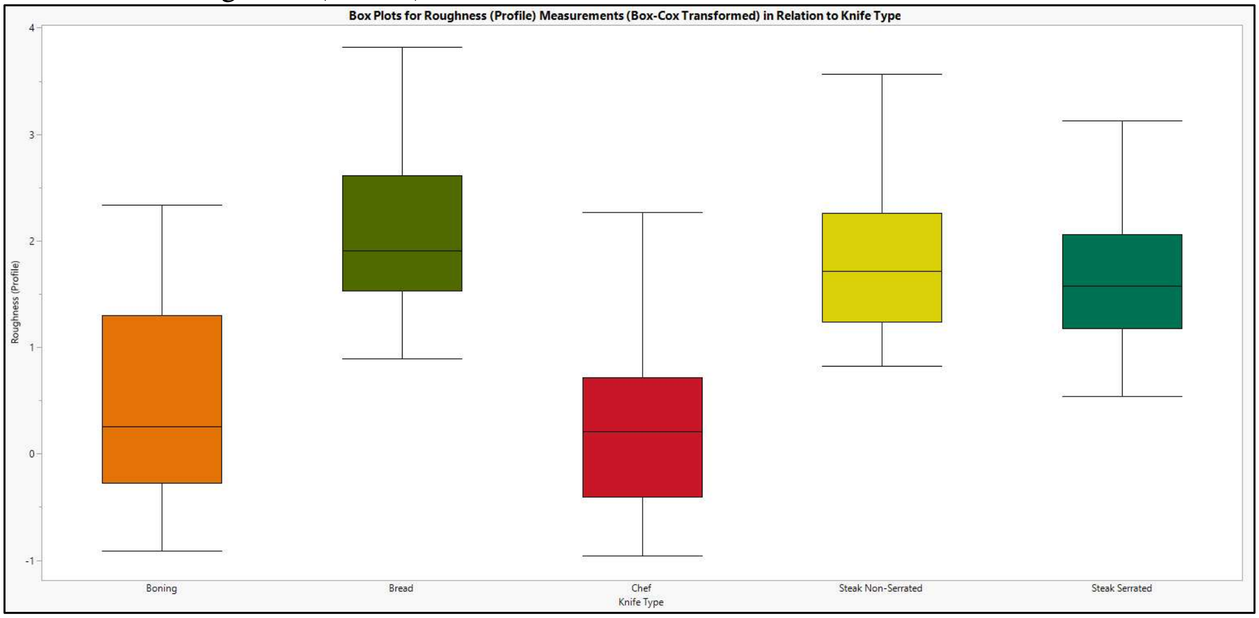

Descriptive Statistics for Roughness (Profile)

Knife Type	**Mark Count**	**Mean**	**Standard Deviation**	**Standard Error Mean**	**Lower 95%**	**Upper 95%**
Chef	28	0.180	0.768	0.145	-0.118	0.477
Boning	28	0.483	0.843	0.159	0.156	0.810
Steak Non-Serrated	28	1.850	0.722	0.136	1.570	2.129
Steak Serrated	28	1.661	0.645	0.122	1.411	1.911
Bread	28	2.049	0.755	0.143	1.756	2.342

Box Plot for Opening Angle (Profile)

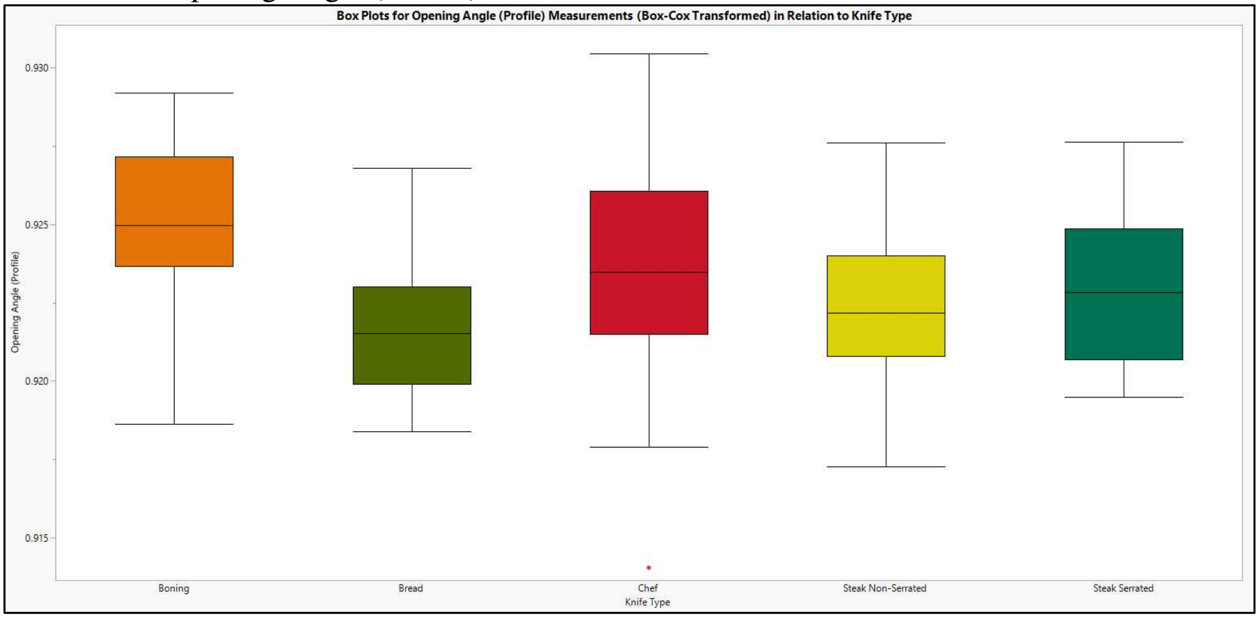

Descriptive Statistics for Opening Angle (Profile)

Knife Type	Mark Count	Mean	Standard Deviation	Standard Error Mean	Lower 95%	Upper 95%
Chef	28	0.923	0.004	0.0007	0.922	0.925
Boning	28	0.925	0.003	0.0005	0.924	0.926
Steak Non-Serrated	28	0.922	0.002	0.0004	0.922	0.923
Steak Serrated	28	0.923	0.002	0.0005	0.922	0.924
Bread	28	0.923	0.002	0.0004	0.921	0.923

Box Plot for Floor Radius (Profile)

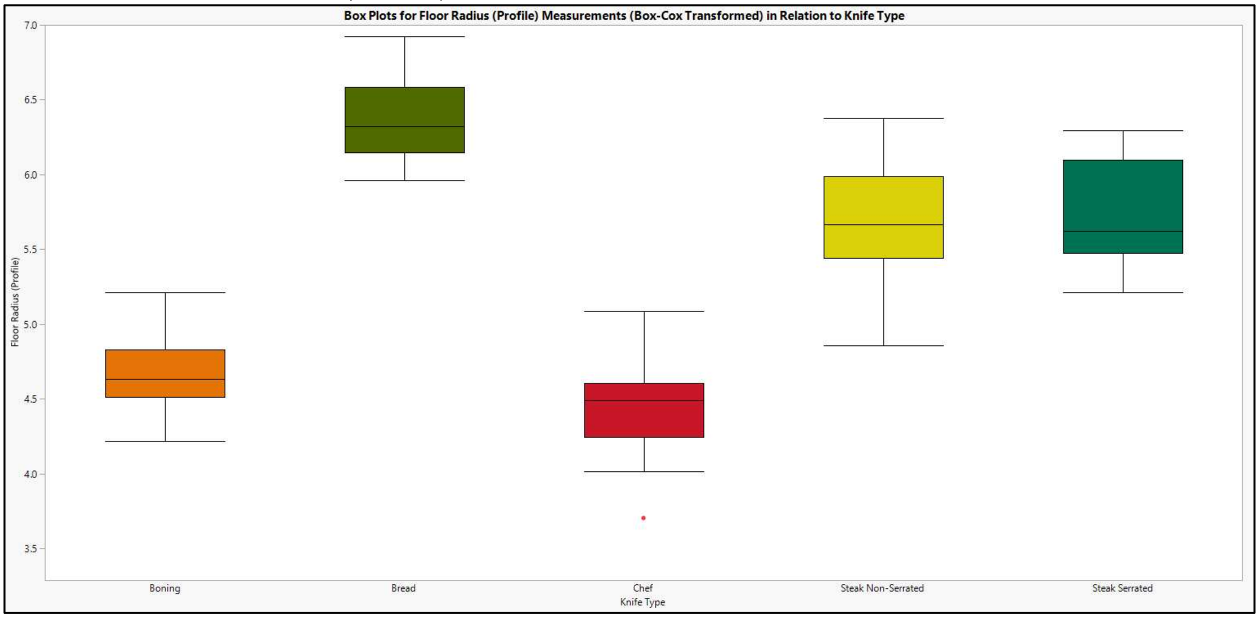

Descriptive Statistics for Floor Radius (Profile)

Knife Type	Mark Count	Mean	Standard Deviation	Standard Error Mean	Lower 95%	Upper 95%
Chef	28	4.447	0.291	0.055	4.334	4.559
Boning	28	4.662	0.213	0.040	4.580	4.745
Steak Non-Serrated	28	5.691	0.335	0.063	5.561	5.821
Steak Serrated	28	5.734	0.348	0.066	5.599	5.869
Bread	28	6.363	0.273	0.052	6.257	6.469

APPENDIX D: DISCRIMINANT SCORES FOR KNIFE TYPE, ALL VARIABLES, TRAINING SET

Row	Actual	SqDist(Actual)	Prob(Actual)	-Log(Prob)	Predicted	Prob(Pred)	Others
1	Boning	8.9266	1.0000	0.000	Boning	1.0000	
2	Boning	7.0284	0.9999	0.000	Boning	0.9999	
3	Boning	7.2369	1.0000	0.000	Boning	1.0000	
4	Boning	5.3448	0.9022	0.103	Boning	0.9022	
5	Boning	1.1774	0.9998	0.000	Boning	0.9998	
6	Boning	5.4124	0.9904	0.010	Boning	0.9904	
7	Boning	8.5633	1.0000	0.000	Boning	1.0000	
8	Boning	9.3566	0.9990	0.001	Boning	0.9990	
9	Boning	11.6503	0.6277	0.466	Boning	0.6277	Chef 0.37
10	Boning	5.6479	0.9461	0.055	Boning	0.9461	
11	Boning	7.7139	0.9854	0.015	Boning	0.9854	
12	Boning	14.6250	0.4343	0.834	Chef	0.5657	
13	Boning	4.7000	0.9986	0.001	Boning	0.9986	
14	Boning	11.9963	1.0000	0.000	Boning	1.0000	
15	Boning	12.3960	0.9887	0.011	Boning	0.9887	
16	Boning	4.9385	0.9994	0.001	Boning	0.9994	
17	Boning	7.6860	1.0000	0.000	Boning	1.0000	
18	Boning	9.2952	0.9997	0.000	Boning	0.9997	
19	Boning	9.2301	0.3409	1.076	Chef	0.6591	
20	Boning	3.8595	0.9997	0.000	Boning	0.9997	
21	Boning	8.3773	0.9995	0.001	Boning	0.9995	
22	Bread	10.1328	1.0000	0.000	Bread	1.0000	
23	Bread	8.2137	0.9999	0.000	Bread	0.9999	
24	Bread	2.0355	1.0000	0.000	Bread	1.0000	
25	Bread	2.2365	0.9999	0.000	Bread	0.9999	
26	Bread	11.7309	1.0000	0.000	Bread	1.0000	
27	Bread	7.4963	1.0000	0.000	Bread	1.0000	
28	Bread	12.4666	1.0000	0.000	Bread	1.0000	
29	Bread	3.5634	1.0000	0.000	Bread	1.0000	
30	Bread	7.3196	0.9959	0.004	Bread	0.9959	
31	Bread	6.2937	1.0000	0.000	Bread	1.0000	
32	Bread	9.9113	1.0000	0.000	Bread	1.0000	
33	Bread	2.6691	1.0000	0.000	Bread	1.0000	
34	Bread	6.5273	0.9998	0.000	Bread	0.9998	
34	Bread	5.7711	1.0000	0.000	Bread	1.0000	
36	Bread	12.4008	1.0000	0.000	Bread	1.0000	
37	Bread	9.0030	0.9958	0.004	Bread	0.9958	
36	Bread	3.3450	1.0000	0.000	Bread	1.0000	
39	Bread	4.7814	0.9999	0.000	Bread	0.9999	
40	Bread	13.9950	1.0000	0.000	Bread	1.0000	
41	Bread	2.1124	0.9983	0.002	Bread	0.9983	
42	Bread	3.6502	0.9999	0.000	Bread	0.9999	
43	Chef	13.2688	1.0000	0.000	Chef	1.0000	
44	Chef	18.2038	1.0000	0.000	Chef	1.0000	
45	Chef	9.3284	1.0000	0.000	Chef	1.0000	

Row	Actual	SqDist(Actual)	Prob(Actual)	-Log(Prob)	Predicted	Prob(Pred)	Others
46	Chef	10.6315	0.9999	0.000	Chef	0.9999	
47	Chef	7.3102	0.9049	0.100	Chef	0.9049	
48	Chef	11.0963	0.9994	0.001	Chef	0.9994	
49	Chef	12.6533	0.9213	0.082	Chef	0.9213	
50	Chef	13.3507	0.7805	0.248	Chef	0.7805	Boning 0.22
51	Chef	9.2260	0.9815	0.019	Chef	0.9815	
52	Chef	19.6927	0.9508	0.050	Chef	0.9508	
53	Chef	13.3286	1.0000	0.000	Chef	1.0000	
54	Chef	10.0921	0.9977	0.002	Chef	0.9977	
55	Chef	10.6213	1.0000	0.000	Chef	1.0000	
56	Chef	7.6852	0.9267	0.076	Chef	0.9267	
57	Chef	17.6691	1.0000	0.000	Chef	1.0000	
58	Chef	18.0058	1.0000	0.000	Chef	1.0000	
59	Chef	10.3043	0.9995	0.001	Chef	0.9995	
60	Chef	16.9381	1.0000	0.000	Chef	1.0000	
61	Chef	9.0893	1.0000	0.000	Chef	1.0000	
62	Chef	7.3705	0.4947	0.704	Boning	0.5053	
63	Chef	8.8490	0.6985	0.359	Chef	0.6985	Boning 0.30
64	Steak Full Blade	6.9449	0.7812	0.247	Steak Full Blade	0.7812	Steak Serrated Portion 0.22
65	Steak Full Blade	10.3585	0.9907	0.009	Steak Full Blade	0.9907	
66	Steak Full Blade	7.4995	0.9533	0.048	Steak Full Blade	0.9533	
67	Steak Full Blade	7.3116	0.9969	0.003	Steak Full Blade	0.9969	
68	Steak Full Blade	3.5824	0.9160	0.088	Steak Full Blade	0.9160	
69	Steak Full Blade	5.7336	0.9919	0.008	Steak Full Blade	0.9919	
70	Steak Full Blade	9.7265	0.6321	0.459	Steak Full Blade	0.6321	Steak Serrated Portion 0.37
71	Steak Full Blade	11.1357	0.9966	0.003	Steak Full Blade	0.9966	
72	Steak Full Blade	5.3450	0.9370	0.065	Steak Full Blade	0.9370	
73	Steak Full Blade	8.5884	0.9918	0.008	Steak Full Blade	0.9918	
74	Steak Full Blade	3.3727	0.9492	0.052	Steak Full Blade	0.9492	
75	Steak Full Blade	4.2002	0.9592	0.042	Steak Full Blade	0.9592	
76	Steak Full Blade	14.1304	1.0000	0.000	Steak Full Blade	1.0000	
77	Steak Full Blade	7.7570	0.9978	0.002	Steak Full Blade	0.9978	
78	Steak Full Blade	12.2827	0.4140	0.882	Steak Serrated Portion	0.5860	
79	Steak Full Blade	11.1170	0.9996	0.000	Steak Full Blade	0.9996	
80	Steak Full Blade	6.3850	0.9473	0.054	Steak Full Blade	0.9473	

Row	Actual	SqDist(Actual)	Prob(Actual)	-Log(Prob)	Predicted	Prob(Pred)	Others
81	Steak Full Blade	6.9025	0.8882	0.119	Steak Full Blade	0.8882	Steak Serrated Portion 0.11
82	Steak Full Blade	3.5707	0.9248	0.078	Steak Full Blade	0.9248	
83	Steak Full Blade	8.9256	0.9983	0.002	Steak Full Blade	0.9983	
84	Steak Full Blade	7.2098	0.9964	0.004	Steak Full Blade	0.9964	
85	Steak Serrated Portion	11.6133	0.9733	0.027	Steak Serrated Portion	0.9733	
86	Steak Serrated Portion	17.2986	1.0000	0.000	Steak Serrated Portion	1.0000	
87	Steak Serrated Portion	6.4094	0.9985	0.001	Steak Serrated Portion	0.9985	
88	Steak Serrated Portion	9.2075	0.2810	1.269	Steak Full Blade	0.7190	
89	Steak Serrated Portion	7.5210	1.0000	0.000	Steak Serrated Portion	1.0000	
90	Steak Serrated Portion	14.3083	0.9996	0.000	Steak Serrated Portion	0.9996	
91	Steak Serrated Portion	6.7271	0.9997	0.000	Steak Serrated Portion	0.9997	
92	Steak Serrated Portion	14.9938	0.9202	0.083	Steak Serrated Portion	0.9202	
93	Steak Serrated Portion	16.8517	1.0000	0.000	Steak Serrated Portion	1.0000	
94	Steak Serrated Portion	9.2218	0.9350	0.067	Steak Serrated Portion	0.9350	
95	Steak Serrated Portion	11.1056	0.9905	0.010	Steak Serrated Portion	0.9905	
96	Steak Serrated Portion	8.1201	0.8564	0.155	Steak Serrated Portion	0.8564	Steak Full Blade 0.11
97	Steak Serrated Portion	9.3576	0.9999	0.000	Steak Serrated Portion	0.9999	
98	Steak Serrated Portion	12.7614	1.0000	0.000	Steak Serrated Portion	1.0000	
99	Steak Serrated Portion	12.0182	0.8546	0.157	Steak Serrated Portion	0.8546	Steak Full Blade 0.15
100	Steak Serrated Portion	7.6227	0.9992	0.001	Steak Serrated Portion	0.9992	
101	Steak Serrated Portion	6.9106	0.4972	0.699	Steak Full Blade	0.5028	
102	Steak Serrated Portion	13.9885	0.9981	0.002	Steak Serrated Portion	0.9981	
103	Steak Serrated Portion	11.6685	0.3433	1.069	Steak Full Blade	0.6567	
104	Steak Serrated Portion	5.2976	0.7519	0.285	Steak Serrated Portion	0.7519	Steak Full Blade 0.25
105	Steak Serrated Portion	7.7536	0.9882	0.012	Steak Serrated Portion	0.9882	

APPENDIX E: DISCRIMINANT SCORES FOR KNIFE TYPE, EXCLUDING VARIABLES, TRAINING SET

Row	Actual	SqDist(Actual)	Prob(Actual)	-Log(Prob)	Predicted	Prob(Pred)	Others
1	Boning	10.98457	0.6459	0.437	Boning	0.6459	Chef 0.35
2	Boning	8.81667	0.8882	0.119	Boning	0.8882	
3	Boning	4.76801	0.9089	0.095	Boning	0.9089	
4	Boning	6.18489	0.7693	0.262	Boning	0.7693	Chef 0.23
5	Boning	2.74359	0.9294	0.073	Boning	0.9294	
6	Boning	3.53858	0.9411	0.061	Boning	0.9411	
7	Boning	9.02905	0.9998	0.000	Boning	0.9998	
8	Boning	10.21780	0.9574	0.044	Boning	0.9574	
9	Boning	8.91572	0.7805	0.248	Boning	0.7805	Chef 0.22
10	Boning	7.41944	0.7880	0.238	Boning	0.7880	Chef 0.21
11	Boning	2.58457	0.9752	0.025	Boning	0.9752	
12	Boning	13.88576	0.1620	1.820	Chef	0.8380	
13	Boning	5.98766	0.9927	0.007	Boning	0.9927	
14	Boning	10.44473	1.0000	0.000	Boning	1.0000	
15	Boning	10.65876	0.3394	1.081	Chef	0.6453	
16	Boning	4.95823	0.9327	0.070	Boning	0.9327	
17	Boning	10.04267	1.0000	0.000	Boning	1.0000	
18	Boning	8.24279	0.9984	0.002	Boning	0.9984	
19	Boning	6.96864	0.5070	0.679	Boning	0.5070	Chef 0.49
20	Boning	5.28672	0.9793	0.021	Boning	0.9793	
21	Boning	5.97934	0.9926	0.007	Boning	0.9926	
22	Bread	5.90373	0.9926	0.007	Bread	0.9926	
23	Bread	7.31722	0.9997	0.000	Bread	0.9997	
24	Bread	4.53993	0.9996	0.000	Bread	0.9996	
25	Bread	3.47020	0.9989	0.001	Bread	0.9989	
26	Bread	6.57947	0.9922	0.008	Bread	0.9922	
27	Bread	3.56101	0.9990	0.001	Bread	0.9990	
28	Bread	13.99775	1.0000	0.000	Bread	1.0000	
29	Bread	4.96233	0.9999	0.000	Bread	0.9999	
30	Bread	6.61245	0.8066	0.215	Bread	0.8066	Steak Serrated Portion 0.12
31	Bread	7.19071	0.9859	0.014	Bread	0.9859	
32	Bread	9.89878	0.9998	0.000	Bread	0.9998	
33	Bread	4.22976	0.9970	0.003	Bread	0.9970	
34	Bread	7.10851	0.9923	0.008	Bread	0.9923	
34	Bread	4.47805	0.9999	0.000	Bread	0.9999	
36	Bread	14.48427	0.9999	0.000	Bread	0.9999	
37	Bread	10.62192	0.8438	0.170	Bread	0.8438	Steak Serrated Portion 0.14
36	Bread	4.56871	0.9977	0.002	Bread	0.9977	
39	Bread	4.63561	0.9936	0.006	Bread	0.9936	
40	Bread	13.41243	1.0000	0.000	Bread	1.0000	
41	Bread	2.34170	0.9812	0.019	Bread	0.9812	
42	Bread	5.79256	0.9663	0.034	Bread	0.9663	
43	Chef	9.59790	0.9479	0.053	Chef	0.9479	

Row	Actual	SqDist(Actual)	Prob(Actual)	-Log(Prob)	Predicted	Prob(Pred)	Others
44	Chef	11.07173	0.9977	0.002	Chef	0.9977	
45	Chef	8.00451	0.8948	0.111	Chef	0.8948	Boning 0.11
46	Chef	8.32083	0.9995	0.000	Chef	0.9995	
47	Chef	4.11660	0.8412	0.173	Chef	0.8412	Boning 0.16
48	Chef	6.31960	0.2993	1.206	Boning	0.7007	
49	Chef	8.50158	0.9176	0.086	Chef	0.9176	
50	Chef	8.78884	0.5544	0.590	Chef	0.5544	Boning 0.45
51	Chef	7.51335	0.9098	0.095	Chef	0.9098	
52	Chef	17.41265	0.8232	0.195	Chef	0.8232	Boning 0.18
53	Chef	10.70110	0.9899	0.010	Chef	0.9899	
54	Chef	8.22256	0.9483	0.053	Chef	0.9483	
55	Chef	9.53544	1.0000	0.000	Chef	1.0000	
56	Chef	6.28815	0.9848	0.015	Chef	0.9848	
57	Chef	11.00582	0.1215	2.108	Boning	0.8774	
58	Chef	16.81083	0.9993	0.001	Chef	0.9993	
59	Chef	8.70475	0.9988	0.001	Chef	0.9988	
60	Chef	12.08240	1.0000	0.000	Chef	1.0000	
61	Chef	6.72537	0.9998	0.000	Chef	0.9998	
62	Chef	4.20544	0.6803	0.385	Chef	0.6803	Boning 0.32
63	Chef	6.93460	0.8259	0.191	Chef	0.8259	Boning 0.17
64	Steak Full Blade	7.58366	0.8558	0.156	Steak Full Blade	0.8558	Steak Serrated Portion 0.14
65	Steak Full Blade	3.32698	0.9186	0.085	Steak Full Blade	0.9186	
66	Steak Full Blade	8.85600	0.8672	0.142	Steak Full Blade	0.8672	Steak Serrated Portion 0.13
67	Steak Full Blade	8.22886	0.8807	0.127	Steak Full Blade	0.8807	Steak Serrated Portion 0.12
68	Steak Full Blade	4.93481	0.9288	0.074	Steak Full Blade	0.9288	
69	Steak Full Blade	8.76116	0.9437	0.058	Steak Full Blade	0.9437	
70	Steak Full Blade	8.92090	0.7497	0.288	Steak Full Blade	0.7497	Steak Serrated Portion 0.25
71	Steak Full Blade	8.51129	0.9855	0.015	Steak Full Blade	0.9855	
72	Steak Full Blade	6.84181	0.8340	0.181	Steak Full Blade	0.8340	Steak Serrated Portion 0.17
73	Steak Full Blade	10.35827	0.6930	0.367	Steak Full Blade	0.6930	Chef 0.15 Steak Serrated Portion 0.15
74	Steak Full Blade	6.45995	0.7919	0.233	Steak Full Blade	0.7919	Steak Serrated Portion 0.20
75	Steak Full Blade	5.25455	0.9432	0.058	Steak Full Blade	0.9432	
76	Steak Full Blade	12.34600	0.8444	0.169	Steak Full Blade	0.8444	Steak Serrated Portion 0.16
77	Steak Full Blade	8.69787	0.9574	0.043	Steak Full Blade	0.9574	
78	Steak Full Blade	12.55730	0.0774	2.559	Steak Serrated Portion	0.9226	

Row	Actual	SqDist(Actual)	Prob(Actual)	-Log(Prob)	Predicted	Prob(Pred)	Others
79	Steak Full Blade	9.13400	0.2735	1.296	Steak Serrated Portion	0.7265	
80	Steak Full Blade	9.33883	0.6761	0.391	Steak Full Blade	0.6761	Steak Serrated Portion 0.32
81	Steak Full Blade	7.75899	0.8877	0.119	Steak Full Blade	0.8877	Steak Serrated Portion 0.11
82	Steak Full Blade	5.78919	0.7642	0.269	Steak Full Blade	0.7642	Steak Serrated Portion 0.24
83	Steak Full Blade	9.50161	0.9932	0.007	Steak Full Blade	0.9932	
84	Steak Full Blade	7.15186	0.9283	0.074	Steak Full Blade	0.9283	
85	Steak Serrated Portion	13.92450	0.4577	0.782	Steak Full Blade	0.5422	
86	Steak Serrated Portion	15.74338	1.0000	0.000	Steak Serrated Portion	1.0000	
87	Steak Serrated Portion	8.79873	0.9320	0.070	Steak Serrated Portion	0.9320	
88	Steak Serrated Portion	8.60807	0.3883	0.946	Steak Full Blade	0.6116	
89	Steak Serrated Portion	8.54738	0.9998	0.000	Steak Serrated Portion	0.9998	
90	Steak Serrated Portion	10.71958	0.9766	0.024	Steak Serrated Portion	0.9766	
91	Steak Serrated Portion	8.05805	0.9961	0.004	Steak Serrated Portion	0.9961	
92	Steak Serrated Portion	8.01449	0.9431	0.059	Steak Serrated Portion	0.9431	
93	Steak Serrated Portion	18.71483	1.0000	0.000	Steak Serrated Portion	1.0000	
94	Steak Serrated Portion	11.40948	0.6636	0.410	Steak Serrated Portion	0.6636	Steak Full Blade 0.34
95	Steak Serrated Portion	11.82646	0.9894	0.011	Steak Serrated Portion	0.9894	
96	Steak Serrated Portion	8.40473	0.2462	1.401	Steak Full Blade	0.7482	
97	Steak Serrated Portion	9.82298	0.9376	0.064	Steak Serrated Portion	0.9376	
98	Steak Serrated Portion	9.15377	0.8588	0.152	Steak Serrated Portion	0.8588	Steak Full Blade 0.14

Row	Actual	SqDist(Actual)	Prob(Actual)	-Log(Prob)	Predicted	Prob(Pred)	Others
99	Steak Serrated Portion	9.93758	0.8971	0.109	Steak Serrated Portion	0.8971	Steak Full Blade 0.10
100	Steak Serrated Portion	7.60963	0.9077	0.097	Steak Serrated Portion	0.9077	
101	Steak Serrated Portion	7.26440	0.5495	0.599	Steak Serrated Portion	0.5495	Steak Full Blade 0.45
102	Steak Serrated Portion	13.83081	0.5850	0.536	Steak Serrated Portion	0.5850	Steak Full Blade 0.41
103	Steak Serrated Portion	12.39936	0.3894	0.943	Steak Full Blade	0.6106	
104	Steak Serrated Portion	6.27312	0.8288	0.188	Steak Serrated Portion	0.8288	Steak Full Blade 0.17
105	Steak Serrated Portion	9.08717	0.9365	0.066	Steak Serrated Portion	0.9365	

APPENDIX F: DISCRIMINANT SCORES FOR BLADE CLASS, ALL VARIABLES, TRAINING SET

Row	Actual	SqDist(Actual)	Prob(Actual)	-Log(Prob)	Predicted	Prob(Pred)	Others
1	Non-Serrated	15.77949	0.9998	0.000	Non-Serrated	0.9998	
2	Non-Serrated	13.41875	1.0000	0.000	Non-Serrated	1.0000	
3	Non-Serrated	16.10493	0.9998	0.000	Non-Serrated	0.9998	
4	Non-Serrated	12.09846	1.0000	0.000	Non-Serrated	1.0000	
5	Non-Serrated	9.18348	1.0000	0.000	Non-Serrated	1.0000	
6	Non-Serrated	10.41672	1.0000	0.000	Non-Serrated	1.0000	
7	Non-Serrated	18.58992	1.0000	0.000	Non-Serrated	1.0000	
8	Non-Serrated	15.24524	0.9987	0.001	Non-Serrated	0.9987	
9	Non-Serrated	12.02374	1.0000	0.000	Non-Serrated	1.0000	
10	Non-Serrated	12.44037	1.0000	0.000	Non-Serrated	1.0000	
11	Non-Serrated	12.68580	1.0000	0.000	Non-Serrated	1.0000	
12	Non-Serrated	15.44276	1.0000	0.000	Non-Serrated	1.0000	
13	Non-Serrated	14.01361	1.0000	0.000	Non-Serrated	1.0000	
14	Non-Serrated	22.70989	1.0000	0.000	Non-Serrated	1.0000	
15	Non-Serrated	18.26971	1.0000	0.000	Non-Serrated	1.0000	
16	Non-Serrated	13.51955	1.0000	0.000	Non-Serrated	1.0000	
17	Non-Serrated	19.22649	1.0000	0.000	Non-Serrated	1.0000	
18	Non-Serrated	17.85254	1.0000	0.000	Non-Serrated	1.0000	
19	Non-Serrated	11.16749	1.0000	0.000	Non-Serrated	1.0000	
20	Non-Serrated	12.77544	1.0000	0.000	Non-Serrated	1.0000	
21	Non-Serrated	15.21177	0.9958	0.004	Non-Serrated	0.9958	
22	Serrated	13.35167	0.9994	0.001	Serrated	0.9994	
23	Serrated	11.43253	1.0000	0.000	Serrated	1.0000	
24	Serrated	5.25434	1.0000	0.000	Serrated	1.0000	
25	Serrated	5.45536	0.9999	0.000	Serrated	0.9999	
26	Serrated	14.94980	0.9999	0.000	Serrated	0.9999	
27	Serrated	10.71517	0.9999	0.000	Serrated	0.9999	
28	Serrated	15.68551	1.0000	0.000	Serrated	1.0000	
29	Serrated	6.78227	1.0000	0.000	Serrated	1.0000	
30	Serrated	10.53851	0.9985	0.002	Serrated	0.9985	
31	Serrated	9.51253	1.0000	0.000	Serrated	1.0000	
32	Serrated	13.13017	1.0000	0.000	Serrated	1.0000	
33	Serrated	5.88798	1.0000	0.000	Serrated	1.0000	
34	Serrated	9.74619	0.9999	0.000	Serrated	0.9999	
34	Serrated	8.98993	1.0000	0.000	Serrated	1.0000	
36	Serrated	15.61970	1.0000	0.000	Serrated	1.0000	
37	Serrated	12.22190	0.9917	0.008	Serrated	0.9917	
36	Serrated	6.56388	0.9999	0.000	Serrated	0.9999	
39	Serrated	8.00031	1.0000	0.000	Serrated	1.0000	
40	Serrated	17.21384	1.0000	0.000	Serrated	1.0000	
41	Serrated	5.33123	0.9988	0.001	Serrated	0.9988	
42	Serrated	6.86903	0.9993	0.001	Serrated	0.9993	
43	Non-Serrated	14.26007	1.0000	0.000	Non-Serrated	1.0000	
44	Non-Serrated	27.85463	1.0000	0.000	Non-Serrated	1.0000	
45	Non-Serrated	15.82389	1.0000	0.000	Non-Serrated	1.0000	

Row	Actual	SqDist(Actual)	Prob(Actual)	-Log(Prob)	Predicted	Prob(Pred)	Others
46	Non-Serrated	14.14516	1.0000	0.000	Non-Serrated	1.0000	
47	Non-Serrated	9.08067	1.0000	0.000	Non-Serrated	1.0000	
48	Non-Serrated	14.63121	1.0000	0.000	Non-Serrated	1.0000	
49	Non-Serrated	13.44560	1.0000	0.000	Non-Serrated	1.0000	
50	Non-Serrated	11.54352	1.0000	0.000	Non-Serrated	1.0000	
51	Non-Serrated	9.42413	1.0000	0.000	Non-Serrated	1.0000	
52	Non-Serrated	22.54424	1.0000	0.000	Non-Serrated	1.0000	
53	Non-Serrated	21.11403	1.0000	0.000	Non-Serrated	1.0000	
54	Non-Serrated	14.34740	1.0000	0.000	Non-Serrated	1.0000	
55	Non-Serrated	15.81159	1.0000	0.000	Non-Serrated	1.0000	
56	Non-Serrated	12.26409	1.0000	0.000	Non-Serrated	1.0000	
57	Non-Serrated	24.34888	1.0000	0.000	Non-Serrated	1.0000	
58	Non-Serrated	30.86403	1.0000	0.000	Non-Serrated	1.0000	
59	Non-Serrated	12.15307	1.0000	0.000	Non-Serrated	1.0000	
60	Non-Serrated	26.56606	1.0000	0.000	Non-Serrated	1.0000	
61	Non-Serrated	13.21595	1.0000	0.000	Non-Serrated	1.0000	
62	Non-Serrated	9.51973	1.0000	0.000	Non-Serrated	1.0000	
63	Non-Serrated	9.06648	1.0000	0.000	Non-Serrated	1.0000	
64	Partially Serrated	9.14309	1.0000	0.000	Partially Serrated	1.0000	
65	Partially Serrated	13.43069	0.9999	0.000	Partially Serrated	0.9999	
66	Partially Serrated	12.17133	0.9997	0.000	Partially Serrated	0.9997	
67	Partially Serrated	12.44208	1.0000	0.000	Partially Serrated	1.0000	
68	Partially Serrated	8.38480	0.9996	0.000	Partially Serrated	0.9996	
69	Partially Serrated	12.63352	0.9999	0.000	Partially Serrated	0.9999	
70	Partially Serrated	12.50420	1.0000	0.000	Partially Serrated	1.0000	
71	Partially Serrated	16.37895	1.0000	0.000	Partially Serrated	1.0000	
72	Partially Serrated	9.49742	1.0000	0.000	Partially Serrated	1.0000	
73	Partially Serrated	15.31445	0.9913	0.009	Partially Serrated	0.9913	
74	Partially Serrated	8.21956	1.0000	0.000	Partially Serrated	1.0000	
75	Partially Serrated	9.34737	1.0000	0.000	Partially Serrated	1.0000	
76	Partially Serrated	21.10231	1.0000	0.000	Partially Serrated	1.0000	
77	Partially Serrated	13.55115	1.0000	0.000	Partially Serrated	1.0000	
78	Partially Serrated	11.31642	1.0000	0.000	Partially Serrated	1.0000	
79	Partially Serrated	17.17557	1.0000	0.000	Partially Serrated	1.0000	
80	Partially Serrated	9.86178	1.0000	0.000	Partially Serrated	1.0000	
81	Partially Serrated	10.81342	1.0000	0.000	Partially Serrated	1.0000	
82	Partially Serrated	7.92169	1.0000	0.000	Partially Serrated	1.0000	
83	Partially Serrated	15.91700	1.0000	0.000	Partially Serrated	1.0000	
84	Partially Serrated	13.69210	1.0000	0.000	Partially Serrated	1.0000	
85	Partially Serrated	12.76613	0.9999	0.000	Partially Serrated	0.9999	
86	Partially Serrated	26.00296	1.0000	0.000	Partially Serrated	1.0000	
87	Partially Serrated	8.64651	1.0000	0.000	Partially Serrated	1.0000	
88	Partially Serrated	8.74033	1.0000	0.000	Partially Serrated	1.0000	
89	Partially Serrated	12.28476	1.0000	0.000	Partially Serrated	1.0000	
90	Partially Serrated	18.32399	1.0000	0.000	Partially Serrated	1.0000	
91	Partially Serrated	10.69483	1.0000	0.000	Partially Serrated	1.0000	
92	Partially Serrated	16.09342	1.0000	0.000	Partially Serrated	1.0000	
93	Partially Serrated	27.97061	1.0000	0.000	Partially Serrated	1.0000	
94	Partially Serrated	9.91299	1.0000	0.000	Partially Serrated	1.0000	
95	Partially Serrated	13.49425	1.0000	0.000	Partially Serrated	1.0000	
96	Partially Serrated	9.69838	0.9838	0.016	Partially Serrated	0.9838	

Row	Actual	SqDist(Actual)	Prob(Actual)	-Log(Prob)	Predicted	Prob(Pred)	Others
97	Partially Serrated	15.48457	0.9997	0.000	Partially Serrated	0.9997	
98	Partially Serrated	19.72314	0.9998	0.000	Partially Serrated	0.9998	
99	Partially Serrated	11.84468	1.0000	0.000	Partially Serrated	1.0000	
100	Partially Serrated	11.82658	1.0000	0.000	Partially Serrated	1.0000	
101	Partially Serrated	8.55149	1.0000	0.000	Partially Serrated	1.0000	
102	Partially Serrated	16.87144	1.0000	0.000	Partially Serrated	1.0000	
103	Partially Serrated	13.79888	1.0000	0.000	Partially Serrated	1.0000	
104	Partially Serrated	7.63339	1.0000	0.000	Partially Serrated	1.0000	
105	Partially Serrated	9.81638	1.0000	0.000	Partially Serrated	1.0000	

APPENDIX G: DISCRIMINANT SCORES FOR BLADE CLASS, EXCLUDING VARIABLES, TRAINING SET

Row	Actual	SqDist(Actual)	Prob(Actual)	-Log(Prob)	Predicted	Prob(Pred)	Others
1	Non-Serrated	9.65777	0.9999	0.000	Non-Serrated	0.9999	
2	Non-Serrated	10.03378	0.9115	0.093	Non-Serrated	0.9115	
3	Non-Serrated	7.40800	1.0000	0.000	Non-Serrated	1.0000	
4	Non-Serrated	8.33074	0.9984	0.002	Non-Serrated	0.9984	
5	Non-Serrated	5.56625	0.9998	0.000	Non-Serrated	0.9998	
6	Non-Serrated	6.70626	1.0000	0.000	Non-Serrated	1.0000	
7	Non-Serrated	14.89968	1.0000	0.000	Non-Serrated	1.0000	
8	Non-Serrated	12.11526	0.9379	0.064	Non-Serrated	0.9379	
9	Non-Serrated	8.35869	1.0000	0.000	Non-Serrated	1.0000	
10	Non-Serrated	9.46642	1.0000	0.000	Non-Serrated	1.0000	
11	Non-Serrated	5.95629	0.9910	0.009	Non-Serrated	0.9910	
12	Non-Serrated	11.43651	1.0000	0.000	Non-Serrated	1.0000	
13	Non-Serrated	8.97809	1.0000	0.000	Non-Serrated	1.0000	
14	Non-Serrated	17.10886	1.0000	0.000	Non-Serrated	1.0000	
15	Non-Serrated	10.36433	0.9897	0.010	Non-Serrated	0.9897	
16	Non-Serrated	6.85507	0.9994	0.001	Non-Serrated	0.9994	
17	Non-Serrated	15.50469	1.0000	0.000	Non-Serrated	1.0000	
18	Non-Serrated	12.66517	1.0000	0.000	Non-Serrated	1.0000	
19	Non-Serrated	7.76045	0.9999	0.000	Non-Serrated	0.9999	
20	Non-Serrated	8.38759	1.0000	0.000	Non-Serrated	1.0000	
21	Non-Serrated	9.00044	0.9998	0.000	Non-Serrated	0.9998	
22	Serrated	5.90373	0.9934	0.007	Serrated	0.9934	
23	Serrated	7.31722	1.0000	0.000	Serrated	1.0000	
24	Serrated	4.53993	0.9989	0.001	Serrated	0.9989	
25	Serrated	3.47020	0.9988	0.001	Serrated	0.9988	
26	Serrated	6.57947	0.9898	0.010	Serrated	0.9898	
27	Serrated	3.56101	0.9983	0.002	Serrated	0.9983	
28	Serrated	13.99775	1.0000	0.000	Serrated	1.0000	
29	Serrated	4.96233	1.0000	0.000	Serrated	1.0000	
30	Serrated	6.61245	0.8608	0.150	Serrated	0.8608	Partially Serrated 0.14
31	Serrated	7.19071	0.9845	0.016	Serrated	0.9845	
32	Serrated	9.89878	0.9999	0.000	Serrated	0.9999	
33	Serrated	4.22976	0.9993	0.001	Serrated	0.9993	
34	Serrated	7.10851	0.9993	0.001	Serrated	0.9993	
34	Serrated	4.47805	1.0000	0.000	Serrated	1.0000	
36	Serrated	14.48427	1.0000	0.000	Serrated	1.0000	
37	Serrated	10.62192	0.8805	0.127	Serrated	0.8805	Partially Serrated 0.12
36	Serrated	4.56871	0.9984	0.002	Serrated	0.9984	
39	Serrated	4.63561	0.9941	0.006	Serrated	0.9941	
40	Serrated	13.41243	1.0000	0.000	Serrated	1.0000	
41	Serrated	2.34170	0.9928	0.007	Serrated	0.9928	
42	Serrated	5.79256	0.9777	0.023	Serrated	0.9777	
43	Non-Serrated	9.02367	1.0000	0.000	Non-Serrated	1.0000	

Row	Actual	SqDist(Actual)	Prob(Actual)	-Log(Prob)	Predicted	Prob(Pred)	Others
44	Non-Serrated	14.19928	1.0000	0.000	Non-Serrated	1.0000	
45	Non-Serrated	8.60361	1.0000	0.000	Non-Serrated	1.0000	
46	Non-Serrated	9.84693	1.0000	0.000	Non-Serrated	1.0000	
47	Non-Serrated	5.14500	1.0000	0.000	Non-Serrated	1.0000	
48	Non-Serrated	5.97740	1.0000	0.000	Non-Serrated	1.0000	
49	Non-Serrated	8.25318	1.0000	0.000	Non-Serrated	1.0000	
50	Non-Serrated	8.16834	0.9999	0.000	Non-Serrated	0.9999	
51	Non-Serrated	6.56659	1.0000	0.000	Non-Serrated	1.0000	
52	Non-Serrated	17.00448	1.0000	0.000	Non-Serrated	1.0000	
53	Non-Serrated	13.26725	0.9848	0.015	Non-Serrated	0.9848	
54	Non-Serrated	10.17534	1.0000	0.000	Non-Serrated	1.0000	
55	Non-Serrated	10.90017	1.0000	0.000	Non-Serrated	1.0000	
56	Non-Serrated	8.45861	1.0000	0.000	Non-Serrated	1.0000	
57	Non-Serrated	8.91892	0.9930	0.007	Non-Serrated	0.9930	
58	Non-Serrated	20.62586	0.9999	0.000	Non-Serrated	0.9999	
59	Non-Serrated	9.02941	1.0000	0.000	Non-Serrated	1.0000	
60	Non-Serrated	19.36862	1.0000	0.000	Non-Serrated	1.0000	
61	Non-Serrated	7.94769	1.0000	0.000	Non-Serrated	1.0000	
62	Non-Serrated	5.06499	1.0000	0.000	Non-Serrated	1.0000	
63	Non-Serrated	6.08915	1.0000	0.000	Non-Serrated	1.0000	
64	Partially Serrated	8.92537	0.9890	0.011	Partially Serrated	0.9890	
65	Partially Serrated	6.00775	0.9999	0.000	Partially Serrated	0.9999	
66	Partially Serrated	10.10157	0.9909	0.009	Partially Serrated	0.9909	
67	Partially Serrated	9.76054	1.0000	0.000	Partially Serrated	1.0000	
68	Partially Serrated	7.72159	0.9904	0.010	Partially Serrated	0.9904	
69	Partially Serrated	12.00760	0.8473	0.166	Partially Serrated	0.8473	Serrated 0.15
70	Partially Serrated	9.31688	1.0000	0.000	Partially Serrated	1.0000	
71	Partially Serrated	12.19871	1.0000	0.000	Partially Serrated	1.0000	
72	Partially Serrated	8.29643	0.9990	0.001	Partially Serrated	0.9990	
73	Partially Serrated	11.06412	0.8471	0.166	Partially Serrated	0.8471	Non-Serrated 0.15
74	Partially Serrated	8.10403	0.9907	0.009	Partially Serrated	0.9907	
75	Partially Serrated	7.95574	1.0000	0.000	Partially Serrated	1.0000	
76	Partially Serrated	13.73202	1.0000	0.000	Partially Serrated	1.0000	
77	Partially Serrated	11.53094	1.0000	0.000	Partially Serrated	1.0000	
78	Partially Serrated	8.89221	1.0000	0.000	Partially Serrated	1.0000	
79	Partially Serrated	6.91980	1.0000	0.000	Partially Serrated	1.0000	

Row	Actual	SqDist(Actual)	Prob(Actual)	-Log(Prob)	Predicted	Prob(Pred)	Others
80	Partially Serrated	9.18494	1.0000	0.000	Partially Serrated	1.0000	
81	Partially Serrated	10.32936	0.9891	0.011	Partially Serrated	0.9891	
82	Partially Serrated	7.01726	1.0000	0.000	Partially Serrated	1.0000	
83	Partially Serrated	13.37294	0.9977	0.002	Partially Serrated	0.9977	
84	Partially Serrated	9.86482	0.9925	0.007	Partially Serrated	0.9925	
85	Partially Serrated	11.88449	0.9999	0.000	Partially Serrated	0.9999	
86	Partially Serrated	20.44297	1.0000	0.000	Partially Serrated	1.0000	
87	Partially Serrated	8.69613	1.0000	0.000	Partially Serrated	1.0000	
88	Partially Serrated	7.98570	0.9996	0.000	Partially Serrated	0.9996	
89	Partially Serrated	11.20945	1.0000	0.000	Partially Serrated	1.0000	
90	Partially Serrated	11.83592	1.0000	0.000	Partially Serrated	1.0000	
91	Partially Serrated	9.97340	1.0000	0.000	Partially Serrated	1.0000	
92	Partially Serrated	7.93276	1.0000	0.000	Partially Serrated	1.0000	
93	Partially Serrated	25.64336	1.0000	0.000	Partially Serrated	1.0000	
94	Partially Serrated	9.88840	1.0000	0.000	Partially Serrated	1.0000	
95	Partially Serrated	12.50898	1.0000	0.000	Partially Serrated	1.0000	
96	Partially Serrated	7.30307	0.9871	0.013	Partially Serrated	0.9871	
97	Partially Serrated	11.56245	0.8872	0.120	Partially Serrated	0.8872	Serrated 0.11
98	Partially Serrated	9.76854	1.0000	0.000	Partially Serrated	1.0000	
99	Partially Serrated	10.66680	1.0000	0.000	Partially Serrated	1.0000	
100	Partially Serrated	7.60346	1.0000	0.000	Partially Serrated	1.0000	
101	Partially Serrated	6.76415	1.0000	0.000	Partially Serrated	1.0000	
102	Partially Serrated	13.68171	1.0000	0.000	Partially Serrated	1.0000	
103	Partially Serrated	11.79969	1.0000	0.000	Partially Serrated	1.0000	
104	Partially Serrated	6.82925	1.0000	0.000	Partially Serrated	1.0000	
105	Partially Serrated	9.27884	0.9999	0.000	Partially Serrated	0.9999	